Appendix A

Supplementary materials for:

Optimizing extraction and targeted capture of ancient environmental DNA for reconstructing past environments using the Palaeo Chip Arctic-1.0 bait-set

Each of the following sets of experiments followed the same protocols for subsampling, library preparation, indexing, qPCR inhibition spike tests, and qPCR total quantifications as described in the main paper. Master mix concentrations for each of the aforementioned reactions can be found in Tables S1–S9. Variations in extraction protocols for testing inhibition clean-up techniques are detailed with the description of that experimental sediment extraction/enrichment test (SET) below, from SET-A to SET-D_2. The following table of contents outlines the sections of this appendix.

List of Tables, Appendix A 2
List of Figures, Appendix A 3
SET-A: Initial explorations 6
SET-A. Extraction 6
SET-A. Bioanalyzer, inhibitor clean-up, and indexing 6
SET-A. Inhibition, qPCR, and DsLp 7
SET-A. Inhibition Index 8
SET-B: Comparing inhibition removal strategies 9
SET-B. Results and interpretations 9
SET-C: Fine-tuning the cold spin 10
SET-D: Optimizing our modified Dabney extraction protocol 11
SET-D. Results and interpretations 12
SET-D. SDS and sarkosyl 13
SET-D. Chloroplast assay of 'purified' extracts with variable Taq 14
SET-E: Additional data for main-text experiment. 15
SET-E. Enrichment: PalaeoChip bait-set design and wet lab procedures. 15
SET-E. Sadoway (2014) PCR metabarcoding 16
SET-E. PCR metabarcoding trnL 17
SET-E. Bioinformatic workflow 17
SET-E. Map-filtered to animal and plant baits. 19
SET-E. Map-filtered to plant reference sequences. 19
SET-E. MapDamage. 20
SET-E. Stringent LCA filtering for unexpected taxa 21
SET-E. Other additional data. 21
Tables 24
Figures 42
Appendix A References 80

List of Tables, Appendix A

Table S1 Final concentrations of components in the proteinase K digestion solution. 24
Table S2 Final concentrations of components in the Dabney binding buffer. 24
Table S3 Final concentrations of components in the blunt-end repair mixture.....24
Table S4 Final concentrations of all components in the adapter ligation mixture. 25
Table S5 Final concentrations of components in the adapter fill-in mixture. 25
Table S6 Primer sequences, PCR master mix, and cycling protocol for indexing amplification..26
Table S7 Inhibition spike test qPCR assay. 27
Table S8 Library adapted short amp total quantification PCR. 28
Table S9 Library adapted *trnL* short amp total quantification PCR. 29
Table S10 Library adapted and indexed long amp total quantification PCR. 30
Table S11 Enrichment mastermixes.....31
Table S12 SET-A sample list. 32
Table S13 SET-B sample list. 33
Table S14 Sonication run parameters. 34
Table S15 SET-C sample list. 35
Table S16 SET-D sample list. 36
Table S17 Metabarcoding qPCR amplification, *trnL*. 37
Table S18 Disabled taxa in MEGAN with NCBI ID. 38
Table S19 Taxon specific mapping summary. 39
Table S20 Bait map-filtered reads *MEGAN* LCA-assignment summary, SET-E. 40
Table S21 Non-map-filtered reads *MEGAN* LCA-assignment summary, SET-E. 40
Table S22 Comparative fold increase in LCA-assigned reads of cold spin extracts with PalaeoChip enrichments over alternative approaches. 41
Table S23 Summary of blank samples and map-filtering counts. 41

List of Figures, Appendix A

Figure S1 Bioanalyzer, high sensitive DNA assay, SET-A. 42
Figure S2 Bioanalyzer, high sensitive DNA assay, SET-A with a 1/10 dilution. 43
Figure S3 SET-A, indexing RFU bar chart for qPCR cycles 1 and 12. 44
Figure S4 SET-A, Inhibition indices of inhibitor clean-up strategies. 45
Figure S5 SET-A, Indexing qPCR reaction of positive control spiked extracts. 46
Figure S6 Components of the inhibition index. 47
Figure S7 Comparing treatments for enzymatic inhibitor removal by their DNA retention. 48
Figure S8 Conceptual balance of overcoming sedaDNA inhibitor co-elution. 49
Figure S9 QPCR indexing reaction to confirm correlation with short amp quantification. 49
Figure S10 Variable duration 4°C centrifuge on the carryover of enzymatic inhibitors and library adapted DNA 50
Figure S11 Total double stranded DNA with variable extract input and blunt-end repair (BER) enzymatic concentrations, SET-C. 51
Figure S12 Core BC 4-2B, variation in co-eluate inhibitor retention by lysing method and inhibitor removal procedure. 52
Figure S13 SET-D Variable lysis disruption and cold spin duration for core BC 4-2B. 53
Figure S14 Variable extract amplification of core LLII 12-217-8, *trn*L ‘endogenous’ qPCR. 54
Figure S15 Variable AmpliTaq Gold concentrations on *trn*L ‘endogenous’ sedaDNA qPCR amplifications. 55
Figure S16 DNA quantification of *trn*L specific library adapted molecules comparing both extraction methods by core 56
Figure S17 QPCR estimated starting concentration averages by extraction type and site for *trn*L metabarcoded extracts 57
Figure S18 Comparing LCA-assignments between Upper Goldbottom (MM12-118b) libraries map-filtered to the plant and animal baits, and those map-filtered to the plant references. 58
Figure S19 Comparing LCA-assignments between Bear Creek (BC 4-2B) libraries map-filtered to the plant and animal baits, and those map-filtered to the plant references. 59
Figure S20 Metagenomic comparison of Upper Goldbottom permafrost core MM12-118b, reads mapped to baits 60

Figure S21 Metagenomic comparison of Lucky Lady II permafrost core LLII-12-84-3, reads mapped to baits 61
Figure S22 Metagenomic comparison of Lucky Lady II permafrost core LLII-12-217-8, reads mapped to baits. 62
Figure S23 Metagenomic comparison of Lucky Lady II permafrost core LLII-12-84-3 with reads mapped to plant references, 1 of 2. 63
Figure S24 Metagenomic comparison of Lucky Lady II permafrost core LLII-12-84-3 with reads mapped to plant references, 2 of 2. 64
Figure S25 Metagenomic comparison of Lucky Lady II permafrost core LLII-12-217-8 with reads mapped to plant references, 1 of 1. 65
Figure S26 Metagenomic comparison of Bear Creek permafrost core BC 4-2B with reads mapped to plant references, 1 of 2. 66
Figure S27 Metagenomic comparison of Bear Creek permafrost core BC 4-2B with reads mapped to plant references, 2 of 2. C.....67
Figure S28 Metagenomic comparison of Upper Goldbottom permafrost core MM12-118b, all reads (not map-filtered), absolute counts.....68
Figure S29 Metagenomic comparison of Lucky Lady II permafrost core LLII-12-84-3, all reads (not map-filtered), absolute counts.....69
Figure S30 Metagenomic comparison of Lucky Lady II permafrost core LLII-12-217-8, all reads (not map-filtered), absolute counts.....70
Figure S31 Metagenomic comparison of Bear Creek permafrost core BC 4-2B, all reads (not map-filtered), absolute counts.....71
Figure S32 Metagenomic comparison of extraction and library blanks, all reads (not map-filtered), absolute counts, bubbles log-scaled. 72
Figure S33 Metagenomic comparison of the metabarcoding blanks from extraction, library preparation, and PCR map-filtered to the plant references (*rbc*L, *mat*K, *trn*L) 73
Figure S34 *MapDamage* plots for *Bison priscus* and *Mammuthus primigenius.* 74
Figure S35 *MapDamage* plots for *Lagopus lagopus* and *Equus caballus.* 75
Figure S36 *MapDamage* plots for *Poa palustris and Artemisia figida.* 76
Figure S37 *MapDamage* plots for *Salix interior* and *Picea glauca.*.....77
Figure S38 *MapDamage* MM12-118b merged replicates plot for *Mammuthus primigenius.*.....78

Figure S39 Histogram of fragment lengths for reads assigned to *Betula sp.* with enrichment and metabarcoding, as well those assigned to *Lupinus sp.* with enrichment for the Upper Goldbottom core (MM12-118b). 79

SET-A: Initial explorations

Our first set of experiments was intended to determine the best sedaDNA extraction strategy to compare shotgun and targeted enrichment sequencing strategies with previously sequenced PCR metabarcoding data collected by Sadoway (2014) on four Yukon sediment cores. However, SET-A informed us that inhibition was a substantial problem with these sediments using our typical in-house demineralization-digestion and Dabney et al. (2013) extraction protocol (hereafter referred to as Dabney), whereas the DNeasy PowerSoil DNA Extraction Kit (hereafter referred to as PowerSoil) only successfully recovered sedaDNA in one of the four cores (with a successful positive control amplification). We felt that this necessitated further experimentation to see if we could overcome enzymatic inhibition and library adapt our target environmental DNA (eDNA) molecules with a high DNA retention purification method. Permafrost core disks from two strata at Lucky Lady II as well as Bear Creek and Upper Goldbottom Creek (Figure 1, main text) were tested to compare a kit-based sediment DNA extraction strategy (PowerSoil) with our in-house Dabney extraction method.

SET-A. Extraction

Samples processed with PowerSoil were extracted following manufacturer specifications. Samples processed using Dabney were first subjected to a two-stage lysis buffer: 1) samples were demineralized in 1 mL of 0.5M EDTA, then rotated continuously for 18 hours at 25°C; 2) samples were then spun down, supernatants were removed, and a proteinase K buffer (Table S1) was added to the sediments to digest overnight at 25°C. The demineralization-digestion supernatants were extracted using a high-volume binding buffer and silica columns following Dabney et al.(2013).

SET-A. Bioanalyzer, inhibitor clean-up, and indexing

Straight and 1/10 diluted extracts were run on an Agilent 2100 Bioanalyzer as a high sensitivity DNA assay (see Figure S1 and Figure S2). Straight extracts from Dabney samples were darkly coloured and failed to produce a detectable DNA signal on the Bioanalyzer (the baseline was unable to be determined), which we suspected was indicative of abundant co-eluted substances that would adversely affect library preparation. We tested whether a 1/10 dilution or additional purification step prior to blunt end repair would sufficiently remove inhibitors for library preparation in the Dabney extracts, or whether the straight uninhibited PowerSoil extracts would perform better (Table S12). In a qPCR indexing reaction (Table S6) following double-

stranded library preparation (DsLp) (Meyer and Kircher, 2010; Kircher et al., 2012), only the positive controls and a single PowerSoil extract from Bear Creek clearly amplified (see Figure S3) despite all samples previously producing positive amplifications and sequence data with a PCR metabarcoding approach (Sadoway, 2014). We suspected that the Dabney extracts were highly inhibited rather than lacking in endogenous DNA. We also suspected that while the PowerSoil kit was effective at removing sedimentary inhibitors, it was ineffective at retaining the kinds of low abundance and highly degraded molecules characteristic of ancient DNA (aDNA).

SET-A. Inhibition, qPCR, and DsLp

In SET-A, a subset of straight extracts, 1/10 and 1/100 diluted extracts, as well as library adapted samples were spiked with the E^3 49 bp standard. Straight and 1/10 extracts prepared with Dabney were completely inhibited (see Figure S4). Even library adapted samples that had two purification steps and 1/100 diluted extracts were partially inhibited during the inhibition spike test. To determine whether these inhibitors were causing library preparation to fail, we spiked our positive control into each of the Dabney extracts and brought the samples through DsLp. The only samples with positive indexing qPCR amplifications were the positive control and the partially inhibited reaction from LLII 12-127-8 (see Figure S5). All other spiked reactions flatlined, which indicates that inhibition was a significant problem when attempting to bring these extracts into libraries using our in-house lysis and extraction techniques. Compared with the kit however, DNeasy PowerSoil was only sporadically successful at retaining sedaDNA despite all of these core samples previously having been found to contain ancient environmental DNA with PCR metabarcoding (D'Costa et al., 2011; Sadoway, 2014). Our follow-up set of experiments was designed to test various inhibitor removal treatments from the PowerSoil kit and other associated methods to minimize inhibition while maximizing the retention of sedaDNA with our in-house extraction protocols.

Most total DNA quantifications in SET-A to SET-D_2 used the short amplification primer sites on the library adapters and were compared against the same library prepared 49-bp oligo standard used in the spike tests (see below, also see Table S8). The total adapted DNA assay was also modified in some instances to quantify the 'endogenous' chloroplast constituent of adapted molecules by pairing the *trn*L P6-loop forward primer-g (Taberlet et al., 2007) with the reverse P7R library adapter primer (IS8, see Table S9). Enk et al. (2013) demonstrated that a single-locus qPCR assay can be used to predict on-target ancient DNA high-throughput sequencing

read counts. Previous analyses (D'Costa et al., 2011; Sadoway, 2014) indicated that ancient vegetation was the most consistently abundant fraction of the biomolecules in these cores, and as such could serve as a rough proxy for assessing aDNA retention for successfully library adapted molecules between various inhibitor removal strategies. For all qPCR results reported here, standard curve metrics are included in the associated captions. Ideal standard curve values are: $R^2 = 1$, slope = -3.3 (or between -3.1 and -3.5), efficiency = 90–105%.

SET-A. Inhibition Index

A positive control spike qPCR assay (King et al., 2009; Enk et al., 2016) was used to assess the relative impact of DNA independent inhibitors (co-eluted substances such as humics that inhibit enzyme function) on the enzymatic amplification efficiency of a spiked amplicon in the presence of template sedaDNA derived from variable lysing and extraction methods (Table S7, see also Figure S6). We suspected that enzymes in library preparation would be inhibited similarly to AmpliTaq Gold polymerase in qPCR. Shifts in the qPCR amplification slope of our spiked oligo with AmpliTaq Gold (due to co-eluted inhibitors in sedaDNA extracts) could then be quantified and used to infer the likelihood of failed adapter ligation due to enzymatic inhibitors (rather than a lack of sedaDNA). Admittedly, AmpliTaq Gold is not a 1:1 stand-in for inhibition sensitivity during blunt-end repair and adapter ligation, as AmpliTaq is among the most sensitive polymerases to inhibition induced reductions in amplification efficiency (Al-Soud and Radstrom, 1998), and due to qPCR specific inhibition such as the reduction in florescence despite successful amplification (Sidstedt et al., 2015). Our experiments do suggest that these enzymes have a very roughly commensurate inhibition sensitivity, insofar as eluates completely inhibited during this spike test are unlikely to successfully undergo library adapter ligation.

To quantify the co-eluted inhibition affecting each spiked amplification, we compared the qPCR slope of an oligo-spiked sedaDNA extract (1 µL of sample eluate spiked with 1 µL of a 49-bp oligo [1000 copies {E^3}], see Table S7) with the qPCR slope of 1 µL E^3 oligo standard in 1 µL of EBT. Average C_q and max relative fluorescence units (RFU) for each PCR replicate (processed in triplicates) were calculated, as was the hill slope of the amplification curve by fitting a variable-slope sigmoidal dose-response curve to the raw fluorescence data using GraphPad Prism v. 7.04 (based on King et al. [2009]). The E^3 oligo-spiked averages (C_q, RFU, and sigmoidal hillslope) were divided by the corresponding E^3 oligo standard amplification value, then averaged together to generate an 'inhibition index' per PCR replicate, which were

averaged again across PCR replicates to determine an extract's inhibition index, ranging from 0–1. In this case, 0 indicates a completely inhibited reaction (no measurable increase in RFU), and 1 indicates a completely uninhibited reaction relative to the spiked E^3 oligo-standard (see Figure S6). Anything above 0.9 (the bottom range for blanks and standards of differing starting quantities) is considered essentially uninhibited insofar as *Taq* polymerase inhibition is concerned (NOTE: Figure 4 [main text] / Figure S8 depicts inhibition as increasing from left to right on the x-axis, which is opposite of how the inhibition index is depicted).

SET-B: Comparing inhibition removal strategies

The second set of experiments tested the following inhibitor removal augmentations to a digestion and Dabney extraction protocol:

1) Physical disruption with PowerBeads (vortexing for 10 minutes) and a proteinase K digestion buffer (see Table S1) (proteinase K was added to each sample individually after vortexing so as to not damage the enzyme, but prior to overnight incubation with continuous oscillation) to release bound DNA.
2) The addition of solution C3 (120 mM aluminum ammonium sulfate dodecahydrate) from the PowerSoil kit prior to Dabney purifications to precipitate inhibitors (maintaining the 1/3 volumes of solution C3 to digest supernatant).
3) A 1 hour 4°C centrifuge at 3900 x *g* with the high-volume Dabney binding buffer in 50 mL tubes to precipitate inhibitors prior to DNA isolation.
4) Sonication with and without a post-sonication purification to disrupt bonds between inhibitors and 'endogenous' sedaDNA (Table S14).

Each combination of these inhibitor removal treatments was used on three cores, subsampled from homogenized triplicates. See Table S13 for the SET-B sample list. The extracts were assayed with a qPCR inhibition spike test (Table S7) then brought through DsLp and quantified using P5/P7 adapter primers (Table S8). A subset of these were also indexed to confirm that the qPCR indexing reaction correlates with our short amplification observations (Figure S9).

SET-B. Results and interpretations

The 4°C centrifuge samples (and sonicated derivatives) outperformed other inhibitor removal treatments in terms of DNA retention (Figure S7). All other treatment variations had low DNA retention, but frequently outperformed the 1 hour 4°C centrifuge variant in the inhibition spike test. Sonication and post-sonication purifications (to re-concentrate DNA) seemed to help with reducing polymerase inhibition in the qPCR spike test, but also resulted in DNA loss compared to their non-sonicated counterparts. The use of PowerSoil beads for physical

disruption resulted in visually clearer extracts and less inhibition than an EDTA based demineralization. Overall, the more treatments utilized, the less inhibition observed, but also the less DNA retained. Solution C3 from the PowerSoil kit was effective at reducing inhibition (both visually in terms of eluate colour retention and in the subsequent inhibition assay), but also resulted in substantial DNA loss. This may explain the results of SET-A where the PowerSoil kit was observed to be effective at removing DNA inhibition but had low DNA retention. The kit is effective with modern sediments and soils, but might precipitate tightly bound organo-mineral complexes (Haile, 2008, p. 18; Arnold et al., 2011, p. 418) in which sedaDNA is preserved. There seems to be an important balance between releasing enough DNA, but not releasing too many inhibitors, as well as removing enough inhibition for enzymatic reactions, while not removing the majority of the 'endogenous' sedaDNA (Figure S8). We also wanted to verify that our short amplification assay roughly correlates with amplification during the qPCR indexing reaction (Figure S9). In this assay we can see that sonication results in fewer adaptable molecules during indexing, which is a trend also apparent in the short amplification assay in Figure S6.

SET-C: Fine-tuning the cold spin

The only viable treatment from SET-B appears to be the 4°C spin. Our follow-up goal was to determine whether we could maximize the inhibitor removal of the spin at various timings, in this case testing 1, 6, and 19 hours (Table S15). We found that increasing the duration of the 4°C spin reduced the polymerase inhibition observed during the qPCR spike test (Figure S10), which correlated with higher quantifications following library adapter ligation (Figure S9). We also attempted to quantify 'endogenous' sedaDNA in extracts prior to adapter ligation using two chloroplast barcoding primer sets, *rbc*L-H1a/H1b (Poinar et al., 1998) and *trn*L P6-loop g/h (Taberlet et al., 2007). However, we found that even in extracts with an inhibition index of ~0.6–0.8 that these assays were uninformative for quantifying pre-DsLp DNA concentrations because the amplification curves were non-standard (the exponential and linear phases had shallower slopes [see Figure S6 for examples]). This was likely due to both DNA-dependent and DNA-independent inhibition. We found that varying the polymerase concentration dramatically changed the extract quantifications on chloroplast amplicons, which will be elaborated on further in section SET-D.

The final experiment with SET-C samples was to assess whether varying the extract input or enzymatic concentration during blunt-end repair (the first phase of DsLp) would affect the

total number of adapter ligated molecules between a highly inhibited sample (BC 4-2B) and an uninhibited sample (LLII 12-217-8) (Figure S11). While there was a reduction in the extraction range of total quantified DNA between replicates of the inhibited core (BC 4-2B) using double the blunt-end repair enzymatic concentrations (T4 polynucleotide kinase and T4 DNA polymerase, see Table S3 for standard concentrations), the effect was marginal. There was also no improvement in halving the extract input in terms of reducing inhibition load on the blunt-end repair enzymes beyond reducing the total adapted DNA by half. Increasing blunt-end repair enzyme concentrations is only recommended for critically important samples where the additional cost is not a concern, as our results suggest that the improvement is marginal.

SET-D: Optimizing our modified Dabney extraction protocol

This final optimization experimental set was intended to fine-tune components of our modified Dabney protocol (Table S16). We wanted to determine whether a physical disruption with PowerBeads is necessary, or if a straight digestion or combined demineralization and digestion buffer is best for releasing sedaDNA (SET-B led us to suspect that EDTA might be releasing too many inhibitors). We also wanted to determine whether the duration of the lysis stage was significant, so 6- and 19-hour lysis variants were tested. Finally, we were interested whether increasing the 4°C spin to two days would plateau our inhibition removal procedure, or if we could further improve the amount of library adapted molecules in highly inhibited cores without losing 'endogenous' sedaDNA. Part-way though this experiment, we also discovered an interesting (initially, admittedly, very frustrating) variable effect on inhibitor retention linked to the lysis detergent. For the first set of samples (SET-D_1) sarkosyl was used as the detergent during lysis instead of SDS. Once this unintended reagent change was discovered (after a series of experiments where the long cold spin was unexpectedly no longer removing inhibition in our most inhibited core sample, BC 4-2B) a second set of homogenized subsamples was taken (SET-D_2) for our highly inhibited core where we switched back to SDS as the lysis detergent. We also conducted tests to quantify 'endogenous' chloroplast sedaDNA on extracts (prior to DsLp) from SET-C and -D samples (as alluded to in section SET-C). However, we are unsatisfied with these assays on purified extracts as they still contain co-eluted inhibition (likely both DNA independent and dependent inhibitors), and as such remain unconvinced by their quantifications. Further work developing these specific extract assays (by improving florescence detection,

improving inhibition removal, increasing polymerase concentrations, or by size selecting out 'viable' DNA fragments) is recommended.

SET-D. Results and interpretations

SET-D experiments yielded five results of interest as observed in Figure S12. First, in column I, there is some indication that increasing the duration of lysis from 9 hours to 19 hours increases inhibitor release (likely as well as DNA release). Inhibitors were not effectively removed during the long cold spin in this instance as sarkosyl appears to be an ineffective detergent to pair with this inhibitor removal technique. This is the only glimpse we observed into the variation of lysis time spans. The optimal interval for our workflow is 19 hours (leaving the samples to oscillate overnight at 35°C). The long cold spin is effective at removing additional inhibition when paired with SDS as observed with columns IV and V in Figure S11. We did not investigate variation in lysis period further as 19 hours is most effective with our workflow and has higher DNA release (as observed in SET-E in the main paper).

Second, the proteinase K buffer with sarkosyl—without either EDTA for demineralization or PowerBeads for physical disruption—has the lowest inhibitor retention (inhibition indices $\gtrsim$0.9) as observed in column II. However, subsequent experiments (detailed in the last SET-D subsection) found that this method also has the worst DNA release.

Third, the detergent used during lysis makes a significant difference in inhibitor retention. All extraction replicates of the inhibited core (BC 4-2B) lysed with the detergent sarkosyl in the proteinase K buffer (with a PowerBead disruption) remain highly inhibited (all failed the inhibition spike test) despite the 4°C inhibition precipitation spin as observed with the inhibition indices in columns III. This is starkly contrasted with column IV where the only experimental change was the use of SDS in the lysing buffer rather than sarkosyl. This was also visually observed in the sarkosyl samples with the lack of a 'dark inhibitor pellet' following the cold spin and much more darkly stained silica-columns and brown-to-black eluates. Our hypothesis for this detergent interaction is detailed in the subsequent SET-D subsection *SDS and sarkosyl*.

Fourth, columns IV and V have equivalent inhibition indices. Subsequent library preparations and short amp quantifications found that increasing the cold spin to 48 hours does slightly increase adapter ligated DNA for both methods (Figure S12). Further, EDTA and

PowerBeads as a means of disrupting organo-mineral sedaDNA complexes have roughly equivalent DNA yields, but PowerBeads do release more DNA on average.

Fifth, there appears to be a saturation point for inhibitor removal (at least qPCR polymerase sensitive inhibitors) after approximately 24 hours with the cold spin with our current reagent concentrations. The cold spin at 48 hours show no difference in inhibition indices. This could potentially be modified with higher concentrations of SDS (discussed further in the following subsection on SDS), but this variant was not tested in our optimizations.

SET-D. SDS and sarkosyl

The most unexpected result of this project was the effect of unintentionally switching detergents on inhibitor precipitation during the 4°C spin. While there is some degree of precipitation during cold centrifugation with a sarkosyl lysing buffer, or even when spinning low-volume purified extracts at room temperature prior to adapter ligation, the marked increase in precipitation with SDS is visually distinct with thick inhibitor pellets forming during the 4°C spin. SDS (sodium dodecyl sulfate) is an anionic surfactant. Surfactants form self-aggregates (micelles) as their concentration increases (Tanford, 1980). These micelles arrange to have exterior hydrophilic heads, and interior hydrophobic tails. Typically, surfactants are present in submicellar concentrations, but these self-aggregate structures can form at sufficiently high concentrations, particularly with constant mixing. Micelles can also co-aggregate with other amphiphilic compounds (those with hydrophobic and hydrophilic domains) such as humic substances (Otto et al., 2003; Koopal et al., 2004), which we suspect is one of the main DNA independent inhibitors in these sediments due to dark colouration (Alaeddini, 2012). SDS precipitates at 4°C and calcium has been found to increase the precipitation of SDS micelles. We hypothesize that our cold spin with high guanidinium concentrations and SDS based digestion buffer (also containing $CaCl_2$ intended for improving proteinase K efficiency) might have created some form of optimal conditions for micelle formation and the subsequent precipitation of humics and other amphiphilic compounds that bound to SDS micelles. It is also possible that pH is involved in humic acid solubility and is affecting this precipitate reaction (Shaban and Mikulaj, 1998), or that proteins also play some role (Schlager et al., 2012), potentially as related to disentangling sedaDNA from its protective organo-mineral complex (Greaves and Wilson, 1969; 1970; Lorenz and Wackernagel, 1987; Ogram et al., 1988; Taylor and Parkinson, 1988; Bezanilla et al., 1995; Blum et al., 1997; Crecchio and Stotzky, 1998; Khanna et al., 2005;

Cleaves et al., 2011). The interaction we have observed here would be of benefit for investigation to further improve the purification of palaeoenvironmental DNA. It is likely that components of the binding or lysing buffers, mixing strategy, or temperature could be tweaked further to improve inhibitor precipitation, thus increasing sedaDNA yield from highly inhibited materials.

SET-D. Chloroplast assay of 'purified' extracts with variable Taq

As discussed in section SET-C, we had intended to test 'endogenous' cpDNA retention and release through our procedure before and after library preparation. However, we found that this assay, either with *rbc*L or *trn*L primers, was not a reliable means of assessing 'endogenous' sedaDNA retention through our inhibition removal technique or library adapter ligation efficiency. We found that even our uninhibited core (LLII 12-217-8) had inconsistent DNA quantifications (Figure S15), largely due to non-standard (shallow) amplification slopes affecting the starting quantity metric in our qPCR assay. It is possible that co-eluted humics not removed during the cold-spin may impact florescence detection with these qPCR assays on extracts (Sidstedt et al., 2015), in addition to directly affecting the polymerase. We found substantial quantification increases when doubling *Taq* concentrations (Figure S14). Despite the overall unreliability of these extract assays however, there are two important pieces of information that can be gleaned. First, there is almost no DNA release during lysis when utilizing just a proteinase K digestion buffer with sarkosyl—meaning, without EDTA or physical disruption from PowerBeads. This complete lack of amplifiable DNA rules out column II (Figure S12) as a viable extraction strategy. We found the least inhibition with this method-core combination (both in terms of its inhibition indices [Figure S15] and visually non-coloured elutes). Second, despite the qPCR inhibition assay detecting minimal inhibition in this core overall with any method, there is still some sort of inhibition in the extracts affecting the efficiency of AmpliTaq Gold polymerase. This might indicate that while this sample has low DNA independent inhibition (humics and other enzymatically inhibitory substances) that do not impact the amplification of spiked, undamaged synthetic amplicons, this sample likely has high DNA dependent inhibition (See Figure 4, main text). Meaning, there might be substantial aDNA damage (such as blocking lesions) or an abundance of extremely short molecules that the *Taq* polymerase is either getting stuck on or stuck amplifying repeatedly, which ultimately leads to poor florescence. This core also had the lowest DNA recovery (see Table 1 [main text] and Figure S16), which when paired

with this assay, suggests that the sedaDNA in this core is more fragmentary and damaged than the other permafrost samples.

Potentially spiking lysing buffers with a known quantity of aDNA sized and damage characteristic non-target DNA, then assaying those synthetic molecules after library preparation with a dual adapter/synthetic target-specific primer set (such as described in Table S9), would be a more reliable means of assessing DNA loss from the cold spin and DNA independent inhibitor effects on library preparation efficiency. However, this assay would not assess DNA dependent inhibition specific to the sedaDNA constituents of the sample. The polymerases used in qPCR amplifications are not directly equivalent to those used in library preparation. Extracts or libraries with florescence inhibition (Sidstedt et al., 2015) might yet be amenable to adapter and indexing ligations, as well as potentially sequencing, but be largely undetectable with *Taq* based qPCR assays unless the reaction is maximally saturated with polymerase to mitigate various forms of inhibition. While potentially feasible with small sample-sets, this strategy would be costly, and likely difficult to standardize across highly variable molecular constituents even within the 'same' homogenized sedimentary sample (however 'homogenized' a sediment sample could be on a molecular scale).

SET-E: Additional data for main-text experiment.

This section reports on details not included in the main-text, including: PalaeoChip Arctic-1.0 bait design and enrichment wet-lab procedures, metabarcoding parameters, a comprehensive bioinformatic workflow, and other supplementary data of use for evaluating the main-text experiment.

SET-E. Enrichment: PalaeoChip bait-set design and wet lab procedures.

The PalaeoChip Arctic-1.0 hybridization enrichment bait-set was designed in collaboration with Arbor Biosciences (where they will be available for purchase) to target whole mtDNA of extinct and extant Quaternary animals (focused primarily on megafauna; number of taxa ≈ 180), and high latitude plant cpDNA based on curated reference databases developed by Sønstebø et al. (2010), Soininen et al. (2015), and Willerslev et al. (2014), initially targeting *trn*L (n ≈ 2100 taxa) (see Appendix B for taxonomic list). This list was queried with the *NCBI Mass Sequence Downloader* software (Pina-Martins and Paulo, 2015) to recover additional nucleotide data from GenBank (Benson et al., 2018) for *trn*L, as well as adding targets for *mat*K and *rbc*L. These three regions were selected as they are among the most sequenced and taxonomically

informative portions of the chloroplast genome (Hollingsworth et al., 2011). Baits were designed in collaboration with Arbor Biosciences to 80 bp with ~3x flexible tiling density, clustered with >96% identity and >83% overlap, and baits were removed with >25% soft-masking (to reduce low complexity baits with a high chance of being off-target in complex environmental samples). Bait sequences were queried with *BLASTn* against the NCBI database on a local computer cluster using a July 2018 database, then inspected in *MEGAN* (Huson et al., 2007; 2016). Baits with a mismatched taxonomic target and *BLASTn* alignment were queried again using a web-blast script (Camacho et al., 2009; NCBI Resource Coordinators, 2018) to determine if these mismatches were due to local database incongruities with the web-based NCBI database. Mismatches were again extracted with *MEGAN*, individually inspected, then removed from the bait-set if determined to be insufficiently specific.

Enrichment Wet lab. Hybridization and bait mixes were prepared to the concentrations in Table S11. For each library, 7 µL of template was combined with 2.95µL of Bloligos (blocking oligos which prevent the hybridization between library adapter sequences). The hybridization and bait mixes were combined and pre-warmed to 60°C, before being combined with the library-Bloligo mixture. The final reaction was incubated for 24 hours at 55°C for bait-library hybridization.

The next day, beads were dispensed (540 µL total between two tubes), washed three times with 200 µL of binding buffer for each tube, then suspended in 270 µL of binding buffer per tube and aliquoted into PCR strips. Baits were captured using 20 µL of the bead suspension per library, incubated at 55°C for 2.5 minutes, finger vortexed and spun down, and incubated for another 2.5 minutes. Beads were pelleted and the supernatant (the non-captured library fraction) was removed and stored at −20°C. The beads were resuspended in 180 µL of 55°C Wash Buffer X and washed four times following the MYbaits V4 protocol. Beads were eluted in 15 µL EBT, PCR reamplified for 12 cycles (Table S6), then purified with MinElute columns following manufacturer's protocols in 15 µL EBT.

SET-E. Sadoway (2014) PCR metabarcoding

Extensive inhibition was observed in the extracts at the time (Sadoway, 2014, p. 8), which was detected using similar qPCR spike tests (see Appendix A, section 'SET-A. Inhibition Index') developed by King et al. (2009), This necessitated a tenfold extract dilution, which were

then amplified in duplicate for each primer set, targeting: *rbc*L (Willerslev et al., 2003; CBOL Plant Working Group, 2009; Hollingsworth, 2011), *trn*L (Taberlet et al., 2007), *16S rRNA* (Höss et al., 1996), *and 12S rRNA* (Kuch et al., 2002), each following cited PCR conditions. The locus *cytochrome b* (*cyt-b*) was also targeted using a set of degenerate primers designed with FastPCR (Kalendar et al., 2011; Sadoway, 2014). *Cyt-b* amplifications were found to be most efficient in 20 µL reactions using AmpliTaq Gold (0.05U/µL), 1X PCR Buffer II, 2.5 mM MgCl2, 0.25 mM dNTPs, 0.5X Evagreen, 250 nM (forward/reverse primers) when cycled with a 3 minute denaturation at 95°C, 45 cycles of 95°C for 30 seconds, and 60°C for 30 seconds (Sadoway, 2014). QPCR products were purified with 10K AcroPrep Pall plates (Pall Canada Direct Ltd., Mississauga, ON, Canada) using a vacuum manifold. QPCR assays were used to pool each amplicon set in equimolar concentrations, which were library prepared and dual-indexed following the same Illumina protocols as described above (Meyer and Kircher, 2010; Kircher et al., 2012). Samples were sequenced on a HiSeq 1500 Rapid Run (2 x 100bp, Illumina Cambridge Ltd, Essex, UK) at the Farncombe Metagenomics Facility (McMaster University, ON) to an approximate target depth of 100,000 reads each.

SET-E. PCR metabarcoding trnL

Components of the *trn*L metabarcoding reaction are detailed in Table S17. Each extract was run in PCR triplicates, and purified using a 10K AcroPrep Pall plate and vacuum manifold in a post-PCR facility. Each well of the AcroPrep membrane was prewet with 50 µL EB and the vacuum was applied for ~10 minutes until almost dry. Post-PCR products were mixed with 100 µL EB per well, added with a multichannel pipette to the AcroPrep plate, and the vacuum manifold was applied until dry (~10 minutes). Wells were washed with another 100 µL EB and vacuumed until dry. 17 µL EBT was added per well and the plate was gently vortexed for 30 minutes. Each well was mixed thoroughly via pipetting, then extract wells were combined to make a single metabarcoded extract from the PCR triplicates for a final volume of ~50 µL. QPCR DNA concentration estimates are reported in Figure S17. Thereafter, these extracts were library prepared identically to the other samples, but all in a post-PCR facility.

SET-E. Bioinformatic workflow

Reads from all library sets (enriched, shotgun sequenced, and PCR metabarcoded) were demultiplexed with *bcl2fastq* (v 1.8.4), converted to bam files with *fastq2bam* (https://github.com/grenaud/BCL2BAM2FASTQ), then trimmed and merged with *leeHom*

(Renaud et al., 2014) using ancient DNA specific parameters (--ancientdna). Reads were then either aligned to a concatenated reference of the animal and plant probes or to a concatenated reference of just the plant target sequences with *network-aware-BWA* (Li and Durbin, 2009) (https://github.com/mpieva/network-aware-bwa) with a maximum edit distance of 0.01 (-n 0.01), allowing for a maximum two gap openings (-o 2), and with seeding effectively disabled (-l 16500). Mapped reads that were merged or unmerged but properly paired were extracted with *libbam* (https://github.com/grenaud/libbam), collapsed based on unique 5' and 3' positions with *biohazard* (https://bitbucket.org/ustenzel/biohazard), and restricted to a minimum length of 24 bp. Mapped reads were string deduplicated using the *NGSXRemoveDuplicates* module of *NGSeXplore* (https://github.com/ktmeaton/NGSeXplore), then queried with *BLASTn* to return the top 100 alignments (-num_alignments 100 -max_hsps 1) against a July 2018 version of the NCBI Nucleotide database on a local computer cluster. Libraries that were not map-filtered to our reference targets (either with the baits or original plant references) were treated identically, although only returned the top 10 alignments to mitigate unwieldy (>20 gb) file sizes. Sequencing summary counts are in Table 1 of the main text.

Blast and fasta files for each sample (unmapped and mapped variants) were passed to *MEGAN* (Huson et al., 2007; 2016) using the following LCA parameters: min-score = 50 (default), max expected (e-value) = 1.0E-5, minimum percent identity = 95% (allows 1 base mismatch at 24 bp, 2 at 50 bp, and 3 at 60 bp to account for cytosine deamination and other aDNA characteristic damage or sequencing errors), top percent consideration of hits based on bit-score = 15% (allows for slightly more conservative taxonomic assignments than the 10% default based on trial and error), minimum read support = 3 or 8 (number of unique reads aligning to an NCBI sequence for that taxon to be considered for LCA, 3 used when mapping to the animal and plant baits, 8 when mapping to the plant references), minimum complexity = 0.3 (default minimum complexity filter), and utilizing the LCA weighted algorithm at 80% (two rounds of analysis that purportedly increases taxon specificity but doubles run time over the native algorithm). Metagenomic profiles were compared in *MEGAN* using absolute read counts. Libraries were not subsampled to an equal depth prior to processing; McMurdie and Holmes (2014) have demonstrated that this rarefying approach is the most ineffective means of accounting for unequally sequenced metagenomic data. Instead, we logarithmically scaled our bubble charts to visually normalize between samples proportionally but retained raw read counts.

There are more sophisticated (and arguably fairer) means of normalizing unequally sequenced libraries, but we feel that this approach does visually normalize well between such variable methodological variants, and streamlines effectively with the *MEGAN* software.

SET-E. Map-filtered to animal and plant baits.

To visualize the taxonomic variability between these replicates, comparative trees in *MEGAN* were summed to the rank of 'order'; animalia was then fully uncollapsed (as the read counts were more manageable compared with plant assignments). Viridiplantae clades were collapsed to higher ranks (higher than 'order') in some cases for summarized visualizations (otherwise there were too many leaves to display at once in a single figure, even when only showing summaries by 'order'). Thereafter, all leaves were selected and visualized with logarithmically scaled bubble charts; additional higher LCA-assigned animalia ranks were also selected where taxonomically informative (for example, reads that could only be conservatively LCA-assigned to Elephantidae or *Mammuthus sp.*, but which in this context likely represent hits to *Mammuthus primigenius* [woolly mammoth]). Low abundance (<3 reads), non-informative and non-target clades (e.g. bacteria, fungi, or LCA-assignments to high ranks) were excluded for visualization purposes.

SET-E. Map-filtered to plant reference sequences.

For the bubble charts mapped to the plant references, the same procedures were followed, although the LCA stringency was increased from a minimum of three unique reads to eight. These libraries were mapped to the plant references to reduce the potential false negatives that might result from the metabarcoding data not mapping well to 80 bp probes. We found that when comparing these two map-filtering strategies, metabarcoded libraries had fewer taxa identified when mapping to the baits compared with mapping to the original plant references (see Figure S18 and Figure S19), which might unfairly bias the data against a metabarcoding approach. To address this limitation, we map-filtered the follow-up *trn*L metabarcoding comparison to the original plant references. We observed that all libraries had increased read counts when using a less restrictive map-filtering strategy.

Probable false positives (e.g. clades with a solely tropical distribution) were excluded from LCA-assignment. This was done to reduce the possibility of database incompleteness (somewhat closely related but as yet unsequenced organisms, either currently present in the

target region or having been extirpated from Beringia), compounded by genetic conservation and/or convergence, driving off-target identifications. See Methods, subsection 10 in the main paper for a discussion of 'oasis taxa' and the problems of false positives and negatives. Our approach of manually removing 'nonsensical' organisms presumes that distributions of plants are roughly comparable to how we have observed them in recent history or through palaeoecological proxies, which is of course a false assumption. These false positive identifications are likely the result of database incompleteness combined with taxonomically non-specific genetic regions, post-mortem DNA modifications, and imperfect alignments. False positives can be somewhat mitigated by using a highly curated local reference database for taxonomic assignment rather than the entire NCBI database, but this also succumbs to *a priori* limitations where one will only find organisms that they intend to find, resulting in false negatives and potentially an over-confidence in taxonomic identifications due to a reverse 'oasis' effect. There is no perfect solution, but we believe our approach strikes a reasonable enough balance to fairly compare between methods here. In retrospect, using a regionally curated, or at least non-redundant *BLAST* database combined with map-filtering to the target organisms (rather than to the baits, or perhaps to the baits but with reference padding to aid with *bwa* mapping) may have been a better approach. Also, the strategy reported by Cribdon et al. (2020) is likely of particular use in similar shotgun or target enriched libraries moving forward, as is increasing *BLAST* top hits to 500 or more.

SET-E. MapDamage.

Taxa with high blast and LCA-assigned read-counts were selected to evaluate damage patterns and fragment length distributions (FLD) (see Table S19 and Figures S33–S37). Enriched libraries were mapped to reference genomes of either the LCA-assigned organism itself (e.g. *Mammuthus primigenius*) or a phylogenetically closely related organism (e.g. *Equus caballus*) if there was no species call or if a reliable reference genome for the probable ancient organism does not yet exist. Mapping followed the aforementioned parameters and software, with an additional map-quality filter to ≥ 30 with *samtools* (https://github.com/samtools/samtools) and passed to *mapDamage* (Jónsson et al., 2013) (v 2.0.3, https://ginolhac.github.io/mapDamage/). Plant chloroplast DNA references were reduced to the target barcoding loci (*trn*L, *rbc*L, and *mat*K), each separated by 100 Ns. Mitochondrial reference genomes were used for animal taxa of interest.

SET-E. Stringent LCA filtering for unexpected taxa

Pine. For sample SET269-MB and a concatenation of samples SET268-En, 269-En, and 270-En, LCA-assignments to *Pinus sp.* are retained (245/545 and 10/42 respectively) when web-*BLASTing* to the top 5000 hits and increasing the *MEGAN*-LCA stringency to 100% identity, a top bit-score consideration of 40%, maximum e-score of 1.0E-8, and minimum 90% read coverage.

Mammoth and horse. LCA-assigned mammoth (n=41) and horse (n=10) reads from the Upper Goldbottom core (~9700 cal yr BP, Figure 4) were extracted, concatenated, and queried with the web-based *BLASTn* to the top 20,000 hits on the NCBI GenBank nuceotide database to assess the reliability of their taxon assignments. LCA parameters were increased to 100% identity and 25% top bit-score consideration. With these more stringent parameters and effectively unlimited alignment references, 3 reads were LCA-assigned to *Mammuthus primigenius, 25 to Mammuthus sp.*, and 11 were identified as Elephantidae. *Equus sp.* retained 5 assigned reads.

SET-E. Other additional data.

. The following list details the additional SET-E data included in this appendix.

1. Map-filtering reference comparisons: Figures S18–S19.
2. Bait-mapped bubble chart extension from main text: Figures S20–S22.
3. Plant metabarcoding (*trn*L) bubble chart extension from main text, Figures S23–S27. A list of 'disabled' taxa in MEGAN is included in Table S18.
4. Non map-filtered comparison of enriched, shotgun, and Sadoway metabarcoding samples: Figures S28–31.
5. Blanks comparison, non map-filtered: Figure S32; Metabarcoding blanks bubble chart, mapped to plant references: Figure S33. See also Table S23 for blank sample summaries.
6. *mapDamage* plots: Figures S34–38. See also Table S19 for *bwa* mapped reference counts.
7. A summation of major clade *MEGAN* LCA-assignments from the main text: Tables S20 and S21.
8. A summary of fold-increases in LCA-assigned DNA comparing the cold spin enriched libraries with alternative approaches: Table S22.
9. Histogram of FLDs between *trn*L metabarcoding and enriched hits to *Betula sp:* Figure S39.

Non map-filtered variants of the enriched, shotgun, and Sadoway metabarcoding samples are included as Figures S28–S31. These were generated identically to the metagenomic bubble charts in the main text, except only the top 10 alignments (rather than top 100) were kept for the non-map filtered blasts to reduce unwieldy file sizes. This is potentially problematic as false-

positives have a higher chance of aligning with so few top hits (due to over-representation of well studied taxa when using the public NCBI nucleotide database); these non-map filtered charts should be interpreted with measured skepticism. Only major prokaryotes are depicted, and within the eukaryotes, only chordates and Viridiplantae shown (to be able to visualize these comparisons relatively succinctly). Additional potentially 'authentic' sedaDNA taxa are identified in the non-map filtered bubble charts. However, most of these potentially authentic taxa are in the curated baits (such as moose, *Alces alces*). So, either 1) those taxa are identified with nuclear or otherwise non-target genetic loci, 2) those reference sequences regions had been clustered or masked in the curated baits (due to being relatively non-specific), which is why they did not map during initial filtering, or 3) the low top alignments (10 versus 100) resulted in less conservative LCA-assignments when not map-filtering the reads, which is why they are not present in the map-filtered, top 100 hits comparison. They might align well to moose (in this example), but also align relatively well to other cervids. This may be why in the map-filtered variant where more top hits are retained, the LCA more conservatively classifies these reads at a higher (less informative) taxonomic rank (e.g. Cervidae or Pecora). It is also worth noting that common sequencing contaminants and adapter-contaminated genomes on NCBI (e.g. camel, carp, wheat) remain in the non-map filtered metagenomic profiles despite attempts to filter out adaptamers (chimeric adapter sequences created during PCR)—whereas these problematic hits are filtered out early in processing by map-filtering. These false positives inflate the read counts in the non-mapped comparisons, particularly with taxa collapsed at such high ranks to allow for the entire metagenomic profile of each core to be easily visualized. These problems make all of the bubble charts for the non map-filtered libraries seem identical; however, this is certainly not the case when carefully observing the reads and their alignments by taxon node in *MEGAN*. For this reason, the non map-filtered comparisons are of minimal interpretive utility overall.

The false positive problem is most obviously apparent with the non map-filtered shotgun data (Figures S28–31). These shotgun samples appear to recapitulate much of the same ecological profile with plant clades collapsed at high taxonomic ranks. This is in part due to an over-abundance of probable false positives, but also reads aligning to regions of the chloroplast and nuclear genomes with few available reference sequences to discriminate between taxonomically specific and deeply conserved loci (in part due to the 'oasis' reference problem as discussed in the main text in reference to Cribdon et al. [2020]). The chloroplast loci *trn*L, *rbc*L,

and *mat*K were selected for targeting (and map-filtering) because of the abundance of reference data available for a wide variety of plants in these loci (particularly arctic species) as a result of concerted barcoding efforts (Sujeevan and Paul, 2007; CBOL Plant Working Group, 2009; Hollingsworth, 2011). But as the huge discrepancies between shotgun data illustrate—insofar as having almost no data when map-filtered to barcoding loci, versus tens of thousands of aligned reads in the non-mapped variants—loci amenable to barcoding efforts constitute an extremely tiny proportion of the nuclear and organelle genetic material released by plants and other organisms into the environment. Despite constant cellular shedding, a tiny fraction of DNA avoids being metabolized by bacteria, incorporated into microbial genomes, or otherwise degraded through a range of chemical and physical processes. Those few surviving molecules (likely far less than 1%) are subsequently preserved through mineral binding and other processes for a time, making them amenable to sedaDNA research. But with eDNA release and rare preservation mechanisms, very few molecules survive overall; fewer still are represented in extant genetic reference databases, fewer are targeted by our baits, and even fewer still can be detected by metabarcoding. Surely much of this shotgun data has utility as the same broad taxonomic trends are observed without any targeting. And this will increasingly be the case moving forward as reference databases are expanded to include genomic-level data from many more species. But at this time, it is difficult to authenticate many of these reads when they only have a handful of hits to poorly sequenced regions of the nuclear genome. These shotgun samples illustrate that a bait-set including a broader suite of informative nuclear and organelle loci (along with a robust regional reference database for expected taxa) is likely to be one of the next best steps when designing a targeting strategy to make full use of the sedimentary genetic archives available for Quaternary research. Currently, it is difficult to trust most of these shotgun reads when they do not map to our curated reference data and contain very few (1-3) *BLAST* hits.

Tables

Table S1 Final concentrations of components in the proteinase K digestion solution.

Proteinase K Digestion Solution	
Component	Final Concentration
Tris-Cl (pH 9.0)	0.02 M
SDS	0.5 %
Proteinase K	0.25 mg/ml
CaCl2	0.01 M
DTT	100 mM
PVP	2.5 %
PTB	5 mM

Samples were digested overnight at 35°C with rotation. Nanopure Barnstead water was used to bring up the volume to the desired concentration. Concentrations based on Karpinski et al. (2016). For samples where sarkosyl was used instead of SDS, the final detergent concentration was unchanged.

Table S2 Final concentrations of components in the Dabney binding buffer.

Dabney Binding Buffer	
Component	Final Concentration
Guanidine Hydrochloride	5 M
Isopropanol (100%)	40 %
Tween-20	0.05 %
3 M Sodium Acetate (pH 5.2)	0.09 M

Nanopure Barnstead water was used to bring up the volume to the desired concentration. Concentrations based on Dabney et al. (2013).

Table S3 Final concentrations of components in the blunt-end repair mixture.

Blunt-End Repair Mixture	
Component	Final Concentration
NE Buffer 2.1	1X
DTT	1 mM
dNTP mix	100 µM
ATP	1 mM
T4 polynucleotide kinase	0.5 U/µL
T4 DNA polymerase	0.1 U/µL

A final volume of 40 µL was used for the mixture and template DNA. Nanopure Barnstead water was used to bring up the volume to the desired concentration.

Table S4 Final concentrations of all components in the adapter ligation mixture.

3. Adapter Ligation Mixture	
Component	Final Concentration
T4 DNA Ligase Buffer	1X
PEG-4000	5%
Adapter Mix	0.5 µM
T4 DNA Ligase	0.125 U/µl
2. Adapter Mix	
IS1_adapter_P5.F	200 µM
IS2_adapter_P7.F	200 µM
IS3_adapter_P5+P7.R	200 µM
Oligo Hybridization Buffer	1X
1. Oligo Hybridization Buffer	
NaCl	500 mM
Tris-Cl, pH 8.0	10 mM
EDTA, pH 8.0	1 mM

Oligo Hybridization Buffer was prepared prior to the Adapter Mix, which was prepared separately for IS1_adapter_P5.F and IS2_adapter_P7.F. These two mixes were then combined after an incubation at 95°C for 10 seconds, and a ramp from 95°C to 12°C at a rate of 0.1°C/sec. A final volume of 40 µl was used for the mixture and template DNA. Nanopure Barnstead water (not listed) was used to bring the volume up to the desired concentration.

Table S5 Final concentrations of components in the adapter fill-in mixture.

Adapter Fill-In Mixture	
Component	Final Concentration
ThermoPol Reaction Buffer	1X
dNTP Mix	250 µM
BST Polymerase (large fragment)	0.4 U/µl

A final volume of 40 µl was used for the mixture and template DNA with the addition of Nanopure Barnstead water to bring the mix up to the desired concentration and volume.

Table S6 Primer sequences, PCR master mix, and cycling protocol for indexing amplification.

Indexing PCR Master Mix			
Component		Final Concentration	
KAPA SYBR®FAST qPCR Master Mix (2X)		1X	
Forward primer		750 nM	
Reverse primer		750 nM	
Primer Sequences			
Forward Primer	AATGATACGGCGACCACCGAGATCTACAC***NNNNNNN***ACACTCTTTCCCTACACGACGCTCTT		
Reverse Primer	CAAGCAGAAGACGGCATACGAGATTAT***NNNNNNN***ACTGGAGTTCAGACGTGT		
Indexing PCR Protocol			
Phase	Temperature (°C)	Time	Cycles
Initial Denaturation	98	3 min	
Denaturation	98	20 sec	Repeated for 8-12 cycles
Annealing	*60*	*20 sec*	
Extension	72	25 sec	
Final Extension	72	3 min	

The N in each primer sequence represents the 7 bp index specific to each primer. A final reaction volume of 40 µl was used for the assay, with 12.5 µl of the adapter ligated DNA libraries. Nanopure Barnstead water (not listed) was used to bring the volume up to the desired concentration.
Fluorescence readings were recorded post-annealing as indicated above with asterisks.

Table S7 Inhibition spike test qPCR assay.

PCR Master Mix			
Component	Final Concentration		
10X PCR Buffer II	1X		
MgCl2	2.5 mM		
dNTP mix	250 µM		
BSA	1 mg/ml		
Forward primer (971)	0.25 µM		
Reverse primer (1040)	0.25 µM		
EvaGreen	0.5X		
AmpliTaq Gold	0.05 U/µL		
Oligo	Sequence (5'–3')		
Forward primer (971_Mamm_Fwd)	CCCTAAACTTTGATAGCTACC		
Reverse primer (1040_Mamm_Rev)	GTAGTTCTCTGGCGGATAGC		
Double stranded 49 bp amplicon based on the mammoth *12S* mitochondrial gene	CCCTAAACTTTGATAGCTACCTTTACAAAGCTATCCGCCAGAGAACTAC		
Input*	Volume		
PCR master mix	8 µL		
sedaDNA extract template	1 µL		
49 bp amplicon spike	1 µL		
PCR Protocol			
Phase	Temperature (^{o}C)	Time	Cycles
Initial Denaturation	95	5 min	
Denaturation	95	30 sec	Repeated for 50 cycles
Annealing	54	30 sec	
Extension	**72**	50 sec	
Final Extension	72	1 min	
Melt Curve	**55–95**	**5 sec per degree**	

*Sample wells = 1 µL template + 1 µL spike. QPCR standard wells = 1 µL spike, 1 µL 0.1X TE. Non-template controls = 2 µL 0.1X TE.

**Fluorescence readings were recorded post-annealing and during the melt curve as indicated above with asterisks.

Assay from Enk et al. (2016).

Nanopure Barnstead water was used to bring the master mix up to the desired concentration and volume.

Table S8 Library adapted short amp total quantification PCR.

PCR Master Mix			
Component	Final Concentration		
KAPA SYBR®FAST qPCR Master Mix (2X)	1X		
Forward primer	0.2 µM		
Reverse primer	0.2 µM		
Oligos	Sequence (5'–3')		
Forward primer (ILPr_shortampP5F_MeyerIS7)	ACACTCTTTCCCTACACGAC		
Reverse primer (ILPr_shortampP7R_MeyerIS8)	GTGACTGGAGTTCAGACGTGT		
Library adapted oligo based on the mammoth *12S* mitochondrial gene *(Priming sites with reverse-complement bolded)*	**ACACTCTTTCCCTACACGAC**GCTCTTCCGATCTCCCTAAACTTTGATAGCTACCTTTACAAAGCTATCCGCCAGAGAACTACAGATCGGAAGAGC**ACACGTCTGAACTCCAGTCAC**		
Input	Volume		
PCR master mix	6 µL		
Library adapted template	4 µL		
PCR Protocol			
Phase	Temperature (°C)	Time	Cycles
Initial Denaturation	95	5 min	
Denaturation	95	30 sec	Repeated for 30 cycles
Annealing + Extension	60	45 sec	
Melt Curve	**65–95**	**5 sec per degree**	

Nanopure Barnstead water was used to bring the mix up to the desired concentration and volume. Oligo based on Enk et al. (2016); primers based Meyer and Kircher (2010).

Table S9 Library adapted *trnL* short amp total quantification PCR.

PCR Master Mix			
Component	Final Concentration		
10X PCR Buffer II	1X		
MgCl2	2.5 mM		
dNTP mix	250 µM		
BSA	1 mg/ml		
Forward primer	0.25 µM		
Reverse primer	0.75 µM		
EvaGreen	0.5X		
AmpliTaq Gold	0.05 U/µL		
Oligos	Sequence (5'–3')		
Forward primer (trnL_P6-g_F)	GGGCAATCCTGAGCCAA		
Reverse primer (ILPr_shortampP7R_MeyerIS8)	GTGACTGGAGTTCAGACGTGT		
Oligo with binding sites for library adapter primers and *trnL* primers from Taberlet et al. (2007). Oligo insert shows no significant similarity with blastn and a top blast hit to Staphylococcus aureus with an E-value of 0.056 using megablast at the time of publication. *(Priming sites with reverse-complement bolded)*	GTGACACTCTTTCCCTACACGACT**GG GCAATCCTGAGCCAA**ATGATATGATT TGAGATATTGATAGAATTGAATGCAT AGTGATAAAAGGATGATATATTAGGA TAGGTGCAGAGACTCAATGGA**ACACG TCTGAACTCCAGTCAC**GTA		
Input	Volume		
PCR master mix	8 µL		
Library adapted template	1 µL		
PCR Protocol			
Phase	Temperature (°C)	Time	Cycles
Initial Denaturation	95	5 min	
Denaturation	95	30 sec	Repeated for 50 cycles
Annealing	51	30 sec	
Extension	*72*	50 sec	
Final Extension	72	1 min	
Melt Curve	*55–95*	*1 sec per degree*	

*Fluorescence readings were recorded post-annealing and during the melt curve as indicated above with asterisks.

Nanopure Barnstead water was used to bring the master mix up to the desired concentration and volume.

Library adapter primer based on Meyer and Kircher (2010); primer *trnL*-g targets the P6 loop of the *trnL* cpDNA intron, and is based on Taberlet et al. (2007).

Table S10 Library adapted and indexed long amp total quantification PCR.

PCR Master Mix			
Component	Final Concentration		
KAPA SYBR®FAST qPCR Master Mix (2X)	1X		
Forward primer	0.2 µM		
Reverse primer	0.2 µM		
Oligos	Sequence (5'–3')		
Forward primer (ILPr_shortampP5F_MeyerIS5)	AATGATACGGCGACCACCGA		
Reverse primer (ILPr_shortampP7R_MeyerIS6)	CAAGCAGAAGACGGCATACGA		
PhiX library adapted control standard from 100 pM to 62.6 fM	AATGATACGGCGACCACCGA *ADAPTER INSERT* TCGTATGCCGTCTTCTGCTTG		
Input	Volume		
PCR master mix	6 µL		
Library adapted and indexed template	4 µL		
PCR Protocol			
Phase	Temperature (°C)	Time	Cycles
Initial Denaturation	95	5 min	1
Denaturation	95	30 sec	Repeated for 35 cycles
Annealing + Extension	60	45 sec	
Cooldown	8	30 sec	1

Nanopure Barnstead water was used to bring the mix up to the desired concentration and volume. Primers from Meyer and Kircher (2010).

Table S11 Enrichment mastermixes.

Hybridization MasterMix	
Component	Final Concentration
Hyb N (19.46X SSPE, 13.5 mM EDTA)	9X, 6.25mM
Hyb D (50X Denhardt's Solution)	8.75X
Hyb S (10% SDS)	0.25%
Hyb R RNAsecure	1.56X
Bait Mixture (200 ng baits per reaction)	11.11 ng/µL
Bait Mixture	
Component	Final Concentration
Plant: 18,672 baits	83.33 ng/rxn
Animal: 57,588 baits	138.89 ng/rxn
Library MasterMix	
Component	Final Concentration
Block A (Illumina bloligos xGens)	0.04 ng/µL
Block C (Human COt-1 DNA)	0.19 ng/µL
Block O (Salmon Sperm DNA)	0.19 ng/µL
Library template input	7 µL
Wash Buffer X (0.2X WB)	
Component	Final Concentration
HYB S (10% SDS)	0.08 %
Wash Buffer (0.1X SSC; 0.1% SDS; 1mM EDTA)	0.2X

Nanopure Barnstead water was used to bring mixes up to the desired concentration and volume.

Table S12 SET-A sample list.

SET ID	Extraction method	Extract clean-up prior to DsLp	Core/sample	Previous ID	Site	Sample Type
SET2	PowerSoil		MM12-118b	GB1	Upper Gold Bottom Creek	Permafrost
SET4	DD-Dabney		MM12-118b	GB1	Upper Gold Bottom Creek	Permafrost
SET5	DD-Dabney	1/10 dilution	MM12-118b	GB1	Upper Gold Bottom Creek	Permafrost
SET6	DD-Dabney	QiaQuick Purification	MM12-118b	GB1	Upper Gold Bottom Creek	Permafrost
SET9	PowerSoil		LLII 12-84-3	LL3	Lucky Lady II	Permafrost
SET10	PowerSoil	1/10 dilution	LLII 12-84-3	LL3	Lucky Lady II	Permafrost
SET13	DD-Dabney		LLII 12-84-3	LL3	Lucky Lady II	Permafrost
SET14	DD-Dabney	1/10 dilution	LLII 12-84-3	LL3	Lucky Lady II	Permafrost
SET15	DD-Dabney	QiaQuick purification	LLII 12-84-3	LL3	Lucky Lady II	Permafrost
SET17	PowerSoil		LLII 12-217-8	LL1	Lucky Lady II	Permafrost
SET19	DD-Dabney		LLII 12-217-8	LL1	Lucky Lady II	Permafrost
SET20	DD-Dabney	1/10 dilution	LLII 12-217-8	LL1	Lucky Lady II	Permafrost
SET21	DD-Dabney	QiaQuick purification	LLII 12-217-8	LL1	Lucky Lady II	Permafrost
SET23	PowerSoil		BC 4-2B	BC	Bear Creek	Permafrost
SET25	DD-Dabney		BC 4-2B	BC	Bear Creek	Permafrost
SET26	DD-Dabney	1/10 dilution	BC 4-2B	BC	Bear Creek	Permafrost
SET27	DD-Dabney	QiaQuick purification	BC 4-2B	BC	Bear Creek	Permafrost
SETPC1	PowerSoil		*N. shastensis*	089	Gypsum Cave, Nevada	Palaeofeces
SETPC2	DD-Dabney		*N. shastensis*	089	Gypsum Cave, Nevada	Palaeofeces
SETBK1 SETBK2	PowerSoil DD-Dabney	**Extraction Blanks**				

Core/previous ID as per Sadoway (2014). All sediment cores from the Yukon.
PowerSoil: DNeasy PowerSoil extraction kit.
DD-Dabney: a two-stage demineralization (0.5 M EDTA) and digestion (proteinase K buffer, see Table S1) (each overnight) followed by purification with a high-volume binding buffer and Roche Diagnostics silica-spin column following Dabney et al.(2013).
DsLp: Double-stranded library preparation (Meyer and Kircher, 2010; Kircher et al., 2012).
PC1/2: Positive control 089, *Nothrotheriops shastensis (*Shasta ground sloth) palaeofeces (Poinar et al., 1998).
Pre-DsLp clean-up with a QiaQuick PCR Purification Kit, or the extract was diluted to 1/10 prior to DsLp.
Observations: Dabney extracts without an additional clean-up were very darkly coloured compared to the clear PowerSoil extracts.

Table S13 SET-B sample list.

Sample Information					Treatment			Sample Information					Treatment				
SET ID	Extract ID	Core	Previous ID	Sample Type	PowerBeads	Solution C3	4°C Spin	SET ID	Extract ID	Core	Previous ID	Sample Type	PowerBeads	Solution C3	4°C Spin	Sonication	Post-sonication purification
SET28	D7a	LLII 12-84-3	LL3	Pf	Y	-	-	**SET73**	D7a	LLII 12-84-3	LL3	Pf	Y	-	-	Y	Y
SET29	D8a	LLII 12-84-3	LL3	Pf	Y	-	Y	**SET74**	D8a	LLII 12-84-3	LL3	Pf	Y	-	Y	Y	Y
SET30	D9a	LLII 12-84-3	LL3	Pf	Y	Y	-	**SET75**	D9a	LLII 12-84-3	LL3	Pf	Y	Y	-	Y	Y
SET31	D10a	LLII 12-84-3	LL3	Pf	Y	Y	Y	**SET76**	D10a	LLII 12-84-3	LL3	Pf	Y	Y	Y	Y	Y
SET32	D11a	LLII 12-84-3	LL3	Pf	-DD	Y	Y	**SET77**	D11a	LLII 12-84-3	LL3	Pf	-DD	Y	Y	Y	Y
SET33	D7b	LLII 12-84-3	LL3	Pf	Y	-	-	**SET78**	D7b	LLII 12-84-3	LL3	Pf	Y	-	-	Y	-
SET34	D8b	LLII 12-84-3	LL3	Pf	Y	-	Y	**SET79**	D8b	LLII 12-84-3	LL3	Pf	Y	-	Y	Y	-
SET35	D9b	LLII 12-84-3	LL3	Pf	Y	Y	-	**SET80**	D9b	LLII 12-84-3	LL3	Pf	Y	Y	-	Y	-
SET36	D10b	LLII 12-84-3	LL3	Pf	Y	Y	Y	**SET81**	D10b	LLII 12-84-3	LL3	Pf	Y	Y	Y	Y	-
SET37	D11b	LLII 12-84-3	LL3	Pf	-Dig	Y	Y	**SET82**	D11b	LLII 12-84-3	LL3	Pf	-Dig	Y	Y	Y	-
SET38	D7c	LLII 12-84-3	LL3	Pf	Y	-	-	**SET83**	D7c	LLII 12-84-3	LL3	Pf	Y	-	-	Y	Y
SET39	D8c	LLII 12-84-3	LL3	Pf	Y	-	Y	**SET84**	D8c	LLII 12-84-3	LL3	Pf	Y	-	Y	Y	-
SET40	D9c	LLII 12-84-3	LL3	Pf	Y	Y	-	**SET85**	D9c	LLII 12-84-3	LL3	Pf	Y	Y	-	Y	-
SET41	D10c	LLII 12-84-3	LL3	Pf	Y	Y	Y	**SET86**	D10c	LLII 12-84-3	LL3	Pf	Y	Y	Y	Y	Y
SET43	D12a	LLII 12-217-8	LL1	Pf	Y	-	-	**SET88**	D12a	LLII 12-217-8	LL1	Pf	Y	-	-	Y	Y
SET44	D13a	LLII 12-217-8	LL1	Pf	Y	-	Y	**SET89**	D13a	LLII 12-217-8	LL1	Pf	Y	-	Y	Y	Y
SET45	D14a	LLII 12-217-8	LL1	Pf	Y	Y	-	**SET90**	D14a	LLII 12-217-8	LL1	Pf	Y	Y	-	Y	Y
SET46	D15a	LLII 12-217-8	LL1	Pf	Y	Y	Y	**SET91**	D15a	LLII 12-217-8	LL1	Pf	Y	Y	Y	Y	Y
SET47	D16a	LLII 12-217-8	LL1	Pf	-DD	Y	Y	**SET92**	D16a	LLII 12-217-8	LL1	Pf	-DD	Y	Y	Y	Y
SET48	D12b	LLII 12-217-8	LL1	Pf	Y	-	-	**SET93**	D12b	LLII 12-217-8	LL1	Pf	Y	-	-	Y	-
SET49	D13b	LLII 12-217-8	LL1	Pf	Y	-	Y	**SET94**	D13b	LLII 12-217-8	LL1	Pf	Y	-	Y	Y	-
SET50	D14b	LLII 12-217-8	LL1	Pf	Y	Y	-	**SET95**	D14b	LLII 12-217-8	LL1	Pf	Y	Y	-	Y	-
SET51	D15b	LLII 12-217-8	LL1	Pf	Y	Y	Y	**SET96**	D15b	LLII 12-217-8	LL1	Pf	Y	Y	Y	Y	-
SET52	D16b	LLII 12-217-8	LL1	Pf	-Dig	Y	Y	**SET97**	D16b	LLII 12-217-8	LL1	Pf	-Dig	Y	Y	Y	-
SET53	D12c	LLII 12-217-8	LL1	Pf	Y	-	-	**SET98**	D12c	LLII 12-217-8	LL1	Pf	Y	-	-	Y	Y
SET54	D13c	LLII 12-217-8	LL1	Pf	Y	-	Y	**SET99**	D13c	LLII 12-217-8	LL1	Pf	Y	-	Y	Y	-
SET55	D14c	LLII 12-217-8	LL1	Pf	Y	Y	-	**SET100**	D14c	LLII 12-217-8	LL1	Pf	Y	Y	-	Y	-
SET56	D15c	LLII 12-217-8	LL1	Pf	Y	Y	Y	**SET101**	D15c	LLII 12-217-8	LL1	Pf	Y	Y	Y	Y	Y
SET58	D17a	BC 4-2B	BC	Pf	Y	-	-	**SET103**	D17a	BC 4-2B	BC	Pf	Y	-	-	Y	Y
SET59	D18a	BC 4-2B	BC	Pf	Y	-	Y	**SET104**	D18a	BC 4-2B	BC	Pf	Y	-	Y	Y	Y
SET60	D19a	BC 4-2B	BC	Pf	Y	Y	-	**SET105**	D19a	BC 4-2B	BC	Pf	Y	Y	-	Y	Y
SET61	D20a	BC 4-2B	BC	Pf	Y	Y	Y	**SET106**	D20a	BC 4-2B	BC	Pf	Y	Y	Y	Y	Y
SET62	D21a	BC 4-2B	BC	Pf	-DD	Y	Y	**SET107**	D21a	BC 4-2B	BC	Pf	-DD	Y	Y	Y	Y
SET63	D17b	BC 4-2B	BC	Pf	Y	-	-	**SET108**	D17b	BC 4-2B	BC	Pf	Y	-	-	Y	-
SET64	D18b	BC 4-2B	BC	Pf	Y	-	Y	**SET109**	D18b	BC 4-2B	BC	Pf	Y	-	Y	Y	-
SET65	D19b	BC 4-2B	BC	Pf	Y	Y	-	**SET110**	D19b	BC 4-2B	BC	Pf	Y	Y	-	Y	-
SET66	D20b	BC 4-2B	BC	Pf	Y	Y	Y	**SET111**	D20b	BC 4-2B	BC	Pf	Y	Y	Y	Y	-
SET67	D21b	BC 4-2B	BC	Pf	-Dig	Y	Y	**SET112**	D21b	BC 4-2B	BC	Pf	-Dig	Y	Y	Y	-
SET68	D17c	BC 4-2B	BC	Pf	Y	-	-	**SET113**	D17c	BC 4-2B	BC	Pf	Y	-	-	Y	Y
SET69	D18c	BC 4-2B	BC	Pf	Y	-	Y	**SET114**	D18c	BC 4-2B	BC	Pf	Y	-	Y	Y	-
SET70	D19c	BC 4-2B	BC	Pf	Y	Y	-	**SET115**	D19c	BC 4-2B	BC	Pf	Y	Y	-	Y	-
SET71	D20c	BC 4-2B	BC	Pf	Y	Y	Y	**SET116**	D20c	BC 4-2B	BC	Pf	Y	Y	Y	Y	Y
SETBK3	D23	Extraction blank			-DD	-	-	**SETBK3-S**	D23	Extraction blank			-DD	-	-	Y	-
SETBK4	D24	Extraction blank			Y	Y	Y	**SETBK4-S**	D24	Extraction blank			Y	Y	Y	Y	-
SETBK5	D25	Extraction blank			Y	Y	Y	**SETBK5-S**	D25	Extraction blank			Y	Y	Y	Y	Y

Core and previous ID as per core slice designation in Sadoway (2014). Pf = permafrost; Y = treatment was used on sample; -DD = 1M EDTA demineralization overnight followed by proteinase K digestion buffer; -Dig = Same as DD without EDTA phase. SET samples on the left half of the divide were not sonicated. For samples on the right half that were, 25 µL of extract was added to 25 µL of EBT (see Table S14 for sonication run parameters). For samples that were sonicated, a subset was purified/concentrated with QiaQuick PCR purification kit back to 25 µL.

Table S14 Sonication run parameters.

Target bp (Peak)	50–150
Peak Incident Power (W)	175
Duty Factor	10%
Cycles per burst	200
Treatment Time (s)	480
Temp (C) (+/-2)	7

Minimum input volume is 50 µL, so 25 µL extracts were diluted with 25 µL EBT to bring up to volume.

Table S15 SET-C sample list.

SET ID	Core	Previous ID	4°C Spin	4°C Timing (hours)
SET118	LLII 12-84-3	LL3	-	-
SET119	LLII 12-84-3	LL3	-	-
SET120	LLII 12-84-3	LL3	-	-
SET121	LLII 12-84-3	LL3	Y	1
SET122	LLII 12-84-3	LL3	Y	1
SET123	LLII 12-84-3	LL3	Y	1
SET124	LLII 12-84-3	LL3	Y	6
SET125	LLII 12-84-3	LL3	Y	6
SET126	LLII 12-84-3	LL3	Y	6
SET127	LLII 12-84-3	LL3	Y	19
SET128	LLII 12-84-3	LL3	Y	19
SET129	LLII 12-84-3	LL3	Y	19
SET130	LLII 12-217-8	LL1	-	-
SET131	LLII 12-217-8	LL1	-	-
SET132	LLII 12-217-8	LL1	-	-
SET133	LLII 12-217-8	LL1	Y	1
SET134	LLII 12-217-8	LL1	Y	1
SET135	LLII 12-217-8	LL1	Y	1
SET136	LLII 12-217-8	LL1	Y	6
SET137	LLII 12-217-8	LL1	Y	6
SET138	LLII 12-217-8	LL1	Y	6
SET139	LLII 12-217-8	LL1	Y	19
SET140	LLII 12-217-8	LL1	Y	19
SET141	LLII 12-217-8	LL1	Y	19
SET142	BC 4-2B	BC	-	-
SET143	BC 4-2B	BC	-	-
SET144	BC 4-2B	BC	-	-
SET145	BC 4-2B	BC	Y	1
SET146	BC 4-2B	BC	Y	1
SET147	BC 4-2B	BC	Y	1
SET148	BC 4-2B	BC	Y	6
SET149	BC 4-2B	BC	Y	6
SET150	BC 4-2B	BC	Y	6
SET151	BC 4-2B	BC	Y	19
SET152	BC 4-2B	BC	Y	19
SET153	BC 4-2B	BC	Y	19
SETBK9	Extraction Blank		Y	1
SETBK10	Extraction Blank		Y	6
SETBK11	Extraction Blank		Y	19
SETLBK12	Library Blank			

All samples were physically disrupted with PowerBeads.

Table S16 SET-D sample list.

Sample Information				Extraction Variants				Sample Information				Extraction Variants			
SET ID	Core	Previous ID	Sample Type	Lysing Method	Detergent	Lysing Timing (hours)	4°C Timing (hours)	SET ID	Core	Previous ID	Sample Type	Lysing Method	Detergent	Lysing Timing (hours)	4°C Timing (hours)
SET160	LLII 12-217-8	LL1	Pf	PowerBead+Digest	Sarkosyl	9	24	SET205	BC 4-2B	BC	Pf	PowerBead+Digest	Sarkosyl	19	48
SET161	LLII 12-217-8	LL1	Pf	PowerBead+Digest	Sarkosyl	9	24	SET206	BC 4-2B	BC	Pf	PowerBead+Digest	Sarkosyl	19	48
SET162	LLII 12-217-8	LL1	Pf	PowerBead+Digest	Sarkosyl	9	24	SET207	BC 4-2B	BC	Pf	PowerBead+Digest	Sarkosyl	19	48
SET163	LLII 12-217-8	LL1	Pf	PowerBead+Digest	Sarkosyl	19	24	SET208	BC 4-2B	BC	Pf	Digest	Sarkosyl	9	24
SET164	LLII 12-217-8	LL1	Pf	PowerBead+Digest	Sarkosyl	19	24	SET209	BC 4-2B	BC	Pf	Digest	Sarkosyl	9	24
SET165	LLII 12-217-8	LL1	Pf	PowerBead+Digest	Sarkosyl	19	24	SET210	BC 4-2B	BC	Pf	Digest	Sarkosyl	9	24
SET166	LLII 12-217-8	LL1	Pf	PowerBead+Digest	Sarkosyl	9	48	SET211	BC 4-2B	BC	Pf	Digest	Sarkosyl	19	24
SET167	LLII 12-217-8	LL1	Pf	PowerBead+Digest	Sarkosyl	9	48	SET212	BC 4-2B	BC	Pf	Digest	Sarkosyl	19	24
SET168	LLII 12-217-8	LL1	Pf	PowerBead+Digest	Sarkosyl	9	48	SET213	BC 4-2B	BC	Pf	Digest	Sarkosyl	19	24
SET169	LLII 12-217-8	LL1	Pf	PowerBead+Digest	Sarkosyl	19	48	SET214	BC 4-2B	BC	Pf	Digest	Sarkosyl	9	48
SET170	LLII 12-217-8	LL1	Pf	PowerBead+Digest	Sarkosyl	19	48	SET215	BC 4-2B	BC	Pf	Digest	Sarkosyl	9	48
SET171	LLII 12-217-8	LL1	Pf	PowerBead+Digest	Sarkosyl	19	48	SET216	BC 4-2B	BC	Pf	Digest	Sarkosyl	9	48
SET172	LLII 12-217-8	LL1	Pf	Digest	Sarkosyl	9	24	SET217	BC 4-2B	BC	Pf	Digest	Sarkosyl	19	48
SET173	LLII 12-217-8	LL1	Pf	Digest	Sarkosyl	9	24	SET218	BC 4-2B	BC	Pf	Digest	Sarkosyl	19	48
SET174	LLII 12-217-8	LL1	Pf	Digest	Sarkosyl	9	24	SET219	BC 4-2B	BC	Pf	Digest	Sarkosyl	19	48
SET175	LLII 12-217-8	LL1	Pf	Digest	Sarkosyl	19	24	SET220	BC 4-2B	BC	Pf	EDTA-Digest	Sarkosyl	9	24
SET176	LLII 12-217-8	LL1	Pf	Digest	Sarkosyl	19	24	SET221	BC 4-2B	BC	Pf	EDTA-Digest	Sarkosyl	9	24
SET177	LLII 12-217-8	LL1	Pf	Digest	Sarkosyl	19	24	SET222	BC 4-2B	BC	Pf	EDTA-Digest	Sarkosyl	9	24
SET178	LLII 12-217-8	LL1	Pf	Digest	Sarkosyl	9	48	SET223	BC 4-2B	BC	Pf	EDTA-Digest	Sarkosyl	19	24
SET179	LLII 12-217-8	LL1	Pf	Digest	Sarkosyl	9	48	SET224	BC 4-2B	BC	Pf	EDTA-Digest	Sarkosyl	19	24
SET180	LLII 12-217-8	LL1	Pf	Digest	Sarkosyl	9	48	SET225	BC 4-2B	BC	Pf	EDTA-Digest	Sarkosyl	19	24
SET181	LLII 12-217-8	LL1	Pf	Digest	Sarkosyl	19	48	SET226	BC 4-2B	BC	Pf	EDTA-Digest	Sarkosyl	9	48
SET182	LLII 12-217-8	LL1	Pf	Digest	Sarkosyl	19	48	SET227	BC 4-2B	BC	Pf	EDTA-Digest	Sarkosyl	9	48
SET183	LLII 12-217-8	LL1	Pf	Digest	Sarkosyl	19	48	SET228	BC 4-2B	BC	Pf	EDTA-Digest	Sarkosyl	9	48
SET184	LLII 12-217-8	LL1	Pf	EDTA-Digest	Sarkosyl	9	24	SET229	BC 4-2B	BC	Pf	EDTA-Digest	Sarkosyl	19	48
SET185	LLII 12-217-8	LL1	Pf	EDTA-Digest	Sarkosyl	9	24	SET230	BC 4-2B	BC	Pf	EDTA-Digest	Sarkosyl	19	48
SET186	LLII 12-217-8	LL1	Pf	EDTA-Digest	Sarkosyl	9	24	SET231	BC 4-2B	BC	Pf	EDTA-Digest	Sarkosyl	19	48
SET187	LLII 12-217-8	LL1	Pf	EDTA-Digest	Sarkosyl	19	24	BK15			E-B	PowerBead+Digest	Sarkosyl	9	
SET188	LLII 12-217-8	LL1	Pf	EDTA-Digest	Sarkosyl	19	24	BK16			E-B	EDTA-Digest	Sarkosyl	9	
SET189	LLII 12-217-8	LL1	Pf	EDTA-Digest	Sarkosyl	19	24	BK17			E-B	PowerBead+Digest	Sarkosyl	19	
SET190	LLII 12-217-8	LL1	Pf	EDTA-Digest	Sarkosyl	9	48	BK18			E-B	EDTA-Digest	Sarkosyl	19	
SET191	LLII 12-217-8	LL1	Pf	EDTA-Digest	Sarkosyl	9	48	SET244	BC 4-2B	BC	Pf	PowerBead+Digest	SDS	19	24
SET192	LLII 12-217-8	LL1	Pf	EDTA-Digest	Sarkosyl	9	48	SET245	BC 4-2B	BC	Pf	PowerBead+Digest	SDS	19	24
SET193	LLII 12-217-8	LL1	Pf	EDTA-Digest	Sarkosyl	19	48	SET246	BC 4-2B	BC	Pf	PowerBead+Digest	SDS	19	24
SET194	LLII 12-217-8	LL1	Pf	EDTA-Digest	Sarkosyl	19	48	SET247	BC 4-2B	BC	Pf	PowerBead+Digest	SDS	19	48
SET195	LLII 12-217-8	LL1	Pf	EDTA-Digest	Sarkosyl	19	48	SET248	BC 4-2B	BC	Pf	PowerBead+Digest	SDS	19	48
SET196	BC 4-2B	BC	Pf	PowerBead+Digest	Sarkosyl	9	24	SET249	BC 4-2B	BC	Pf	PowerBead+Digest	SDS	19	48
SET197	BC 4-2B	BC	Pf	PowerBead+Digest	Sarkosyl	9	24	SET250	BC 4-2B	BC	Pf	EDTA-Digest	SDS	19	24
SET198	BC 4-2B	BC	Pf	PowerBead+Digest	Sarkosyl	9	24	SET251	BC 4-2B	BC	Pf	EDTA-Digest	SDS	19	24
SET199	BC 4-2B	BC	Pf	PowerBead+Digest	Sarkosyl	19	24	SET252	BC 4-2B	BC	Pf	EDTA-Digest	SDS	19	24
SET200	BC 4-2B	BC	Pf	PowerBead+Digest	Sarkosyl	19	24	SET253	BC 4-2B	BC	Pf	EDTA-Digest	SDS	19	48
SET201	BC 4-2B	BC	Pf	PowerBead+Digest	Sarkosyl	19	24	SET254	BC 4-2B	BC	Pf	EDTA-Digest	SDS	19	48
SET202	BC 4-2B	BC	Pf	PowerBead+Digest	Sarkosyl	9	48	SET255	BC 4-2B	BC	Pf	EDTA-Digest	SDS	19	48
SET203	BC 4-2B	BC	Pf	PowerBead+Digest	Sarkosyl	9	48	BK19			E-B	PowerBead+Digest	SDS	19	24
SET204	BC 4-2B	BC	Pf	PowerBead+Digest	Sarkosyl	9	48	BK20			E-B	EDTA-Digest	SDS	19	48

Pf = permafrost; E-B = extraction blank. SET-D_1 in grey (left and upper right sections), SET-D_2 in blue (bottom right section).

Table S17 Metabarcoding qPCR amplification, *trnL*.

PCR Master Mix			
Component	Final Concentration		
10X PCR Buffer II	1X		
MgCl2	1.5 mM		
dNTP mix	250 µM		
BSA	1 mg/ml		
Forward primer	0.25 µM		
Reverse primer	0.25 µM		
EvaGreen	1X		
AmpliTaq Gold	0.65 U/µL		
Oligos	Sequence (5'–3')		
Forward primer (trnL_P6-g_F)	GGGCAATCCTGAGCCAA		
Reverse primer (trnL_P6-h_R)	CCATTGAGTCTCTGCACCTATC		
Oligo with binding sites for library adapter primers and *trnL* primers from Taberlet et al. (2007). Oligo insert shows no significant similarity with BLASTn and a top blast hit to Staphylococcus aureus with an E-value of 0.056 using megablast at the time of publication. *(Priming sites with reverse-complement bolded)*	GTGACACTCTTTCCCTACACGACT**GG GCAATCCTGAGCCAA**ATGATATGATT TGAGATATTGATAGAATTGAATGCAT AGTGATAAAAGGATGATATATTAG**GA TAGGTGCAGAGACTCAATGG**AACAC GTCTGAACTCCAGTCACGTA		
Input	Volume		
PCR master mix	24 µL		
Extract template	1 µL		
PCR Protocol			
Phase	Temperature (°C)	Time	Cycles
Initial Denaturation	95	5 min	
Denaturation	95	30 sec	Repeated for 45 cycles
Annealing	52	30 sec	
Extension	*72*	50 sec	
Final Extension	72	1 min	

*Fluorescence readings were recorded post-annealing as indicated above with asterisks. Nanopure Barnstead water was used to bring the master mix up to the desired concentration and volume. trn*L*-g/h targets the P6 loop of the *trnL* cpDNA intron, and is based on Taberlet et al. (2007) with a custom in-house standard for quantification (SET-E).

Table S18 Disabled taxa in MEGAN with NCBI ID.

[2323] unclassified Bacteria	[78725] Cleistes
[2706] Citrus	[78760] Epistephium
[3298] Zamiaceae	[79318] Irvingia
[3520] Casuarinaceae	[85234] Oncotheca
[3642] Lecythidaceae	[85241] Plagiopteron
[3680] Begoniaceae	[93758] Corchorus
[3733] Moringaceae	[100370] Croton
[3737] Sapotaceae	[102805] Barnadesioideae
[3805] Bauhinia	[106722] Dorstenia
[4268] Malpighiaceae	[112800] Achariaceae
[4328] Proteaceae	[112827] Lacistemataceae
[4420] Victoria	[112836] Paropsia
[4441] Camellia	[124867] Pandaceae
[4527] Oryza	[126560] Picconia
[4613] Bromeliaceae	[134367] hybrid subtypes
[4618] Zingiberales	[142700] Pimelea
[4672] Dioscorea	[149357] Cissus
[4710] Arecaceae	[156614] environmental samples <viruses,unclassified bacterial viruses>
[12908] unclassified sequences	[163724] Crotalarieae
[13394] Capparis	[163736] Podalyrieae
[13484] Dianella	[169618] Ixoroideae
[13669] Sarcandra	[169619] Cinchonoideae
[14107] Restionaceae	[169659] Psychotrieae
[16472] Goodeniaceae	[173686] Santiria
[16739] Piperaceae	[179710] Homalium
[19955] Ebenaceae	[180118] Mammea
[21910] Verbenaceae	[186616] environmental samples <viruses,superkingdom Viruses>
[22063] Monimiaceae	[214912] Sterculioideae
[22973] Chrysobalanaceae	[225222] Platysace
[23808] Simaroubaceae	[226089] Elatostema
[24942] Dilleniaceae	[233879] Putranjivaceae
[26000] Elaeocarpaceae	[235594] Bridelieae
[26122] Gesneriaceae	[238071] Samydeae
[26778] Nothofagaceae	[238073] Scolopieae
[28384] other sequences	[238074] Prockieae
[37820] Hydrostachys	[238075] Abatieae
[39173] Ocimum	[239467] Phyteuma
[39613] Loeseneriella	[246513] Coldenia
[40029] Rhizophoraceae	[256812] Pera
[41867] Stilbaceae	[261082] Goniothalamus
[42220] Curtisiaceae	[324786] Pomaderreae
[43690] Canarium	[325293] Phyliceae
[43707] Meliaceae	[367897] environmental samples <viruses,unclassified DNA viruses>
[44985] Hyacinthaceae	[494674] Gypothamnium
[47936] environmental samples <proteobacteria,phylum Proteobacteria>	[768725] Prunus hybrid cultivar
[48479] environmental samples <bacteria,superkingdom Bacteria>	[1003877] Benincaseae
[48510] environmental samples <archaea,superkingdom Archaea>	[1445966] Gnetidae
[53907] Ormosia	[1446378] Araucariales
[55234] Monotoca	[1504452] Osmelia
[55390] Adinandra	[1525719] Palicoureeae
[56627] Ochnaceae	[1648022] Parapholiinae
[58436] Argostemma	[1699513] Myrtoideae
[58963] Moraea	[1895897] Pombalia
[60092] Vinca	[1978182] Detarioideae
[61964] environmental samples <eukaryotes,superkingdom Eukaryota>	[2060783] Scyphostegioideae
[65009] Dipterocarpoideae	[2231387] dalbergioids sensu lato
[69062] Globularia	[2233854] mirbelioid clade
[72403] Clusia	[2233855] indigoferoid/millettioid clade
[77014] Melicope	[2304098] Cayratieae
[77071] Cecropia	[2508080] Crocoideae

This list is a combination of *MEGANs* default and intentionally disabled taxa. Sporadic mishits to some species within these families or genera were identified in this work and parallel Beringian analyses. It is believed much of this is driven by an abundance of genetic research on specific organisms (what Cribdon et al. [2020] refers to as ‘oasis taxa’), compounded by database incompleteness for some Quaternary Holarctic plant taxa. The highest possible rank at which no taxa within the clade have a Holarctic distribution were selected to be disabled for simplicity (rather than individually disabling a wide set of species due to robust genetic research on those clades), SET-E.

Table S19 Taxon specific mapping summary at a minimum length of 24 bp and mapping quality of 30.

Library	Core	Extraction	*Bison priscus* NC_027233	*Equus caballus* NC_001640	*Mammuthus primigenius* NC_007596	*Lagopus lagopus* NC_035568	*Picea glauca* NC_028594	*Poa palustris* NC_027484	*Salix interior* NC_024681	*Artemisia frigida* NC_020607
L-SET-256-En			6	0	3	14	1,723	0	37,569	3,645
L-SET-257-En	MM12-118b	PowerSoil	1	0	0	7	1,279	298	15,097	1,371
L-SET-258-En			2	0	1	24	1,212	263	14,894	1,495
L-SET-259-En			2	4	2	110	130	218	4,236	1,023
L-SET-260-En	LLII 12-84-3	PowerSoil	5	1	5	74	196	294	5,214	1,209
L-SET-261-En			1	0	1	63	136	196	3,419	917
L-SET-262-En			5	4	3	3	17	227	113	1,080
L-SET-263-En	LLII 12-217-8	PowerSoil	6	2	0	1	20	106	93	850
L-SET-264-En			9	7	3	1	33	171	169	1,671
L-SET-265-En			37	4	2	7	52	920	1,518	939
L-SET-266-En	BC 4-2B	PowerSoil	35	8	8	10	95	953	1,453	977
L-SET-267-En			26	7	2	13	79	1,477	1,864	1,149
L-SET-268-En			103	47	44	**245**	13,524	11,502	**141,195**	34,802
L-SET-269-En	MM12-118b	Modified Dabney	106	45	83	201	12,396	**10,791**	113,197	29,313
L-SET-270-En			104	32	37	178	**14,575**	10,480	112,797	30,262
L-SET-271-En			74	49	59	1,798	**10,170**	13,523	92,828	**37,685**
L-SET-272-En	LLII 12-84-3	Modified Dabney	82	59	67	**1,611**	9,921	12,811	85,995	36,168
L-SET-273-En			78	51	61	**1,950**	9,718	12,694	**96,063**	36,377
L-SET-274-En			89	58	17	21	533	**1,551**	1,731	**6,462**
L-SET-275-En	LLII 12-217-8	Modified Dabney	80	81	31	21	444	1,484	1,426	4,455
L-SET-276-En			74	43	13	14	231	727	745	2,226
L-SET-277-En			**1,466**	**427**	**311**	127	**4,907**	**20,006**	**30,198**	**26,042**
L-SET-278-En	BC 4-2B	Modified Dabney	**1,034**	**338**	**131**	123	3,082	13,724	20,619	15,035
L-SET-279-En			**1,541**	**370**	**221**	113	3,770	16,781	26,821	18,734
L-SET-BK22-En	Ext. Blank	PowerSoil	0	0	0	0	0	0	0	0
L-SET-BK23-En	Ext. Blank	Modified Dabney	0	0	0	1	0	0	0	0
L-SET-Bk24-En	Library Blank		0	0	0	0	0	0	0	0

Figures S34–S38 report *MapDamage* profiles for highlighted cells. Note: these reads are not filtered to those that solely map to their associated reference. Mapping to each reference was done independently (SET-E).

Table S20 Bait map-filtered reads *MEGAN* LCA-assignment summary, SET-E.

SedaDNA Extraction	Targeting Strategy	Total reads	Map-filtered summation				Map-filtered select major clade summations (reads mapped-to-baits, string de-duplicated, ≥ 24bp)											
			Mapped-to-baits*		*BLASTn* aligned & *MEGAN* assigned		Bacteria and Archaea		Fungi		Metazoa		Virdiplantae		No *BLASTn* hits		Not LCA-assigned	
PowerSoil	Enrichment	14,292,697	41,592	**0.3%**	36,693	***0.3%***	15	**0.0%**	0	**0.0%**	143	**0.3%**	36,507	**87.8%**	2,149	**5.2%**	2,750	**6.6%**
Modified Dabney	Enrichment	15,516,557	961,734	**6.4%**	835,364	***5.6%***	282	**0.0%**	56	**0.0%**	8,152	**0.8%**	826,203	**85.9%**	68,228	**7.1%**	58,132	**6.0%**
PowerSoil	Shotgun	6,071,164	161	**0.0%**	50	***0.0%***	0	**0.0%**	0	**0.0%**	0	**0.0%**	50	**31.1%**	103	**64.0%**	8	**5.0%**
Modified Dabney	Shotgun	14,911,050	2,216	**0.0%**	470	***0.0%***	4	**0.2%**	0	**0.0%**	8	**0.4%**	449	**20.3%**	1,642	**74.1%**	104	**4.7%**
D'Costa et al.	Metabarcoding	1,097,644	3176	**0.3%**	3078	***0.3%***	0	**0.0%**	0	**0.0%**	463	**14.6%**	2,608	**82.1%**	57	**1.8%**	41	**1.3%**

Map-filtered summation: percent of total reads.
Map-filtered major clade summations: percent of mapped-to-baits*.

Table S21 Non-map-filtered reads *MEGAN* LCA-assignment summary, SET-E.

SedaDNA Extraction	Targeting Strategy	Total reads	Non-map-filtered select major clade summations (string de-duplicated and ≥ 24bp)											
			Bacteria & Archea		Fungi		Metazoa		Virdiplantae		No *BLASTn* hits		Not LCA-assigned	
PowerSoil	Enrichment	14,292,697	243,941	**1.7%**	3,234	**0.0%**	40,345	**0.3%**	462,592	**3.2%**	9,178,308	**64.2%**	877,851	**6.1%**
Modified Dabney	Enrichment	15,516,557	127,382	**0.8%**	11,354	**0.1%**	93,089	**0.6%**	1,685,455	**10.9%**	9,368,011	**60.4%**	526,480	**3.4%**
PowerSoil	Shotgun	6,071,164	113,216	**1.9%**	728	**0.0%**	24,177	**0.4%**	44,852	**0.7%**	4,997,565	**82.3%**	488,337	**8.0%**
Modified Dabney	Shotgun	14,911,050	150,986	**1.0%**	3,141	**0.0%**	87,745	**0.6%**	233,197	**1.6%**	11,863,278	**79.6%**	499,037	**3.3%**
D'Costa et al.	Metabarcoding	1,097,644	43	**0.0%**	0	**0.0%**	20,245	**1.8%**	76,953	**7.0%**	14,097	**1.3%**	17,690	**1.6%**

Non-map-filtered major clade summations: percent of total reads.

Table S22 Comparative fold increase in LCA-assigned reads of cold spin extracts with PalaeoChip enrichments over alternative approaches.

Mapped-to-baits, LCA-assigned					
	Extraction Method:	PowerSoil		SedaDNA modified Dabney	D'Costa et al. 2001
	Targeting Strategy:	Enrichment	Shotgun	Shotgun	Metabarcoding
SedaDNA modified Dabney extraction paired with targeted enrichment	MM12-118b	15.7x	5,497.1x	1,020.6x	24.7x
	LLII 12-84-3	19.3x	7,024.8x	1,152.1x	59.9x
	LLII 12-217-8	7.7x	1,763.2x	351.7x	1.2x
	BC 4-2B	15.8x	9,826.3x	2,371.7x	4.7x
	Average	**14.6x**	**6,027.9x**	**1,224.0x**	**22.6x**

Mapped-to-plant references, LCA-assigned							
	Extraction Method:	PowerSoil			SedaDNA modified Dabney		D'Costa et al. 2001
	Targeting Strategy:	Metabarcoding	Enrichment	Shotgun	Metabarcoding	Shotgun	Metabarcoding
SedaDNA modified Dabney extraction paired with targeted enrichment	MM12-118b	23.0x	5.0x	3,514.5x	17.8x	1,414.3x	5.5x
	LLII 12-84-3	20.6x	9.1x	6,977.6x	19.5x	1,366.4x	12.7x
	LLII 12-217-8	2.3x	2.6x	1,132.5x	2.9x	421.7x	0.3x
	BC 4-2B	6.3x	7.3x	58,281.9x	5.8x	2,856.4x	0.9x
	Average	**13.0x**	**6.0x**	**17,476.6x**	**11.5x**	**1,514.7x**	**4.9x**

SET-E.

Table S23 Summary of blank samples and map-filtering counts.

Sample Type	Sample	DNA Targeting Strategy	Extraction Method	Total Reads	Bait mapped & LCA-assigned*	LCA-Assigned of Total	Plant ref mapped & LCA-assigned**	LCA-Assigned of Total
Extraction Blank	SETBK22-SG	Shotgun	PowerSoil	2,756,360	0	0.0%	0	0.0%
	SETBK22-En	Enrichment		102,752	0	0.0%	0	0.0%
	SETBK22-MB	Metabarcoding		628,453	*nm*		156	0.0%
Extraction Blank	SETBK23-SG	Shotgun	SedaDNA Modified Dabney	1,748,595	0	0.0%	0	0.0%
	SETBK23-En	Enrichment		1,186	0	0.0%	0	0.0%
	SETBK23-MB	Metabarcoding		987,906		0.0%	50	0.0%
Library Blank	SETBK24-SG	Shotgun	*NA*	2,841,911	0	0.0%	0	0.0%
	SETBK24-En	Enrichment		677	0	0.0%	0	0.0%
	SETBK24-MB	Metabarcoding		578,123	*nm*		16	0.0%
PCR blank	SETBK25-MB	Metabarcoding		973,729	*nm*		41	0.0%

*Reads map-filtered to animal and plant baits, size filtered to ≥ 24 bp, de-duplicated, *BLASTn* aligned, and MEGAN LCA assigned. **Reads map-filtered to plant references, with the same subsequent filtering parameters. *Nm* = not mapped to animal/plant baits. Enriched has low total read counts due to off-target exclusion expected with targeted capture, combined with equimolar pooling with samples. See Figures S32–S33 for blank bubble charts, *SET-E.*

Figures

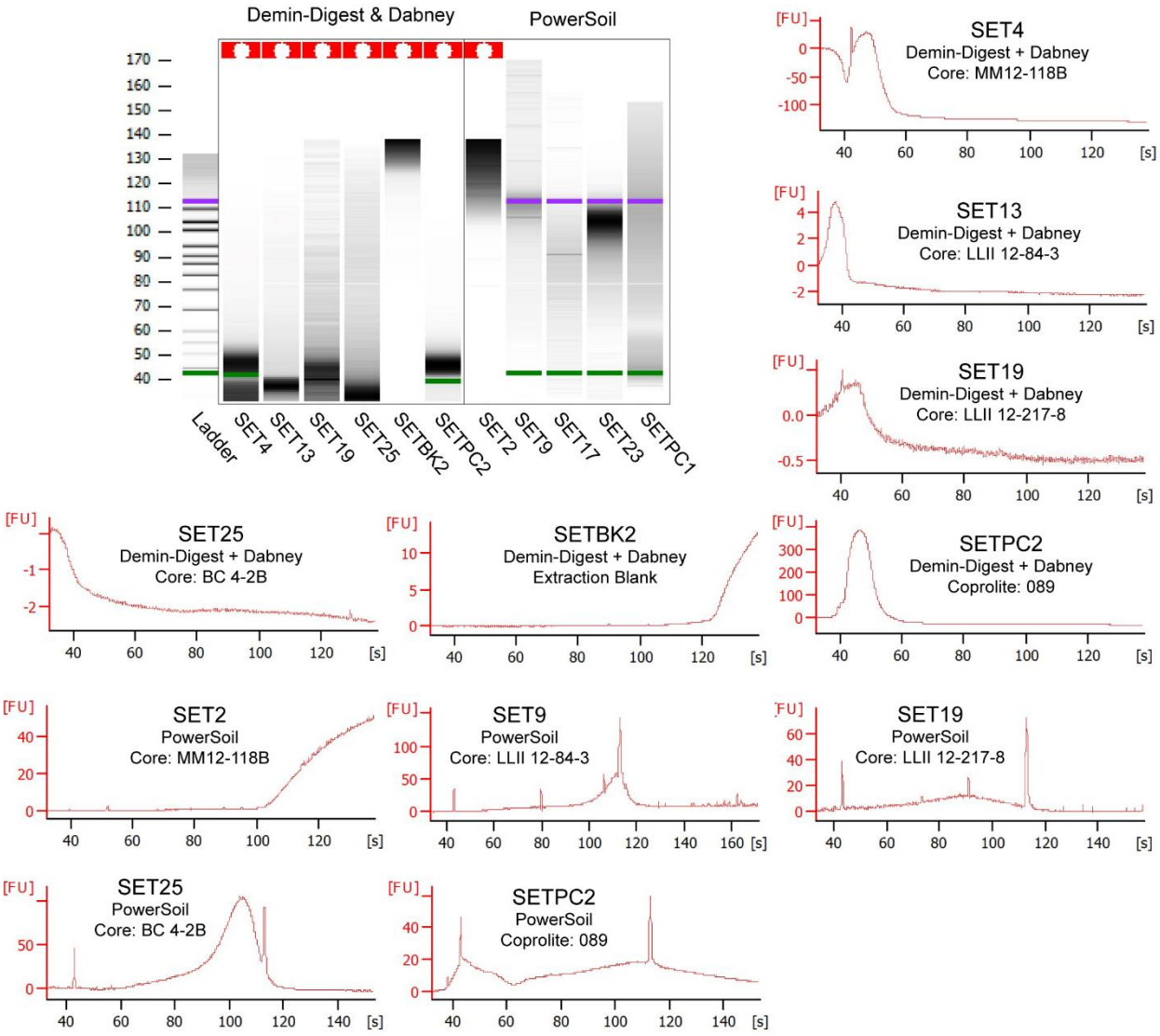

Figure S1 Bioanalyzer, high sensitive DNA assay, SET-A.
Run on an Agilent 2100 Bioanalyzer. Note that lanes 2-8 failed (too darkly coloured to detect baseline florescence), likely due to a high inhibition (humic) load.
PowerSoil: DNeasy PowerSoil extraction kit.
Demin-Digest + Dabney: demineralization (0.5 M EDTA) and digestion (proteinase K buffer, see Table 2) (each overnight separately) followed by purification with a high-volume binding buffer and silica column following Dabney et al. (2013).
089: *N. shastensis* palaeofeces from (Poinar et al., 1998).
Core ID as per Sadoway (2014).

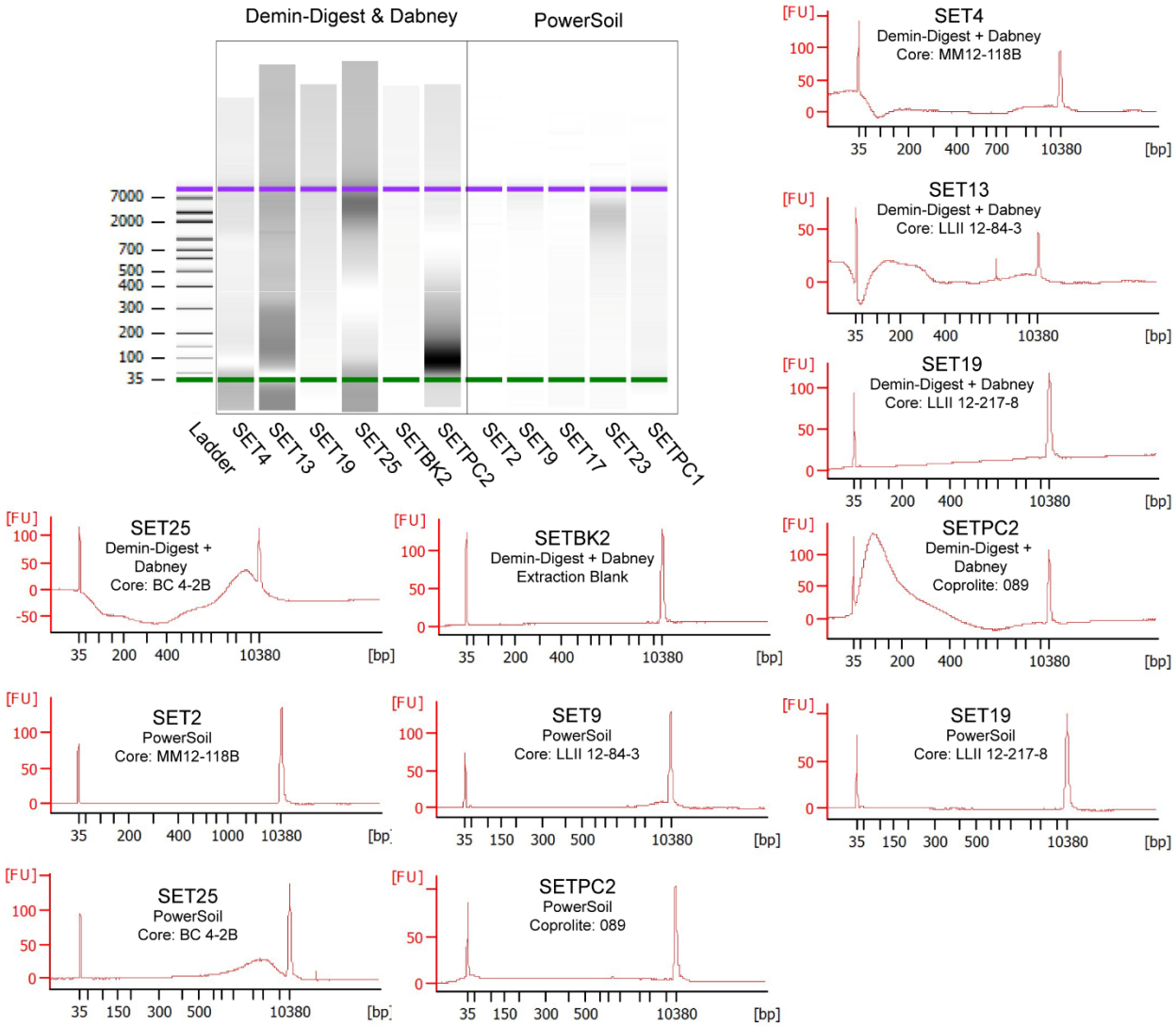

Figure S2 Bioanalyzer, high sensitive DNA assay, SET-A with a 1/10 dilution.
Run on an Agilent 2100 Bioanalyzer.
PowerSoil: DNeasy PowerSoil extraction kit.
Demin-Digest + Dabney: demineralization (0.5 M EDTA) and digestion (proteinase K buffer, see Table 2) (each overnight separately) followed by purification with a high-volume binding buffer and silica column following Dabney et al. (2013).
089: *N. shastensis* palaeofeces from (Poinar et al., 1998).
Core ID as per Sadoway (2014).

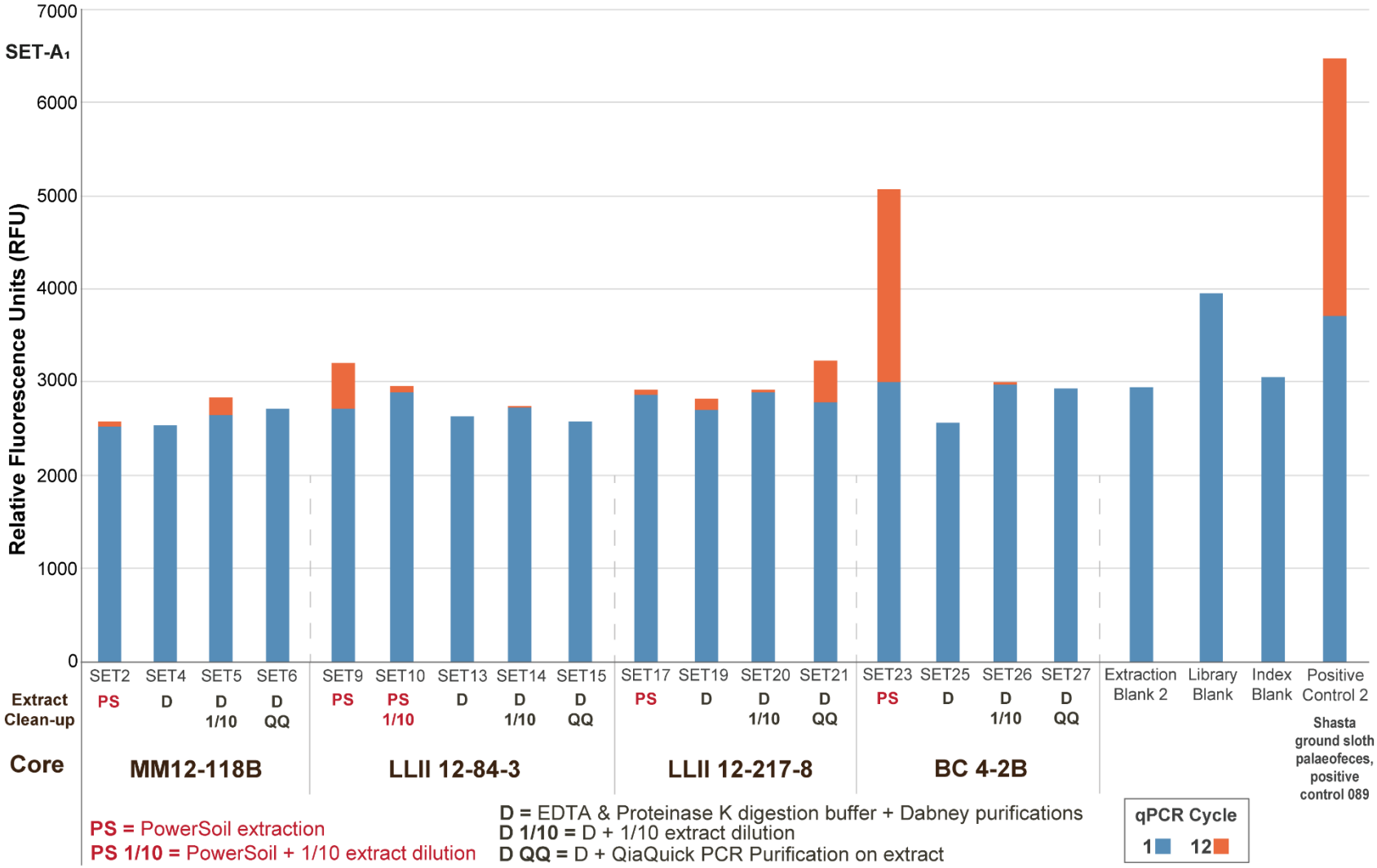

Figure S3 SET-A, indexing RFU bar chart for qPCR cycles 1 and 12.
Extract clean-up indicates how the purified elutes were 'cleaned' prior to double stranded library preparation.

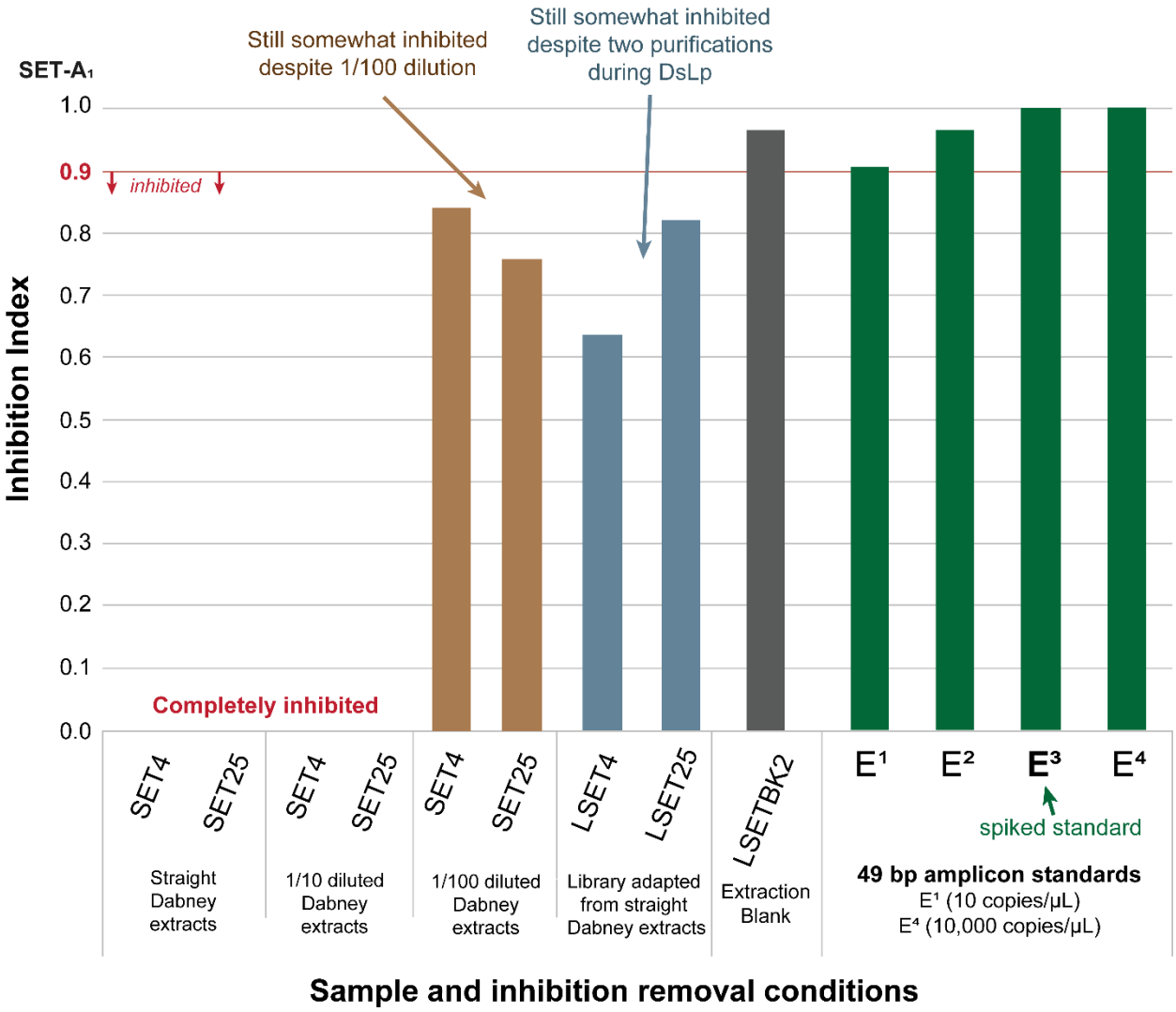

Figure S4 SET-A, Inhibition indices of inhibitor clean-up strategies.
First three column sets are extracts that were spiked for the assay. SET samples with a preceding 'L' denote libraries that were assayed for inhibition.

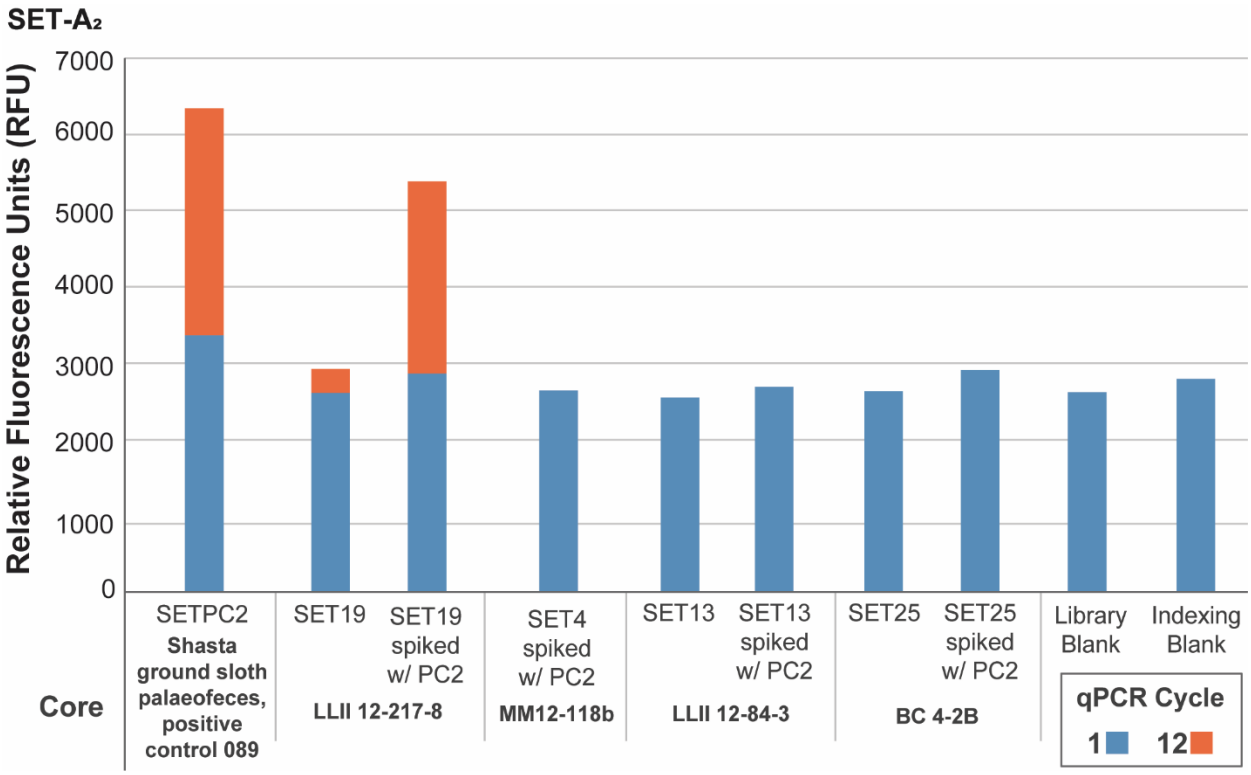

Figure S5 SET-A, Indexing qPCR reaction of positive control spiked extracts prior to library preparation.
The SET4 extract was exhausted; only SET4 with a positive control spike was tested in this experiment.

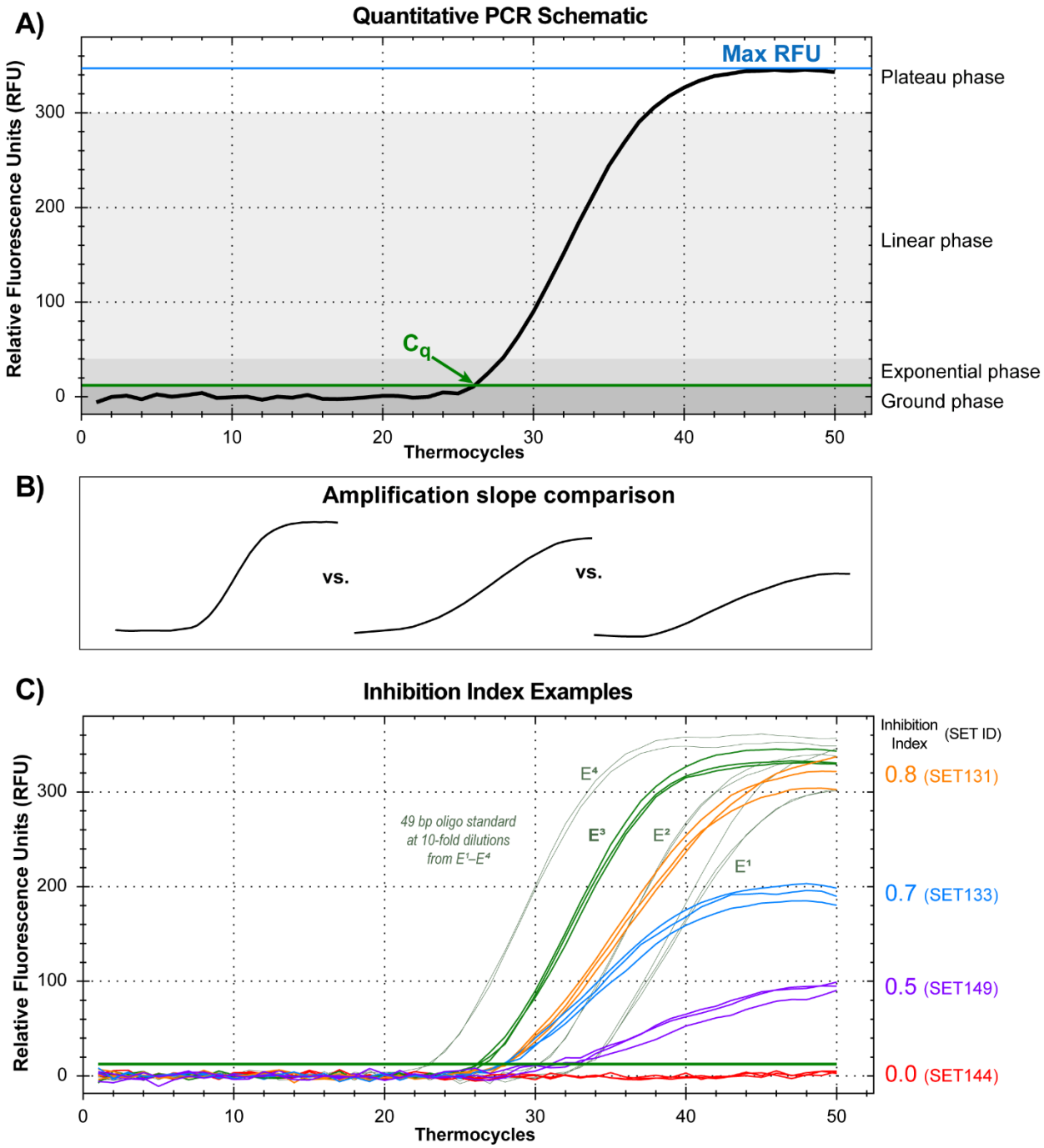

Figure S6 Components of the inhibition index.
A) A standard qPCR reaction showing C_q and max RFU. **B)** A comparison of various amplification slopes from a typical reaction (left), towards increasingly inhibited reactions (right). **C)** Example inhibition indices derived from averaging the C_q, max RFU, and by fitting a variable-slope sigmoidal dose-response curve to the raw fluorescence data (using GraphPad Prism v. 7.04) based on King et al.(2009) for each PCR replicate by sample against the spiked E^3 standard. Inhibition index values <0.5 tend to occur when individual PCR replicates fail in a triplicate series; blanks and standard serial dilutions E^2 and E^1 tend to have inhibition indices >0.9 despite their 10- and 100-fold reduction in starting DNA causing a 3 or 6 cycle C_q shift. QPCR standard curve: E = 94.2%, R^2 = 0.997, slope = −3.469. See Table S7 for PCR assay specifications.

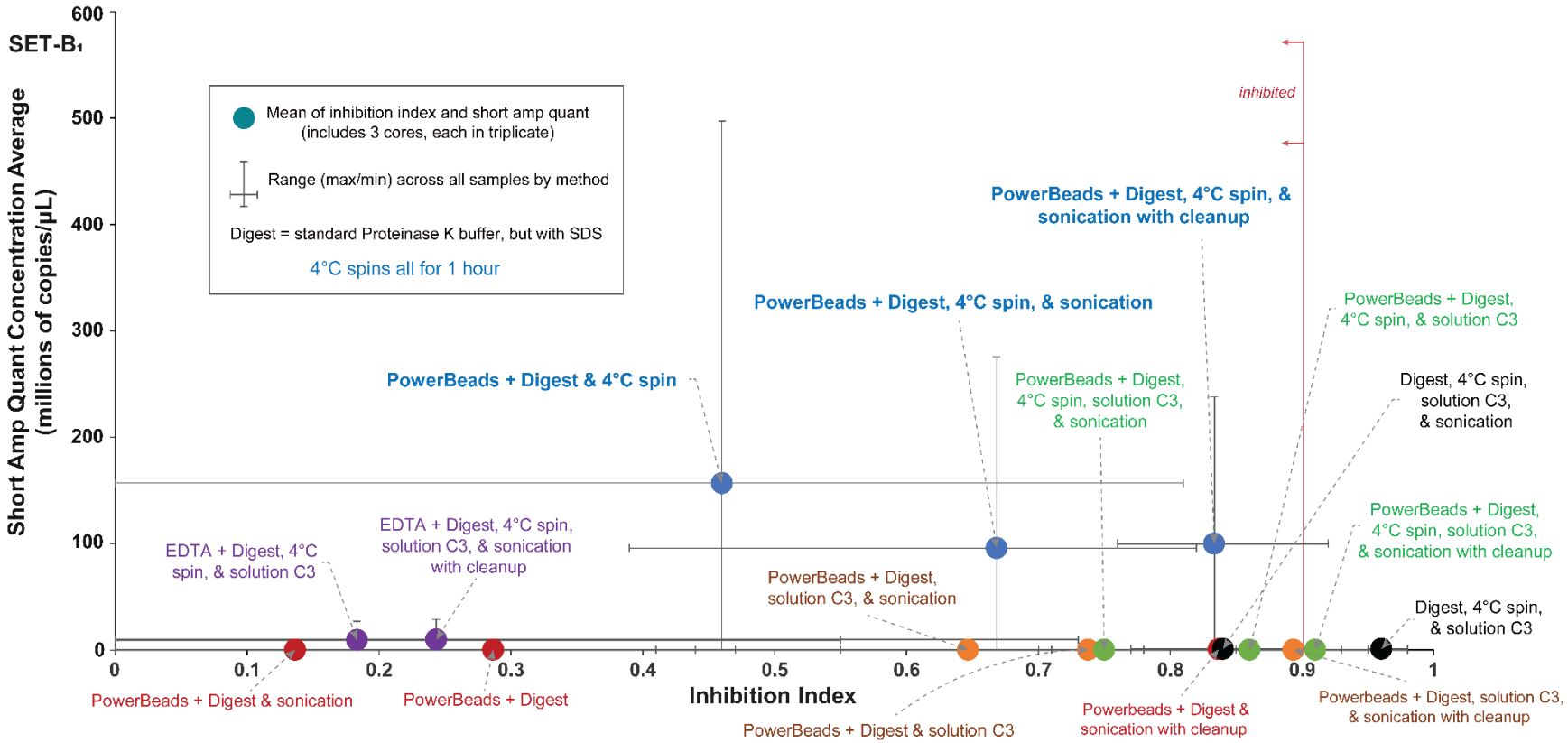

Figure S7 SET-B, comparing treatments for enzymatic inhibitor removal by their DNA retention.
Details for the short amp DNA quantification can be found in Table S8. See Table S7 and Figure E14 (main text) for details on the inhibition index. See Table S13 for SET-B sample list. Short amp qPCR standard curves for plates 1 and 2 respectively: E = 103.8% and 92.4%, R^2= 0.999 and 0.995, slope = −3.234 and −3.519.

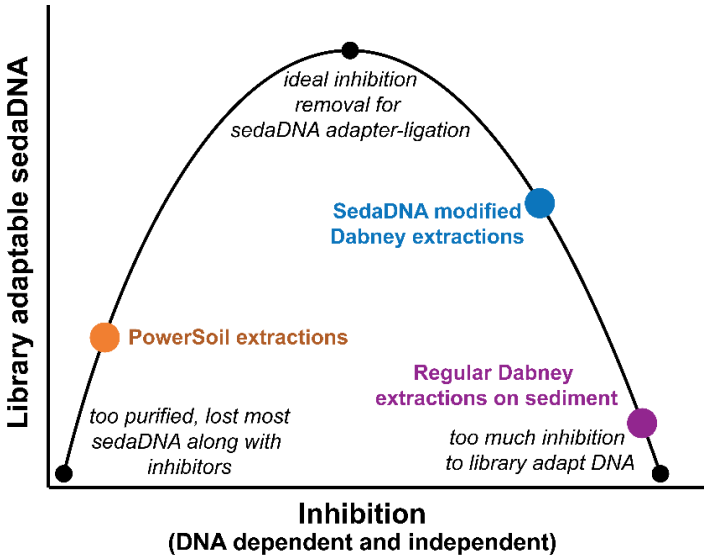

Figure S8 Conceptual balance of overcoming sedaDNA inhibitor co-elution.

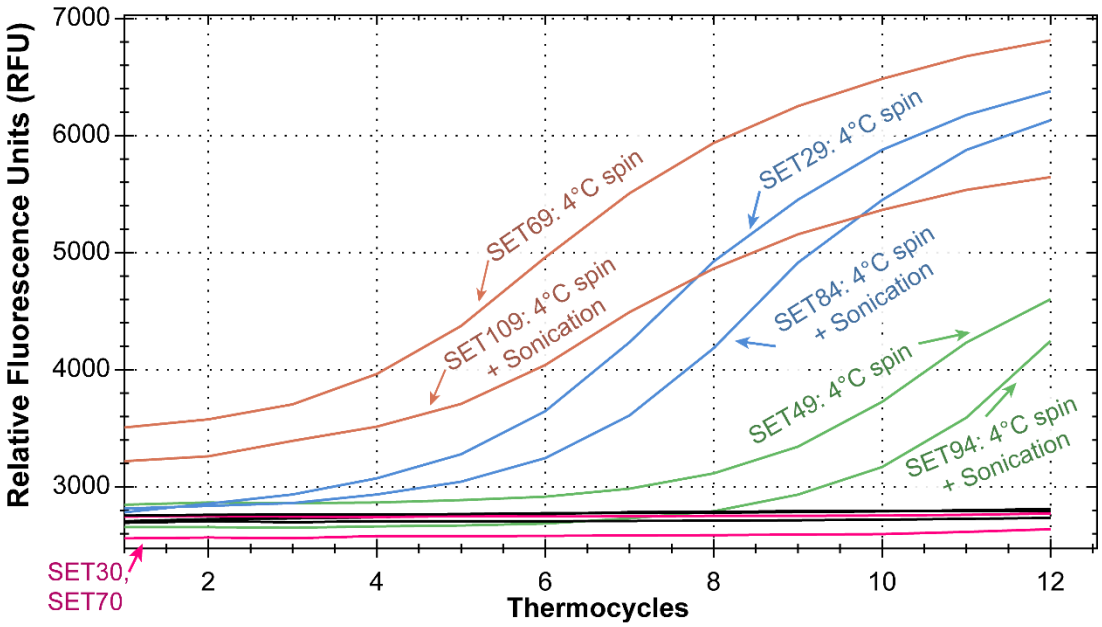

SET-B1

SET ID	Core	PowerBeads	PowerSoil Solution	1 hour 4°C Spin	Sonication	Post-Sonication Purification
SET69	BC 4-2B	Y	-	Y	-	-
SET109	BC 4-2B	Y	-	Y	Y	-
SET29	LLII 12-84-3	Y	-	Y	-	-
SET84	LLII 12-84-3	Y	-	Y	Y	-
SET49	LLII 12-217-8	Y	-	Y	-	-
SET94	LLII 12-217-8	Y	-	Y	Y	-
SET30	LLII 12-84-3	Y	Y	-	-	-
SET70	BC 4-2B	Y	Y	-	-	-

Figure S9 SET-B, qPCR indexing reaction to confirm correlation with short amp quantification. See Table S6 for indexing qPCR specifications. See Table S13 for SET-B sample list.

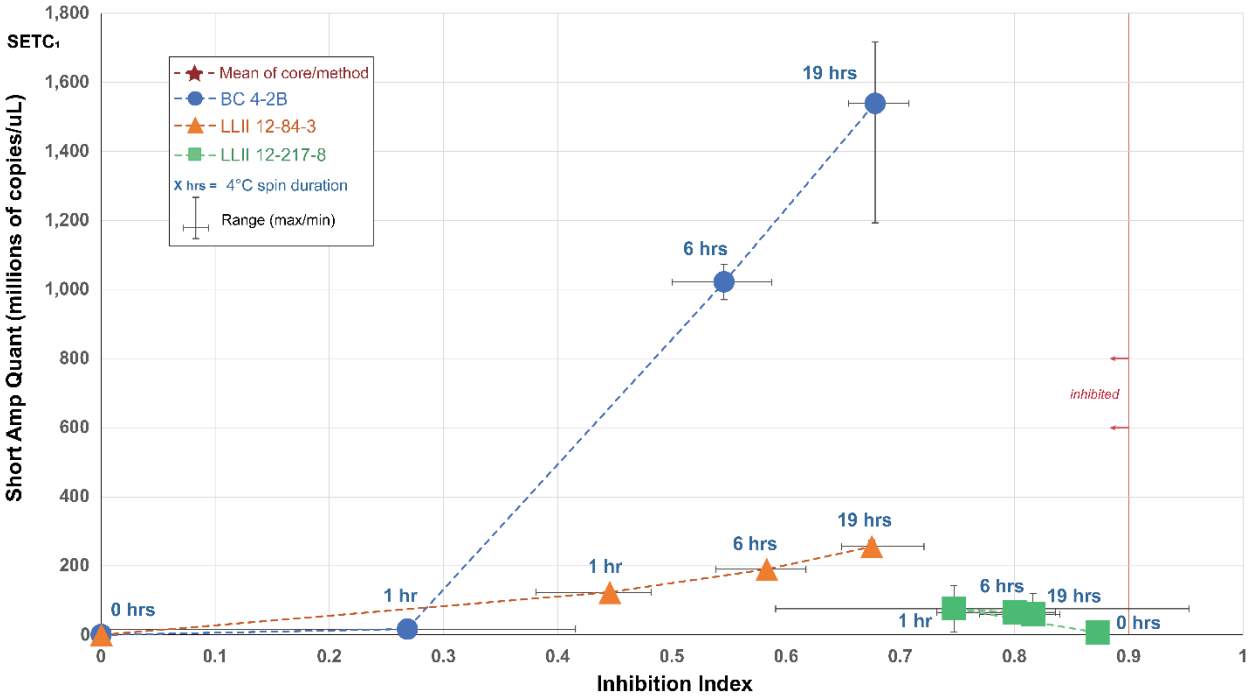

Figure S10 Variable duration 4°C centrifuge on the carryover of enzymatic inhibitors and library adapted DNA, SET-C. Short amp qPCR standard curve: E = 100.7%, R^2= 0.998, slope = −3.306. See Table S15 for sample list.

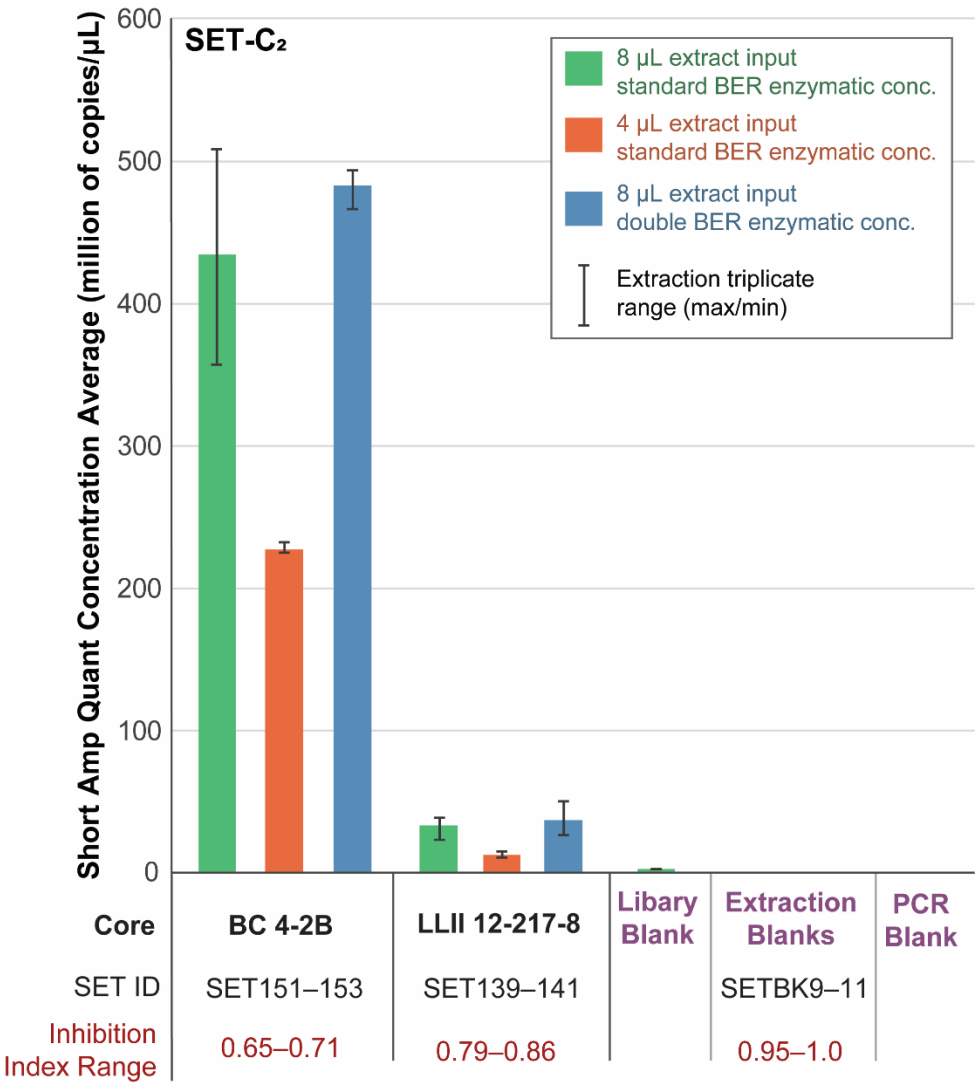

Figure S11 Total double stranded DNA with variable extract input and blunt-end repair (BER) enzymatic concentrations, SET-C.
BER enzymatic conc. = blunt-end repair enzymatic concentrations. PCR triplicate used to determine DNA concentration average per SET sample. Extraction triplicate used to determine mean and range of DNA concentration average by method and core. Short amp qPCR standard curve: E = 100.3%, R^2= 0.992, slope = −3.314. An inhibition index < 0.9 is considered inhibited (to some degree).

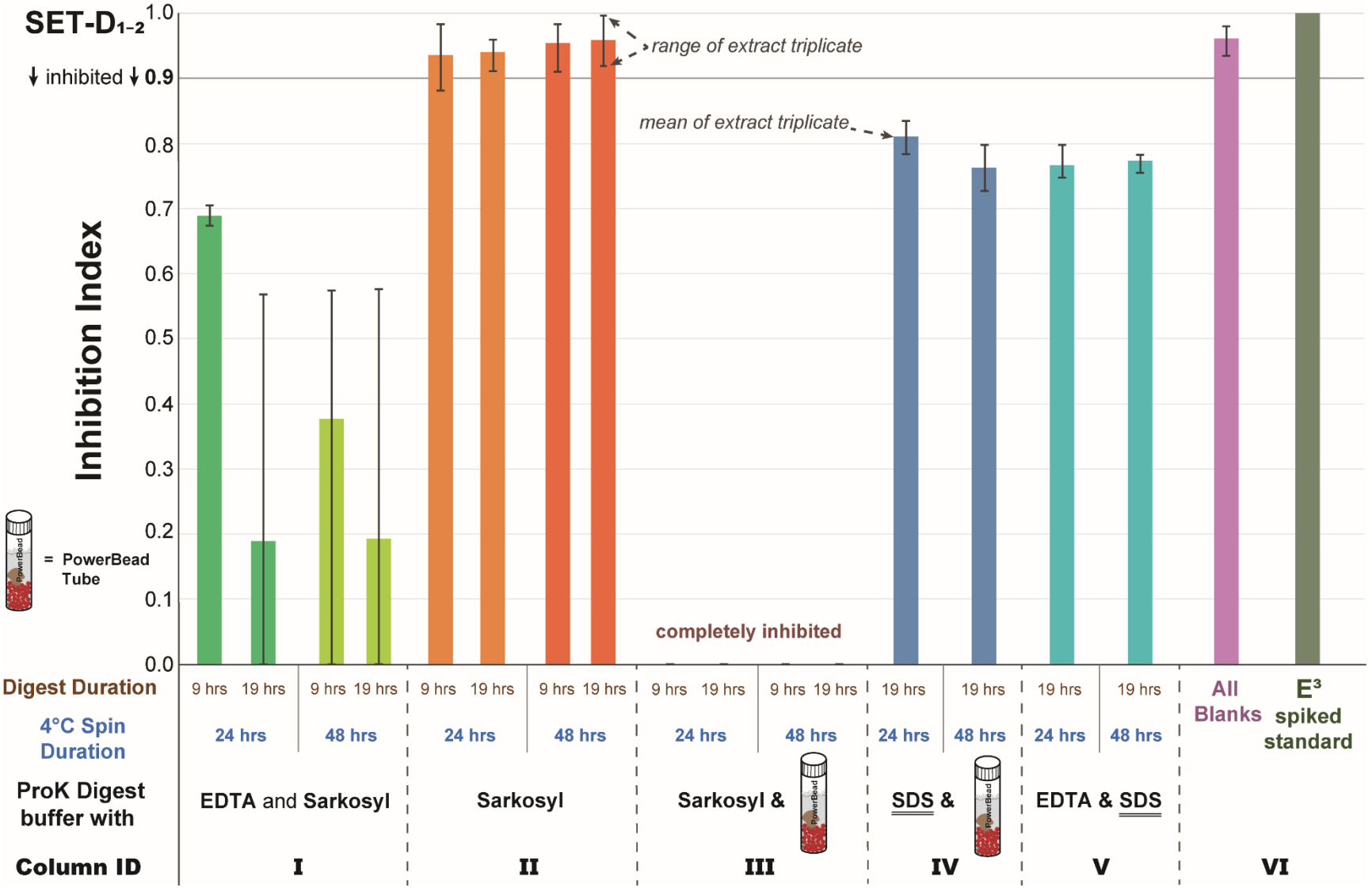

Figure S12 SET-D, core BC 4-2B, variation in co-eluate inhibitor retention by lysing method and inhibitor removal procedure. PCR triplicate used to determine inhibition index per SET sample. Extraction triplicate used to determine mean and range of inhibition indices by method and core. See Table S16 for sample list.

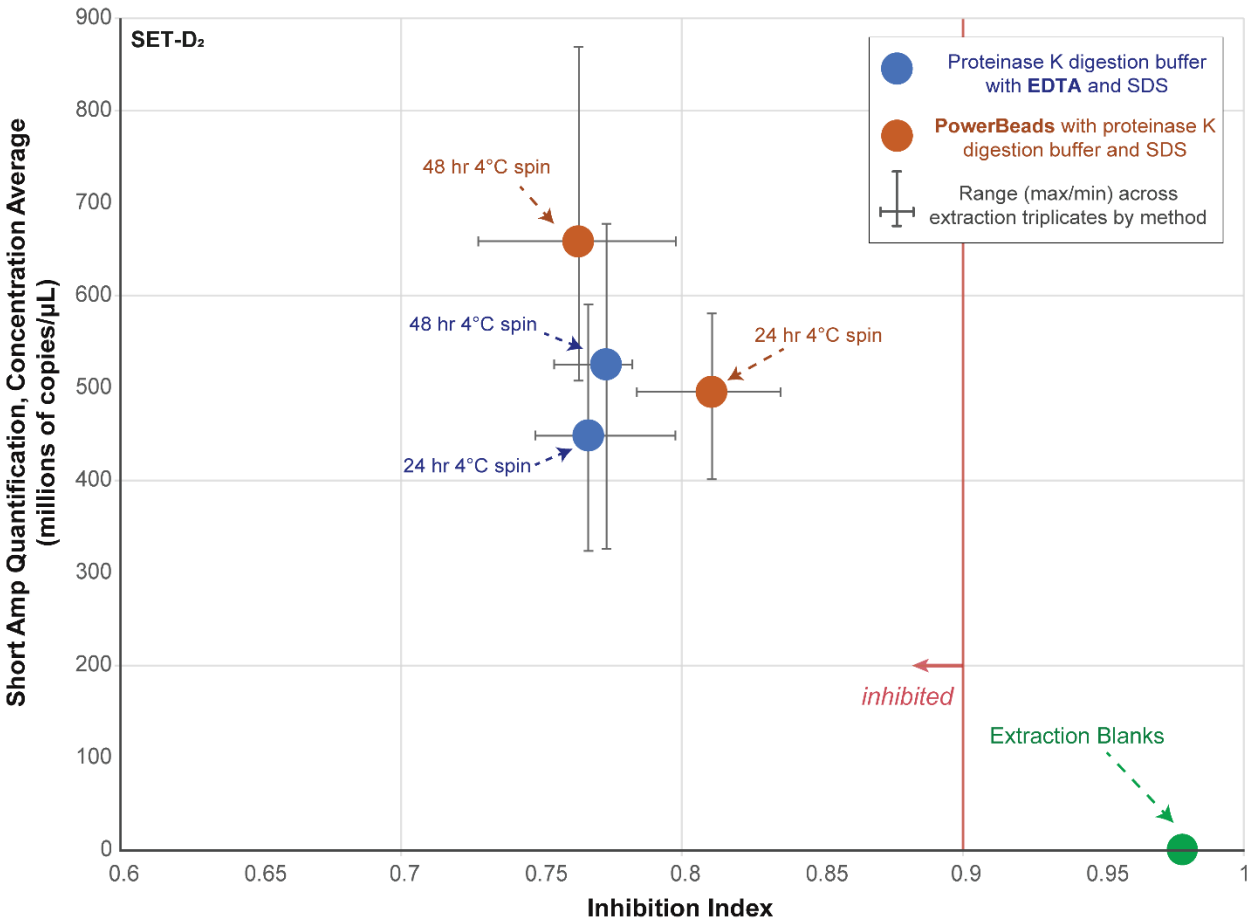

Figure S13 SET-D Variable lysis disruption and cold spin duration for core BC 4-2B. Details for the short amp DNA quantification can be found in Table S8. See Table S7 and Figure S6 (main text) for details on the inhibition index. See Table S16 for SET-D sample list. PCR triplicates used to determine average copies per µL per SET sample. Extraction triplicates used to determine mean and range of inhibition indices and short amp quantifications by method. Short amp qPCR standard curve: E = 100.5%, R^2= 0.998, slope = −3.310.

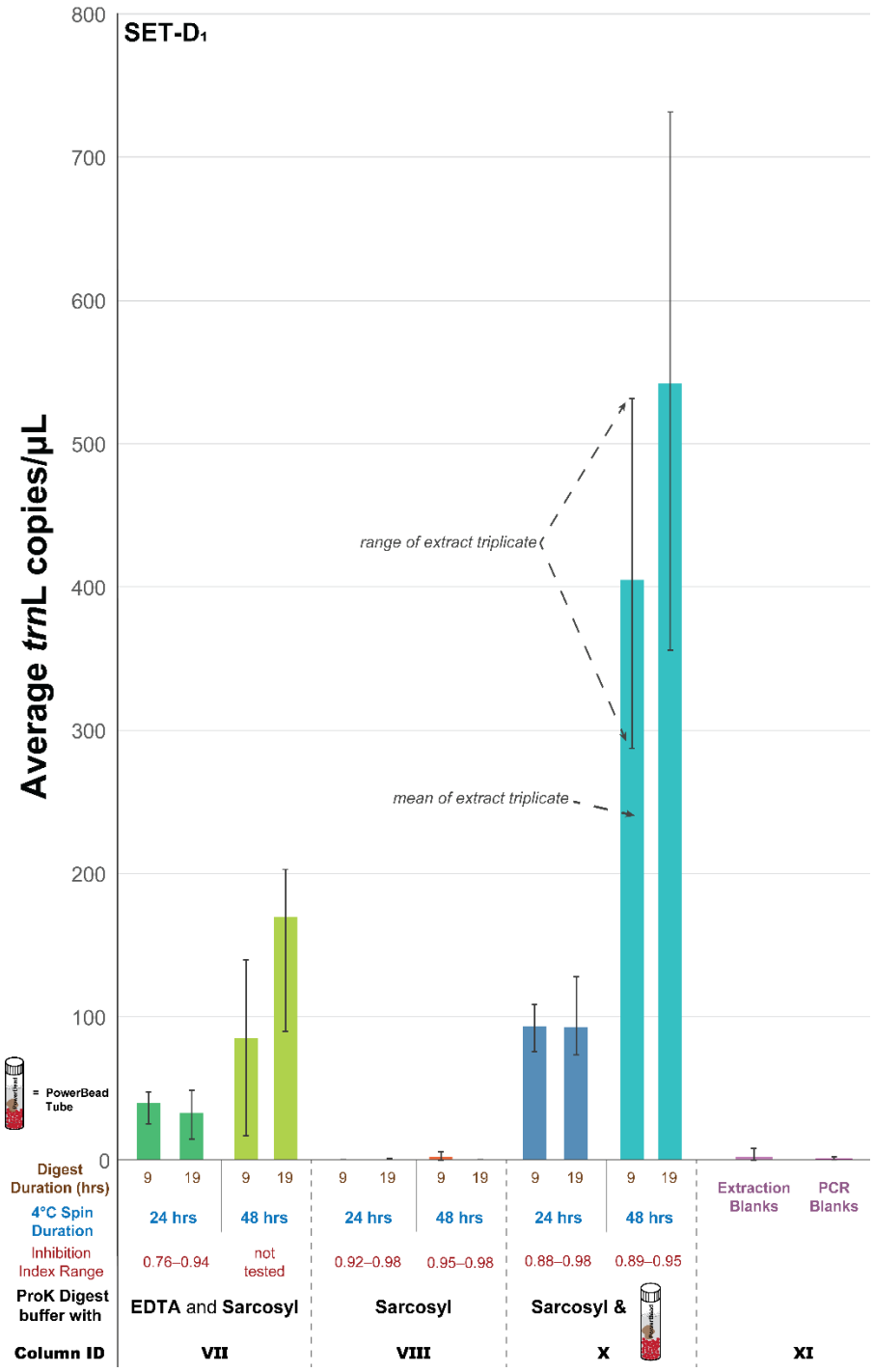

Figure S14 Variable extract amplification of core LLII 12-217-8, *trn*L 'endogenous' qPCR. This core sample had low inhibition in all experiments, regardless of the inhibition removal technique used. It was the only "uninhibited" sample in the SET-A positive control spike test (Figure S5). The wide variation in DNA concentrations is due to non-standard PCR amplification curves. As such, *these values are unreliable indicators of actual DNA concentration in the extracts*. This data was included despite being unreliable because it shows that column VIII has no amplifiable DNA and no inhibition, ruling it out as a potential lysis option (as related to column II in Figure S11). PCR triplicates used to determine average *trn*L copies per µL per SET sample. Extraction triplicate used to determine mean and range of inhibition indices by method. See Table S16 for sample list. QPCR standard curves for plates 1 and 2 respectively: E = 97.5% and 101.1%, R^2= 0.983 and 0.985, slope = −3.373 and −3.296. Column IDs correlated with Figure S11 and Figure S14.

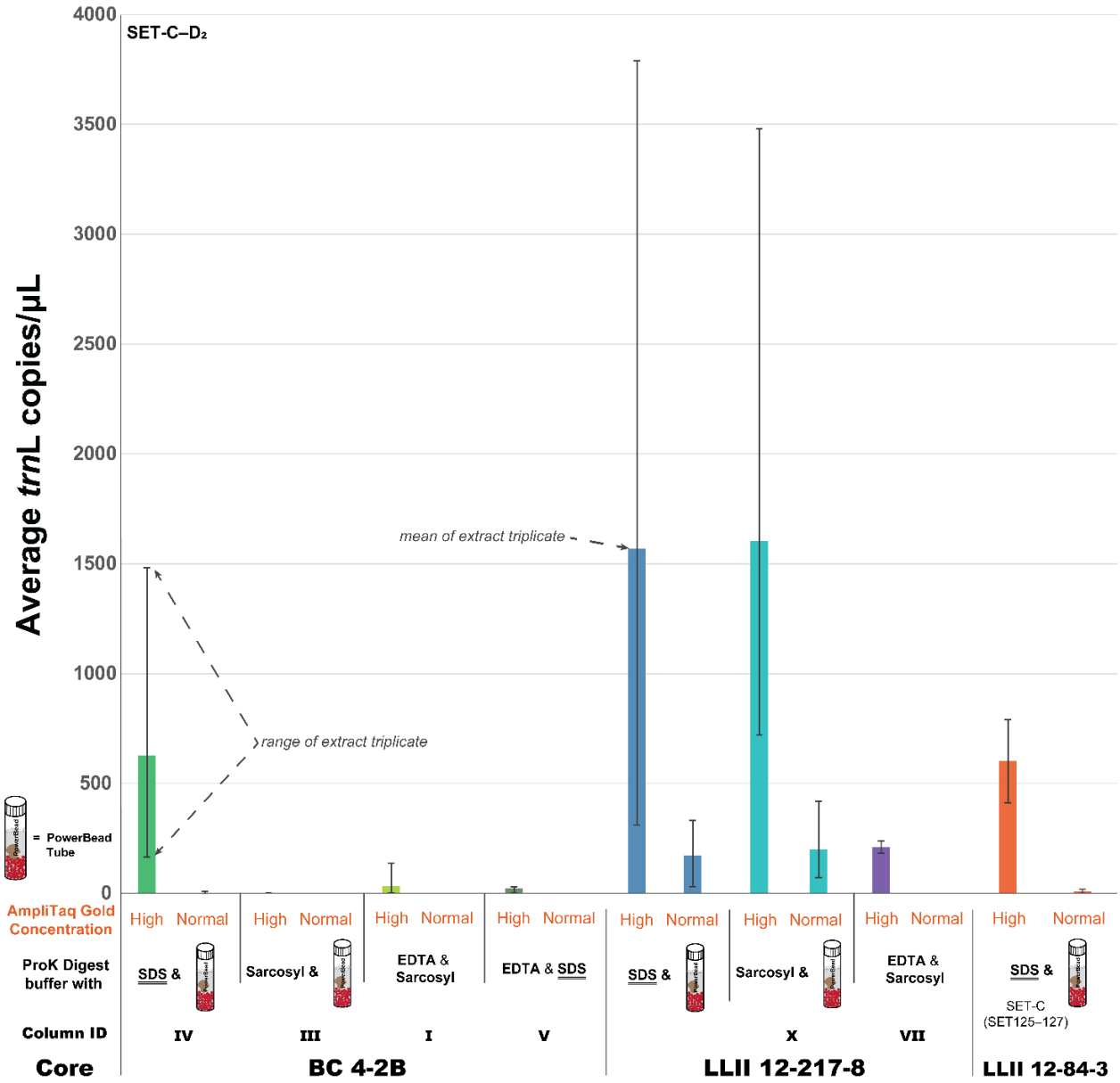

Figure S15 Variable AmpliTaq Gold concentrations on *trn*L 'endogenous' sedaDNA qPCR amplifications.

The wide variation in DNA concentration is due to non-standard PCR amplification curves. As such, *these values are unreliable indicators of actual DNA concentration in the extracts.* This data was included despite being unreliable because it shows that there is some sort of inhibition affecting these extracts, even for the core with low levels of inhibition (LLII 12-217-8, e.g. Figure S5). PCR triplicates used to determine average *trn*L copies per µL per SET sample. Extraction triplicate used to determine mean and range of inhibition indices by method. QPCR standard curve: E = 103.8%, R^2= 0.983 and 0.992, slope = −3.234. Column IDs correlated with Figure S11 and Figure S13.

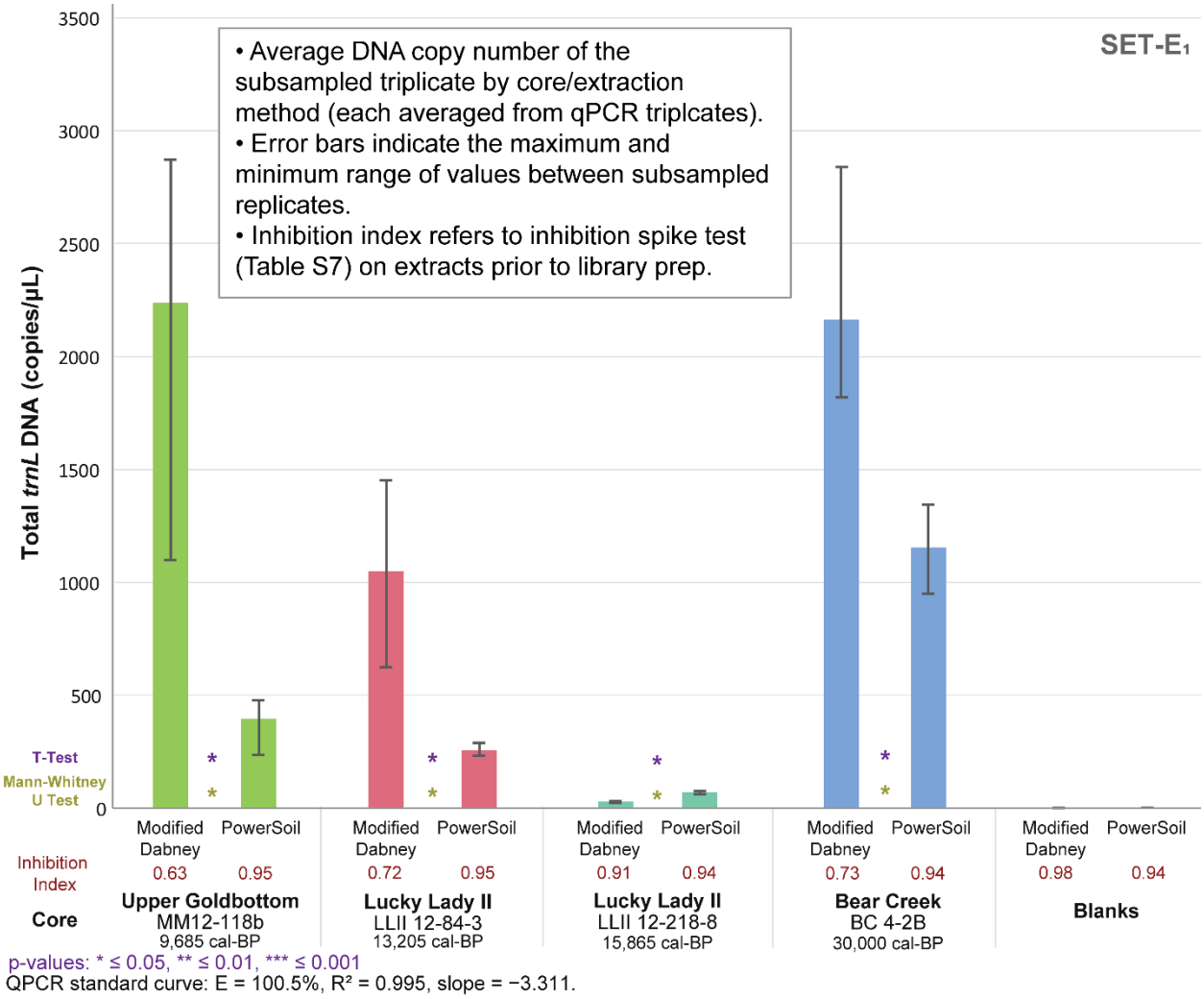

Figure S16 DNA quantification of *trn*L specific library adapted molecules comparing both extraction methods by core (see Table S9 for qPCR specifications). Core LLII 12-217-8 consistently has low DNA recovery, but also a low co-elution of DNA independent inhibition.

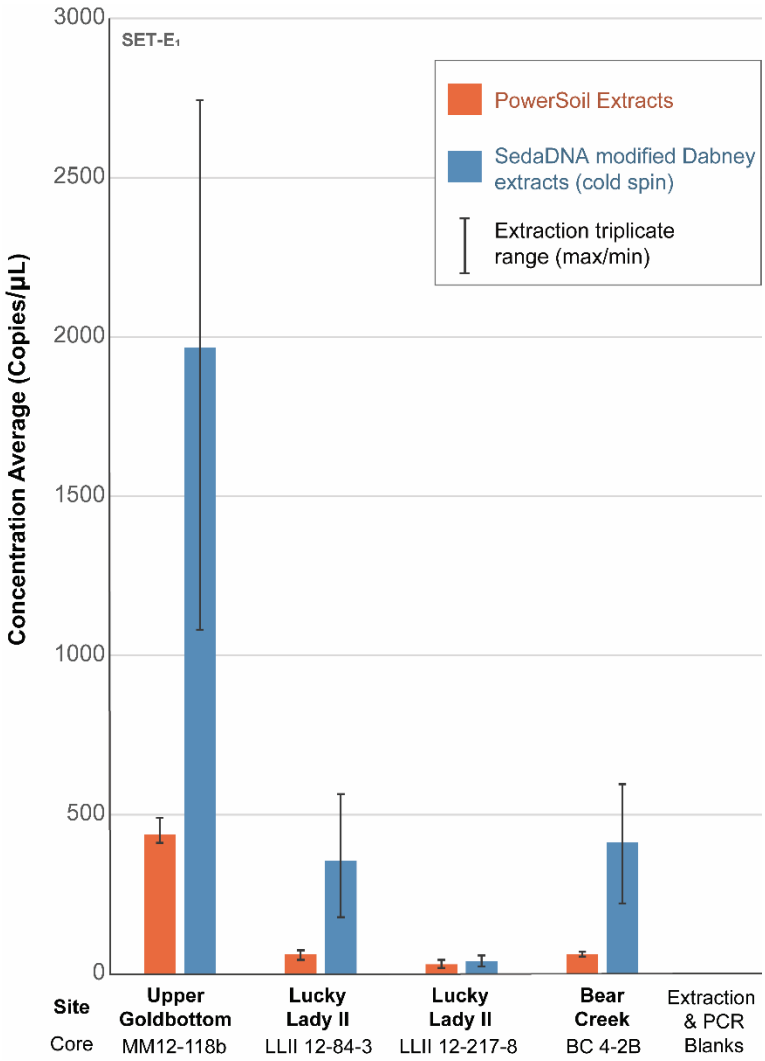

Figure S17 QPCR estimated starting concentration averages by extraction type and site for *trn*L metabarcoded extracts. QPCR standard curve: E = 97.6%, R^2 = 0.998, slope = −3.381.

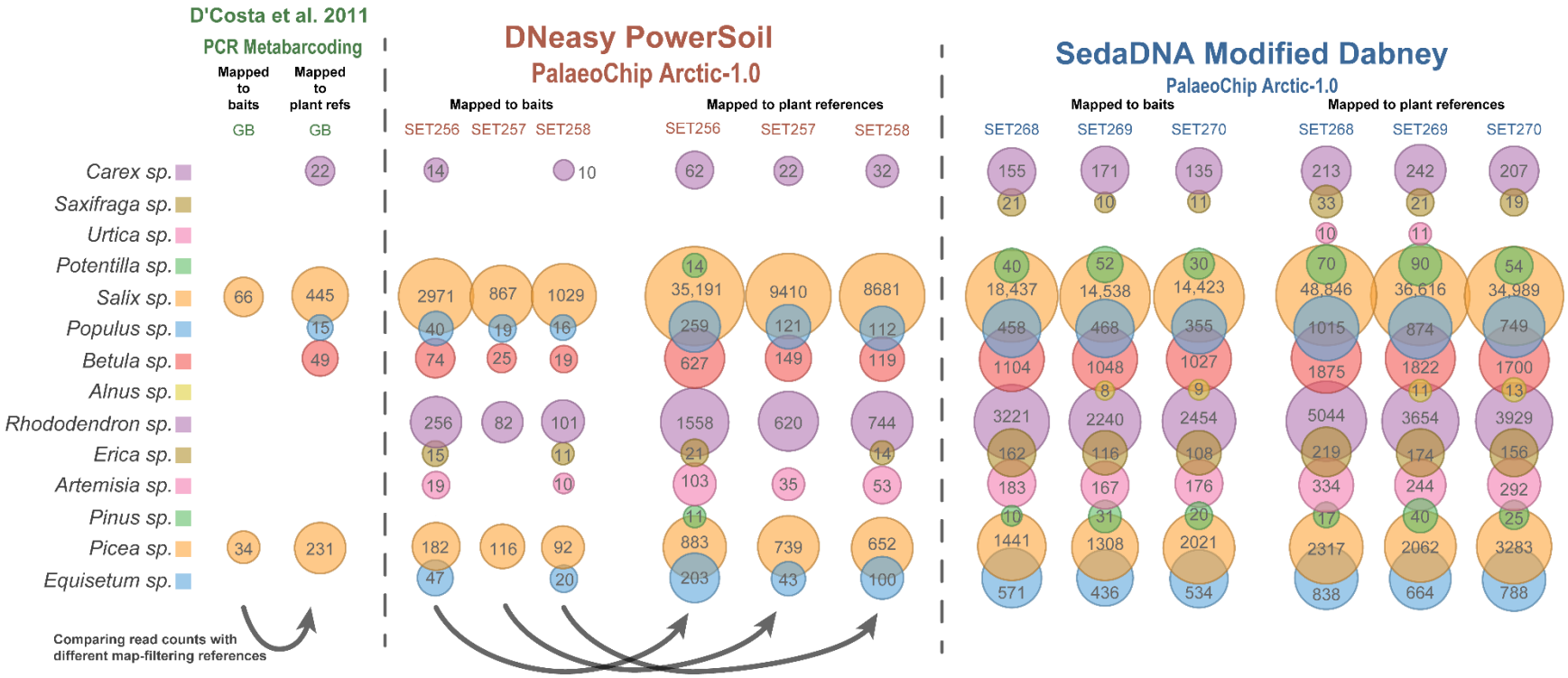

Figure S18 Comparing LCA-assignments between Upper Goldbottom (MM12-118b) libraries map-filtered to the plant and animal baits, and those map-filtered to the plant references. The baits are more conservative for map-filtering, but also might be more biased against metabarcoding reads that do not map well against tiled baits. This can be seen in the first two columns where some taxa are absent from the bait map-filtered variants (SET-E).

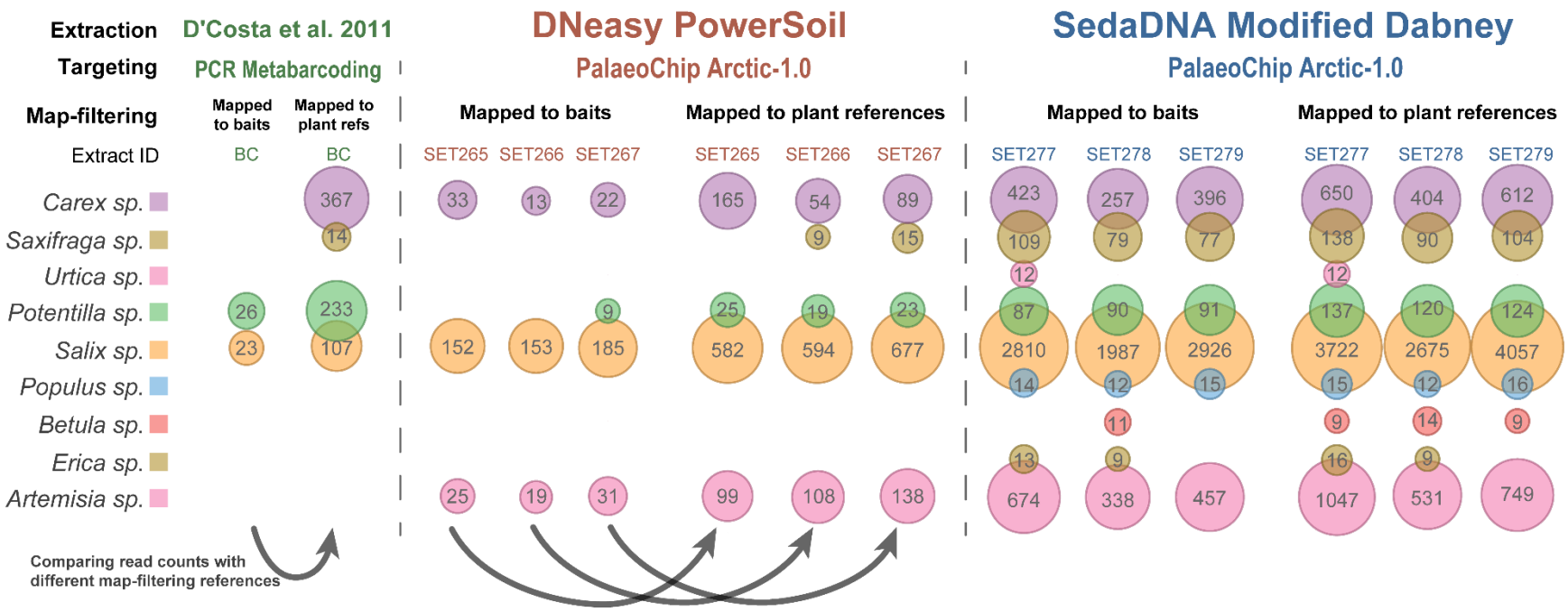

Figure S19 Comparing LCA-assignments between Bear Creek (BC 4-2B) libraries map-filtered to the plant and animal baits, and those map-filtered to the plant references. The baits are more conservative for map-filtering, but also might be more biased against metabarcoding reads that do not map well against tiled baits. This can be seen in the first two columns where some taxa are absent from the bait map-filtered variants (SET-E).

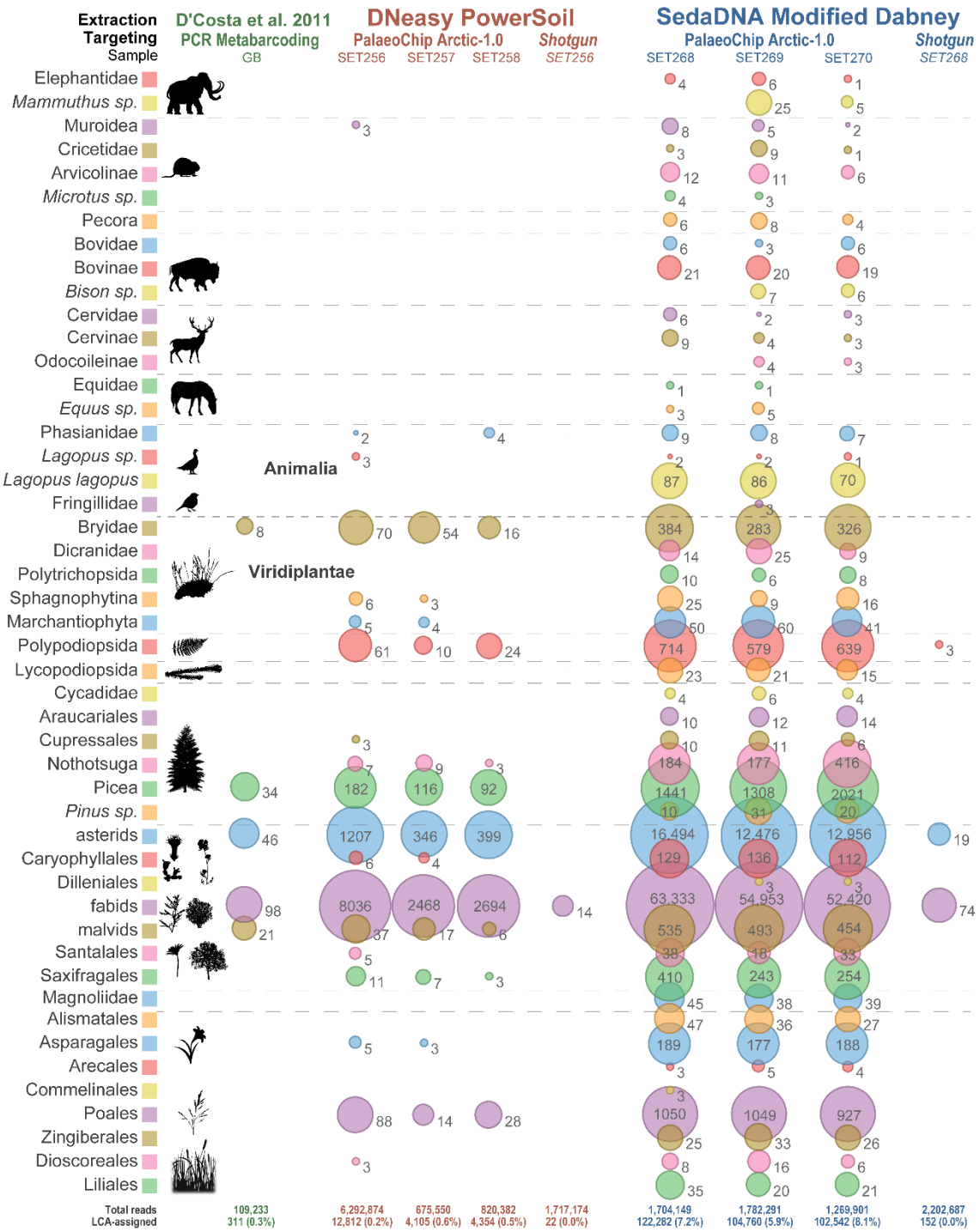

Figure S20 Metagenomic comparison of Upper Goldbottom permafrost core MM12-118b. Reads mapped to animal and plant baits and compared with absolute counts and logarithmically scaled bubbles. Core slice dated to 9,685 cal yr BP (Sadoway, 2014; Mahony, 2015). Values indicate total reads assigned to that taxon node for Animalia, and a clade summation of reads for Viridiplantae. Note: hits to Arecales, Zingiberales, and Diosoreales (along with potentially some others) are likely false positives driven by uneven reference coverages within Commelinids (see Methods subsection 10 in the main text for a discussion of this challenge).

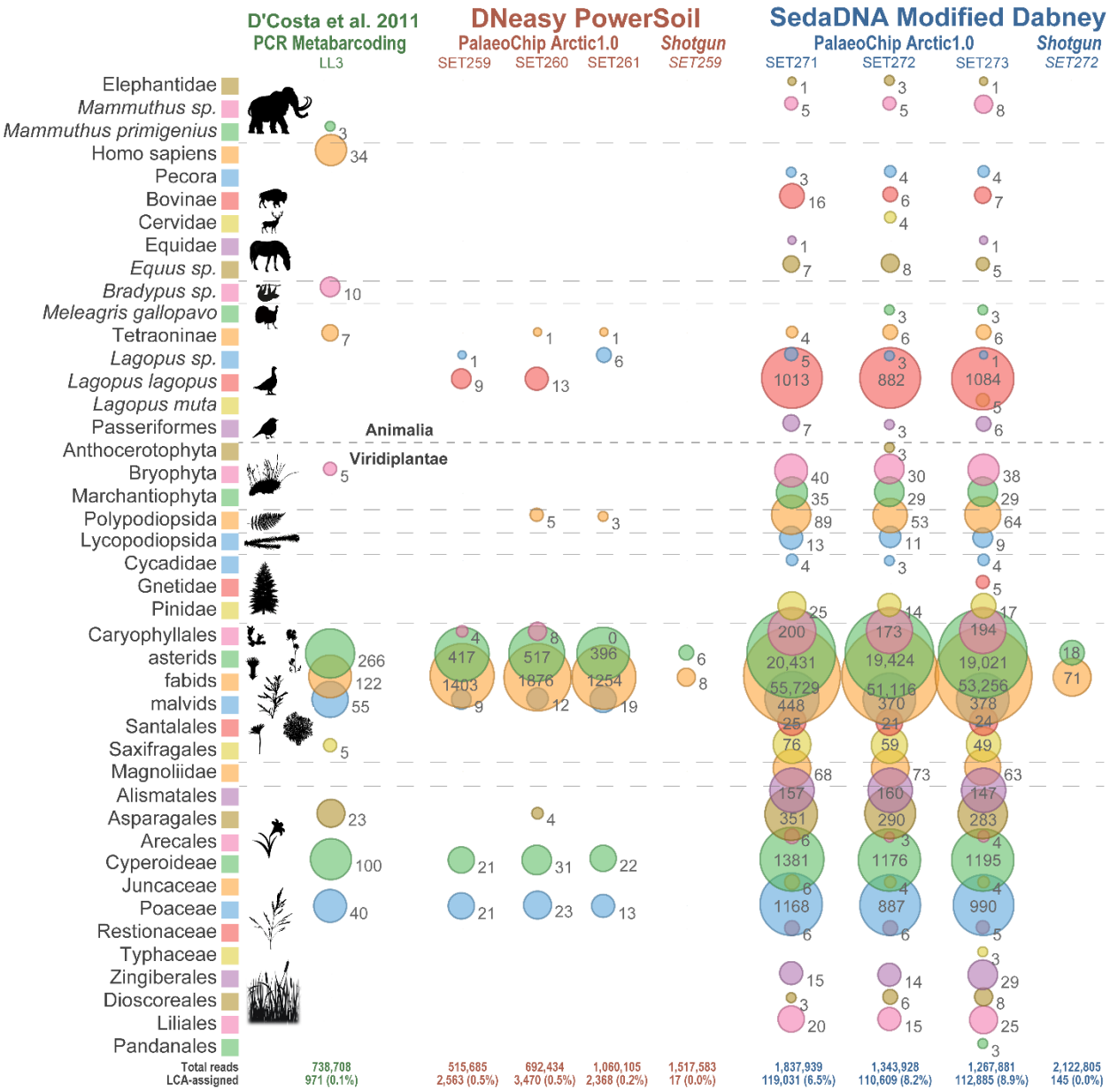

Figure S21 Metagenomic comparison of Lucky Lady II permafrost core LLII-12-84-3, reads mapped to baits, logarithmically scaled bubbles. Core slice dated to 13,205 cal yr BP (Sadoway, 2014). Values indicate total reads assigned to that taxon node for Animalia, and a clade summation of reads for Viridiplantae. See Table 1 for read summaries (SET-E). Note: hits to Arecales, Zingiberales, and Diosoreales (along with potentially some others) are likely false positives driven by uneven reference coverages within Commelinids (see Methods subsection 10 in the main text for a discussion of this challenge).

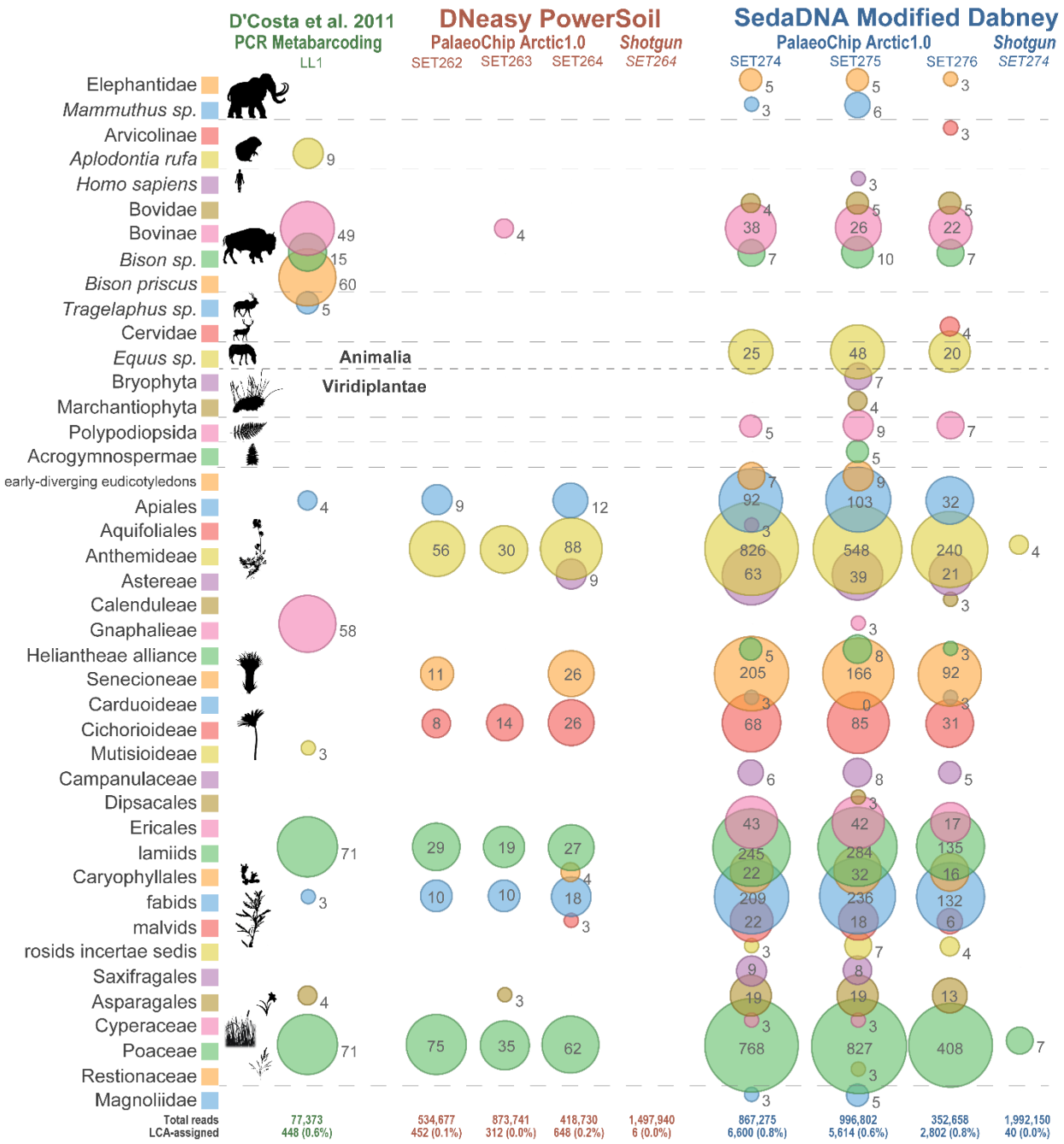

Figure S22 Metagenomic comparison of Lucky Lady II permafrost core LLII-12-217-8, reads mapped to baits, logarithmically scaled bubbles. Core slice dated to 15,865 cal yr BP (Sadoway, 2014). Values indicate total reads assigned to that taxon node for Animalia, and a clade summation of reads for Viridiplantae. See Table 1 for read summaries (SET-E). Note: hits to Arecales, Zingiberales, and Diosoreales (along with potentially some others) are likely false positives driven by uneven reference coverages within Commelinids (see Methods subsection 10 in the main text for a discussion of this challenge).

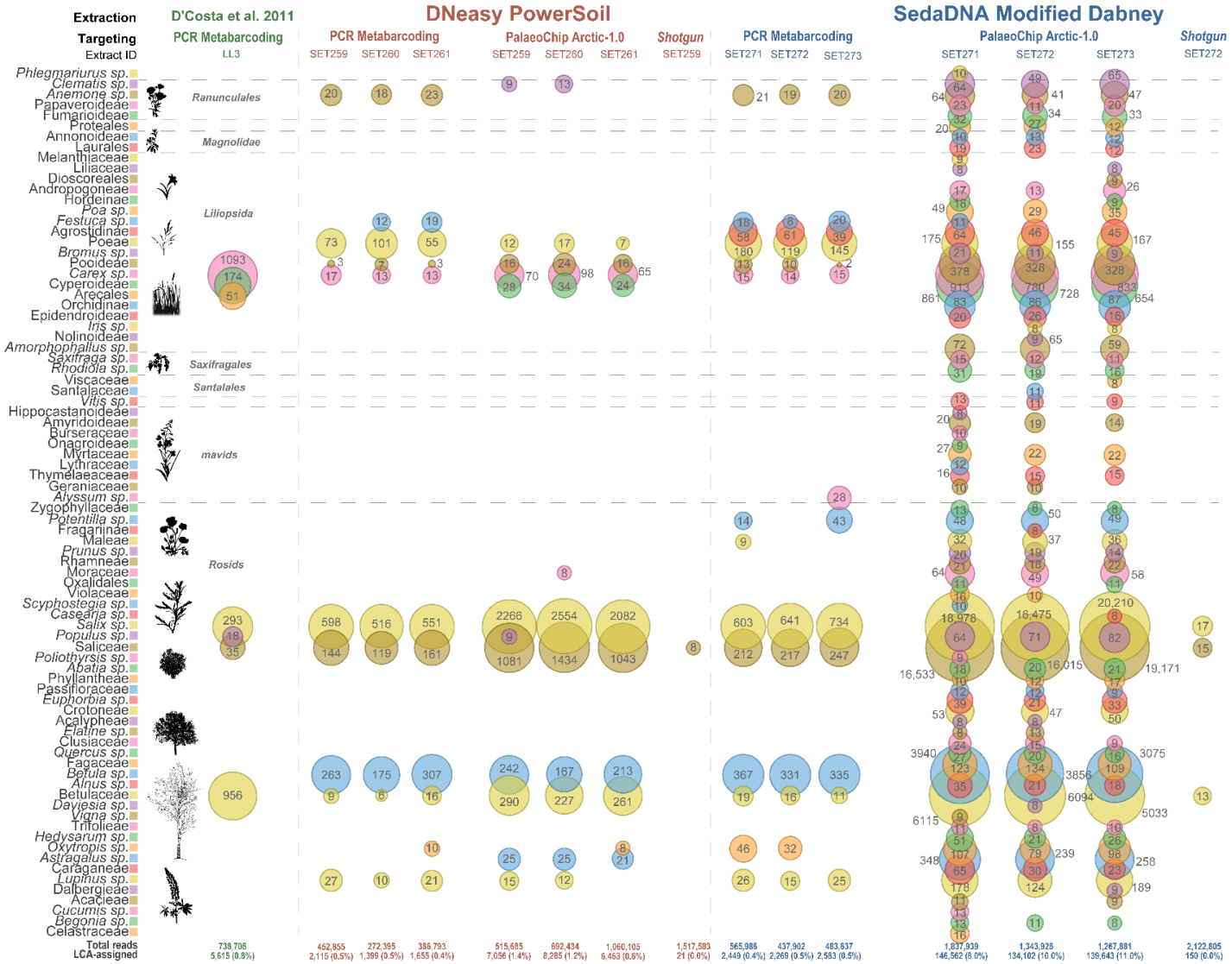

Figure S23 Metagenomic comparison of Lucky Lady II permafrost core LLII-12-84-3 with reads mapped to plant references, 1 of 2. Compared with absolute counts and logarithmically scaled bubbles. Core slice dated to 13,205 cal yr BP (Sadoway, 2014). Values indicate total reads assigned to that taxon node (SET-E).

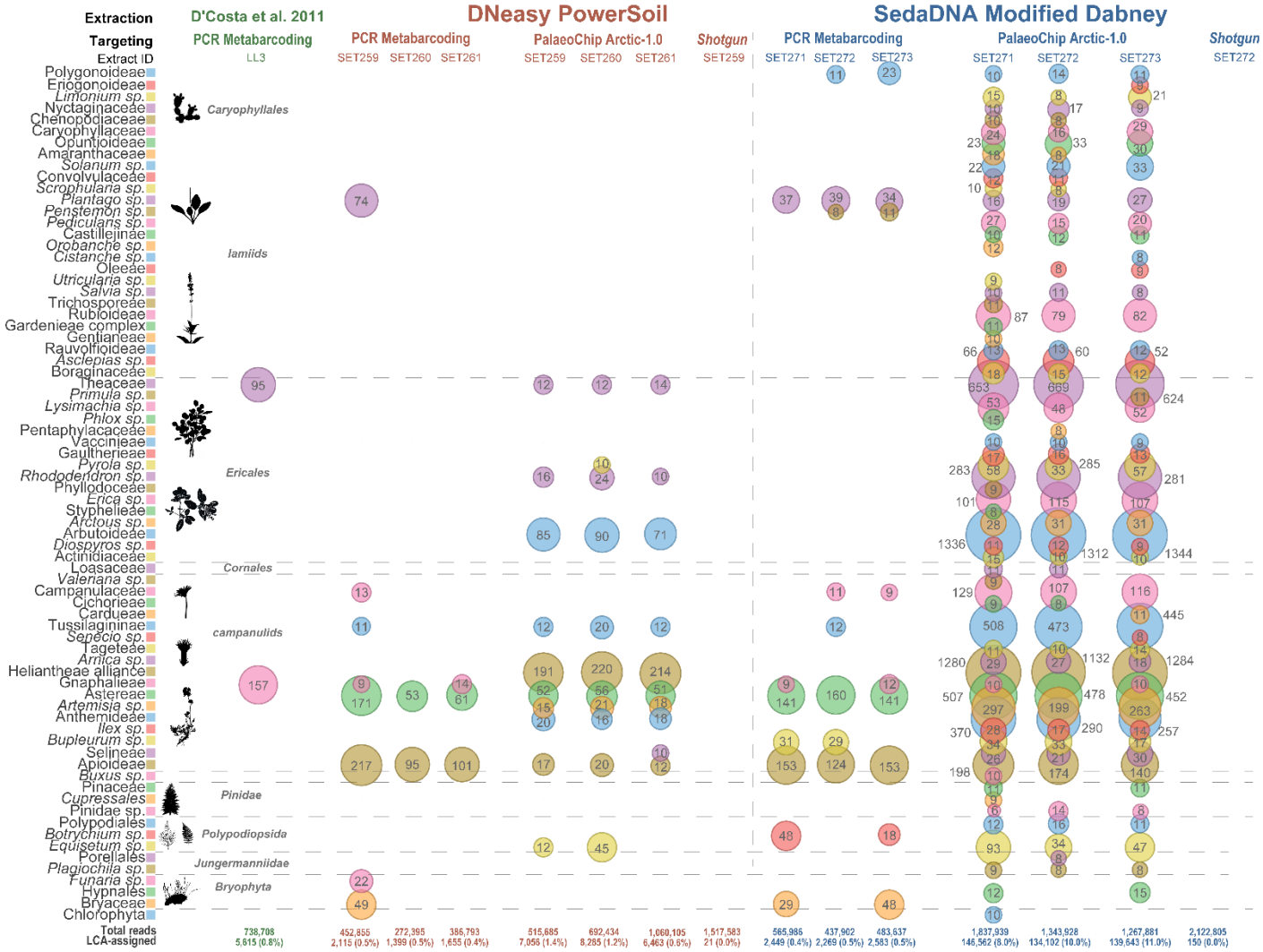

Figure S24 Metagenomic comparison of Lucky Lady II permafrost core LLII-12-84-3 with reads mapped to plant references, 2 of 2. Compared with absolute counts and logarithmically scaled bubbles. Core slice dated to 13,205 cal yr BP (Sadoway, 2014). Values indicate total reads assigned to that taxon node (SET-E).

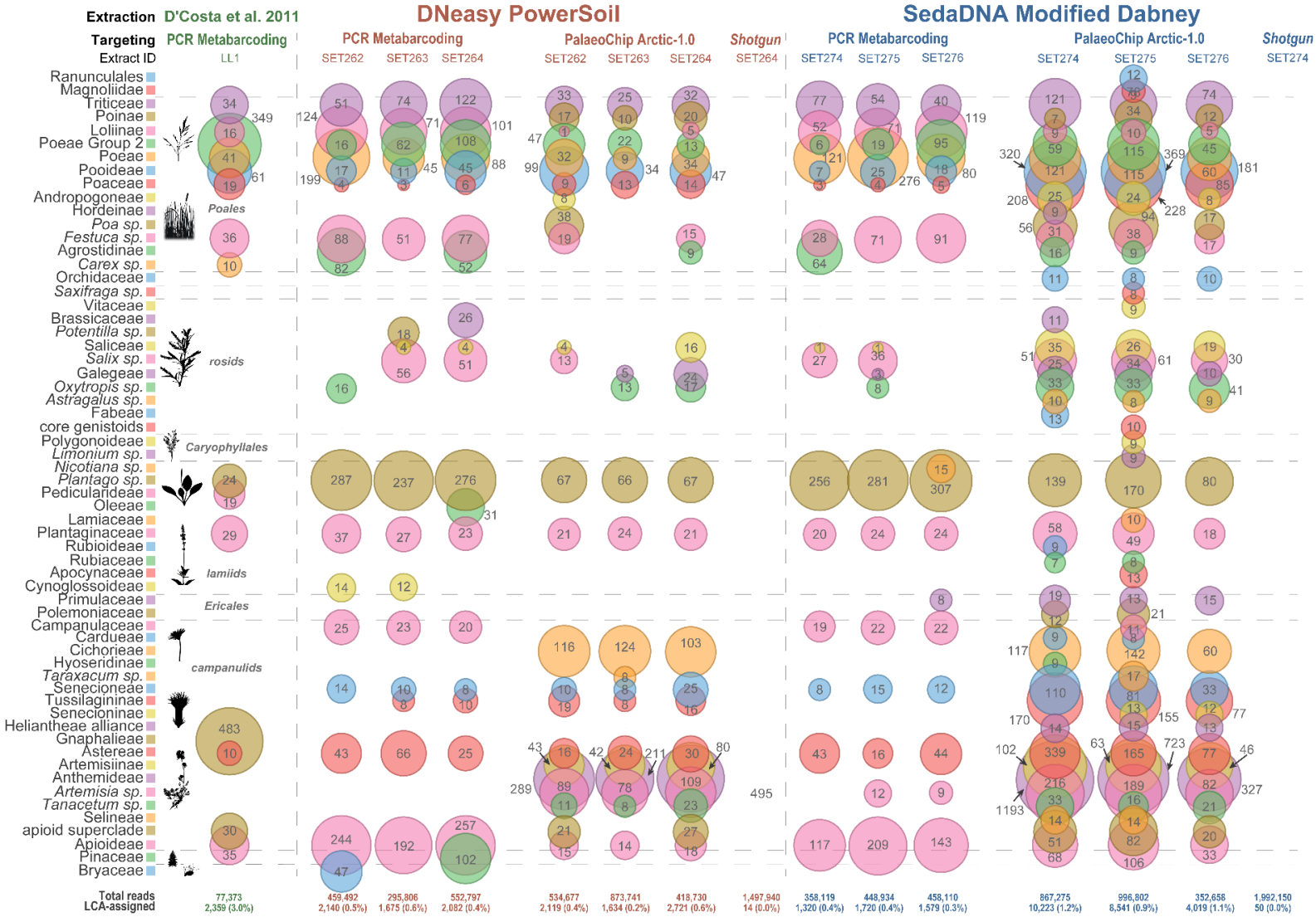

Figure S25 Metagenomic comparison of Lucky Lady II permafrost core LLII-12-217-8 with reads mapped to plant references, 1 of 1. Compared with absolute counts and logarithmically scaled bubbles. Core slice dated to 15,865 cal yr BP (Sadoway, 2014). Values indicate total reads assigned to that taxon node (SET-E). Note: this is the routinely poorly performing core, which we believe contains and abundance of highly degraded DNA and minimal DNA independent inhibition.

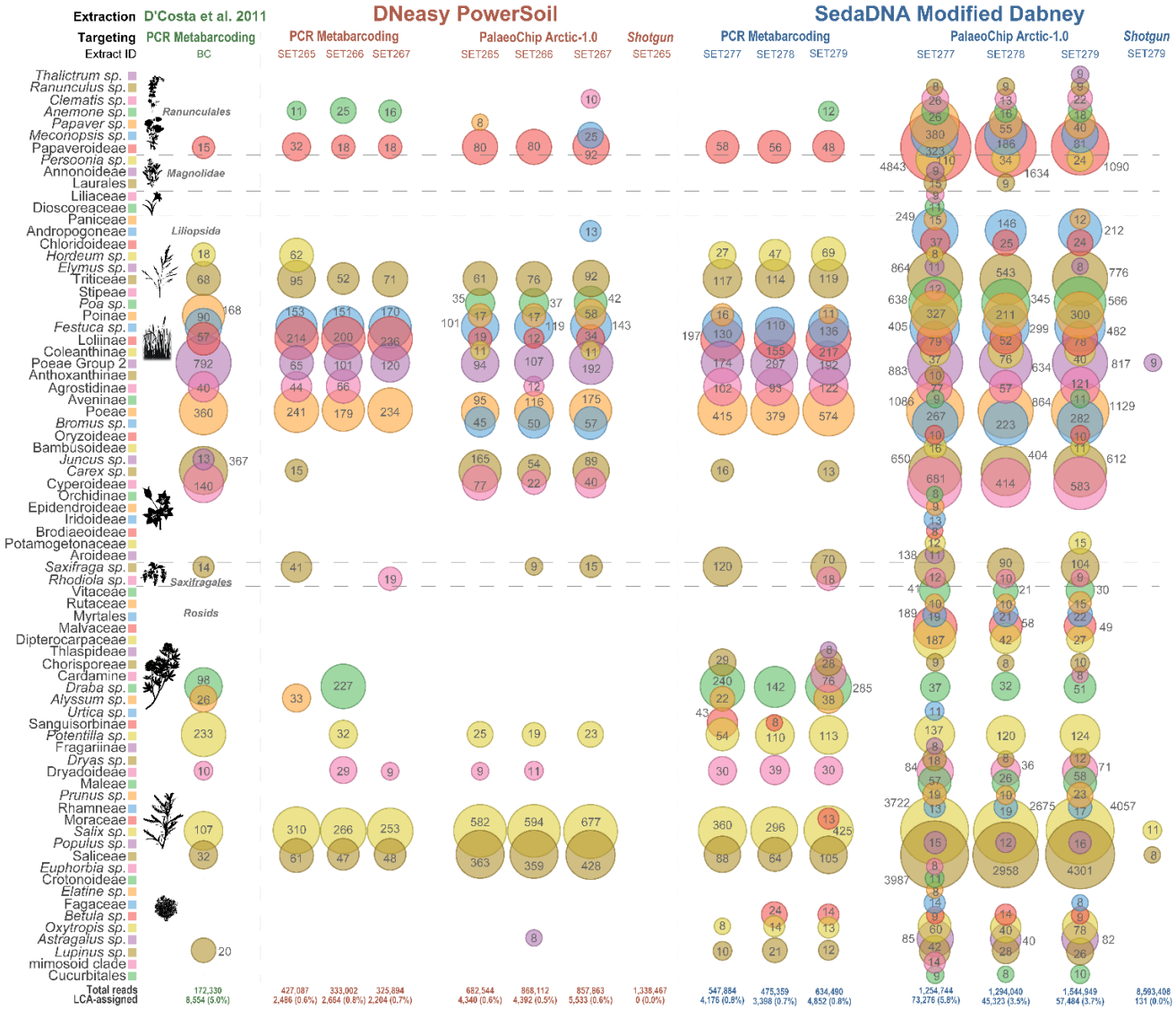

Figure S26 Metagenomic comparison of Bear Creek permafrost core BC 4-2B with reads mapped to plant references, 1 of 2. Compared with absolute counts and logarithmically scaled bubbles. Core slice dated to ~30,000 cal yr BP (D'Costa et al., 2011; Sadoway, 2014; Mahony, 2015). Values indicate total reads assigned to that taxon node (SET-E).

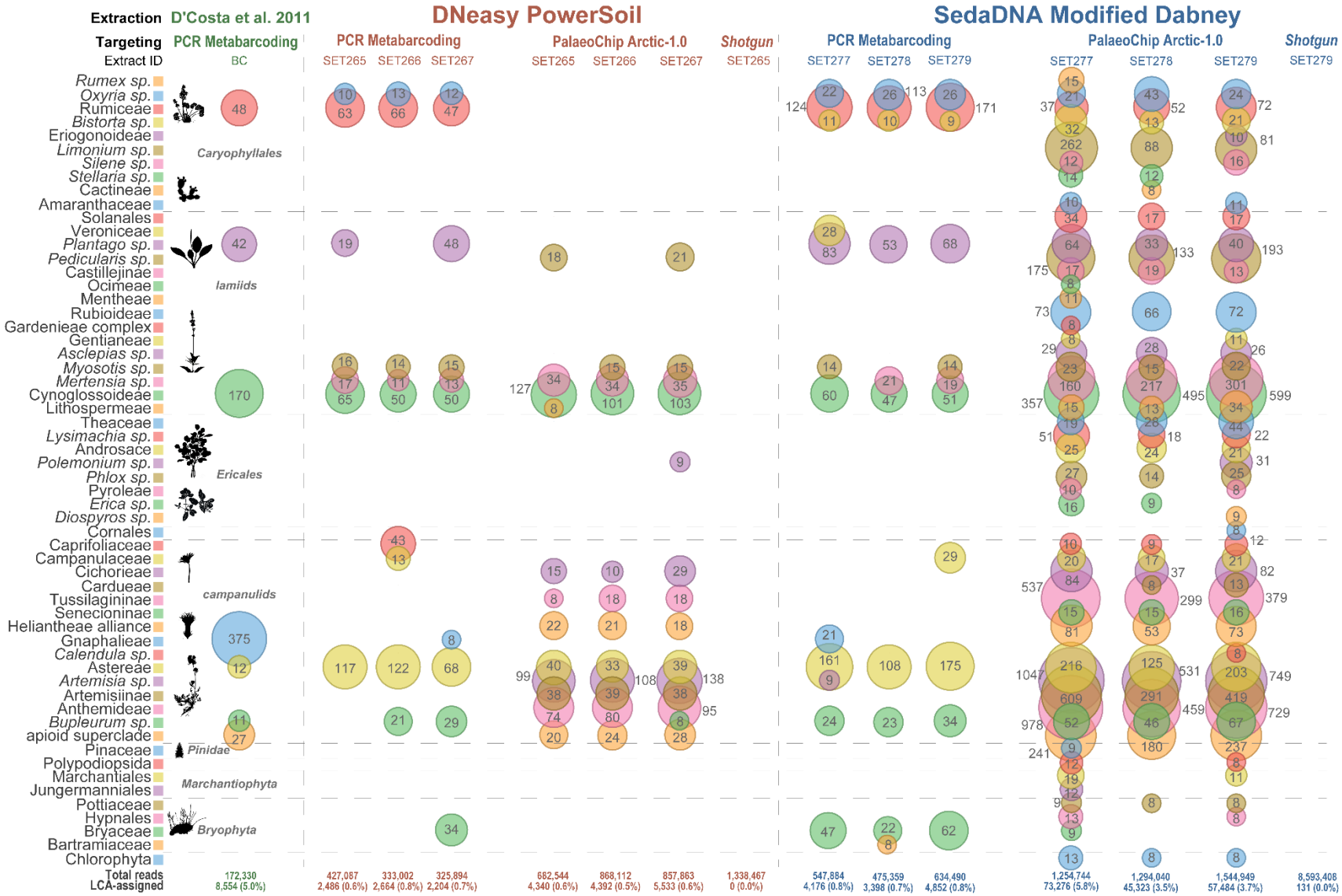

Figure S27 Metagenomic comparison of Bear Creek permafrost core BC 4-2B with reads mapped to plant references, 2 of 2. Compared with absolute counts and logarithmically scaled bubbles. Core slice dated to ~30,000 cal yr BP (D'Costa et al., 2011; Sadoway, 2014; Mahony, 2015). Values indicate total reads assigned to that taxon node (SET-E).

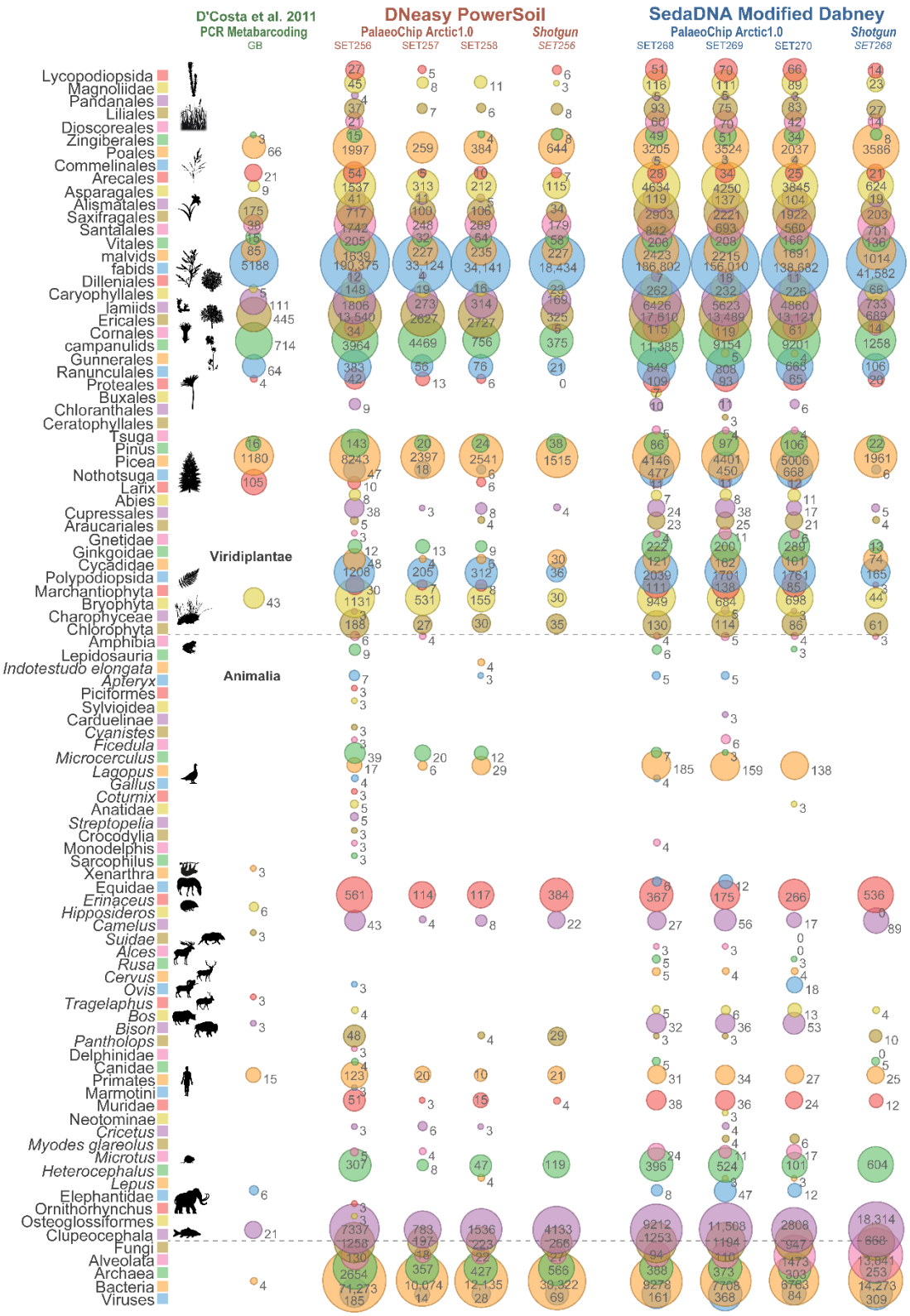

Figure S28 Metagenomic comparison of Upper Goldbottom permafrost core MM12-118b, all reads (not map-filtered), absolute counts, bubbles log-scaled. Core slice dated to 9,685 cal yr BP (Sadoway, 2014; Mahony, 2015). Values indicate total reads assigned to that taxon node for Animalia, and a clade summation of reads for Viridiplantae (SET-E).

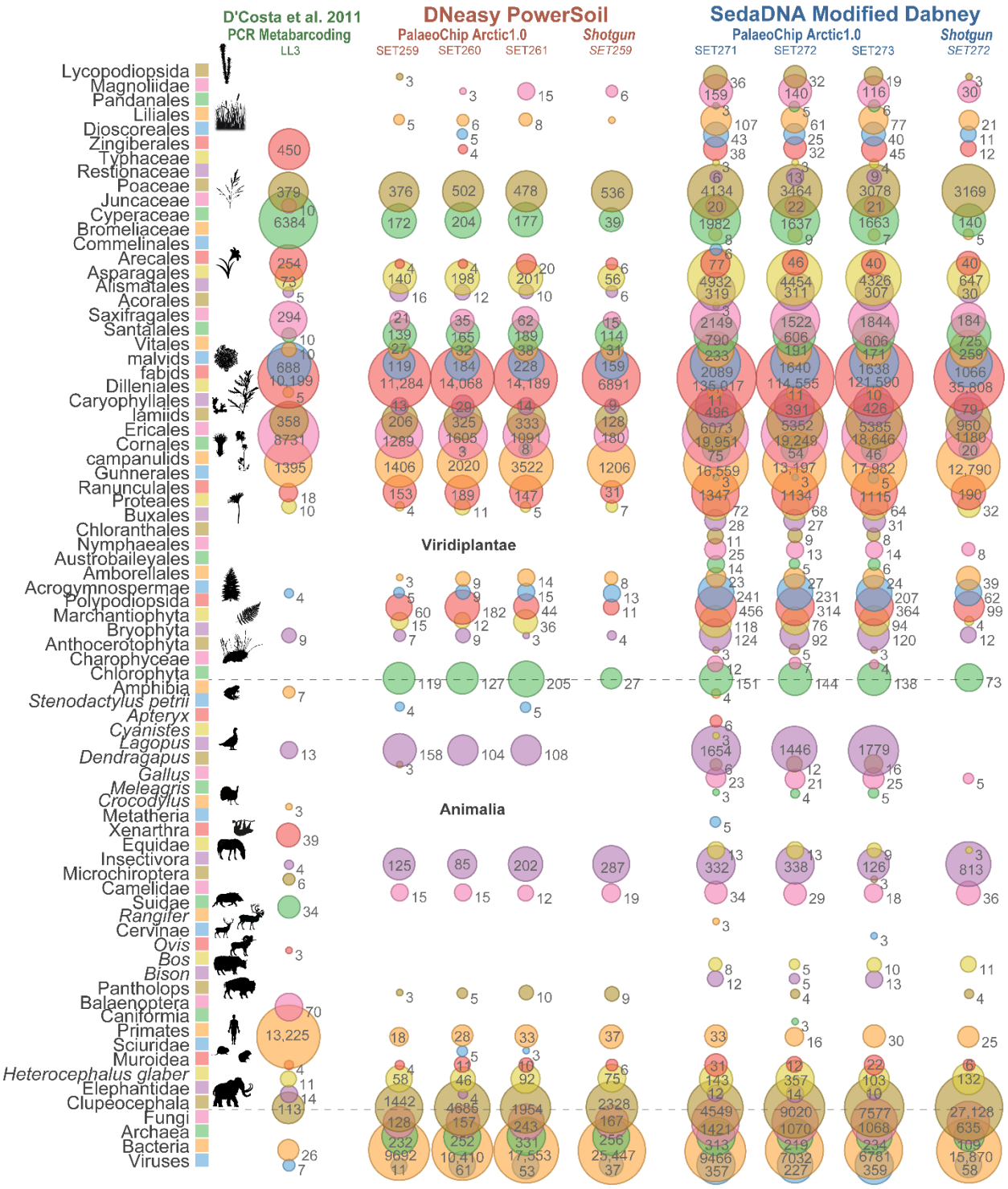

Figure S29 Metagenomic comparison of Lucky Lady II permafrost core LLII-12-84-3, all reads (not map-filtered), absolute counts, bubbles log-scaled. Core slice dated to 13,205 cal yr BP (Sadoway, 2014). Values indicate total reads assigned to that taxon node for Animalia, and a clade summation of reads for Viridiplantae (SET-E).

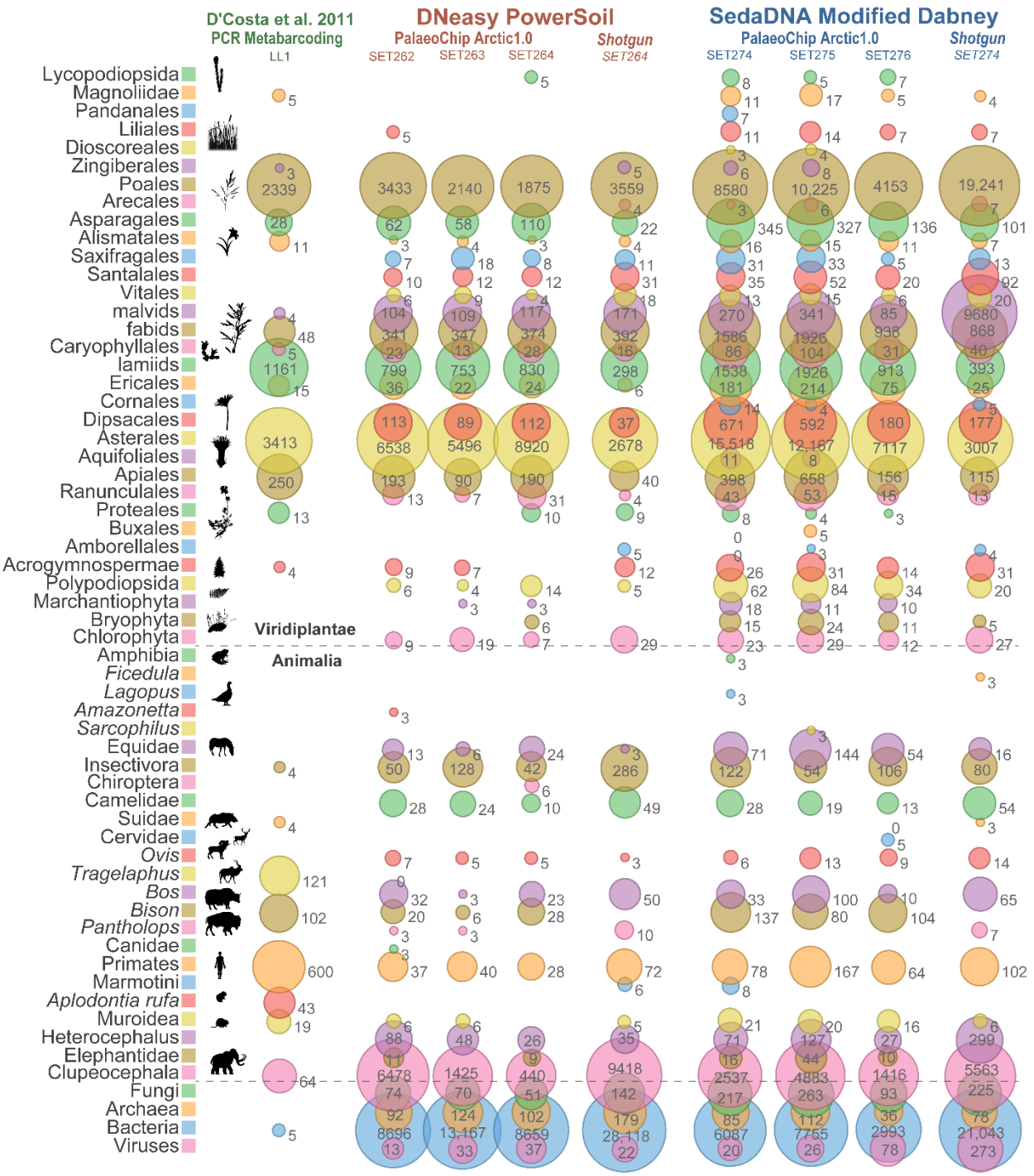

Figure S30 Metagenomic comparison of Lucky Lady II permafrost core LLII-12-217-8, all reads (not map-filtered), absolute counts, bubbles log-scaled. Core slice dated to 15,865 cal yr BP (Sadoway, 2014). Values indicate total reads assigned to that taxon node for Animalia, and a clade summation of reads for Viridiplantae (SET-E).

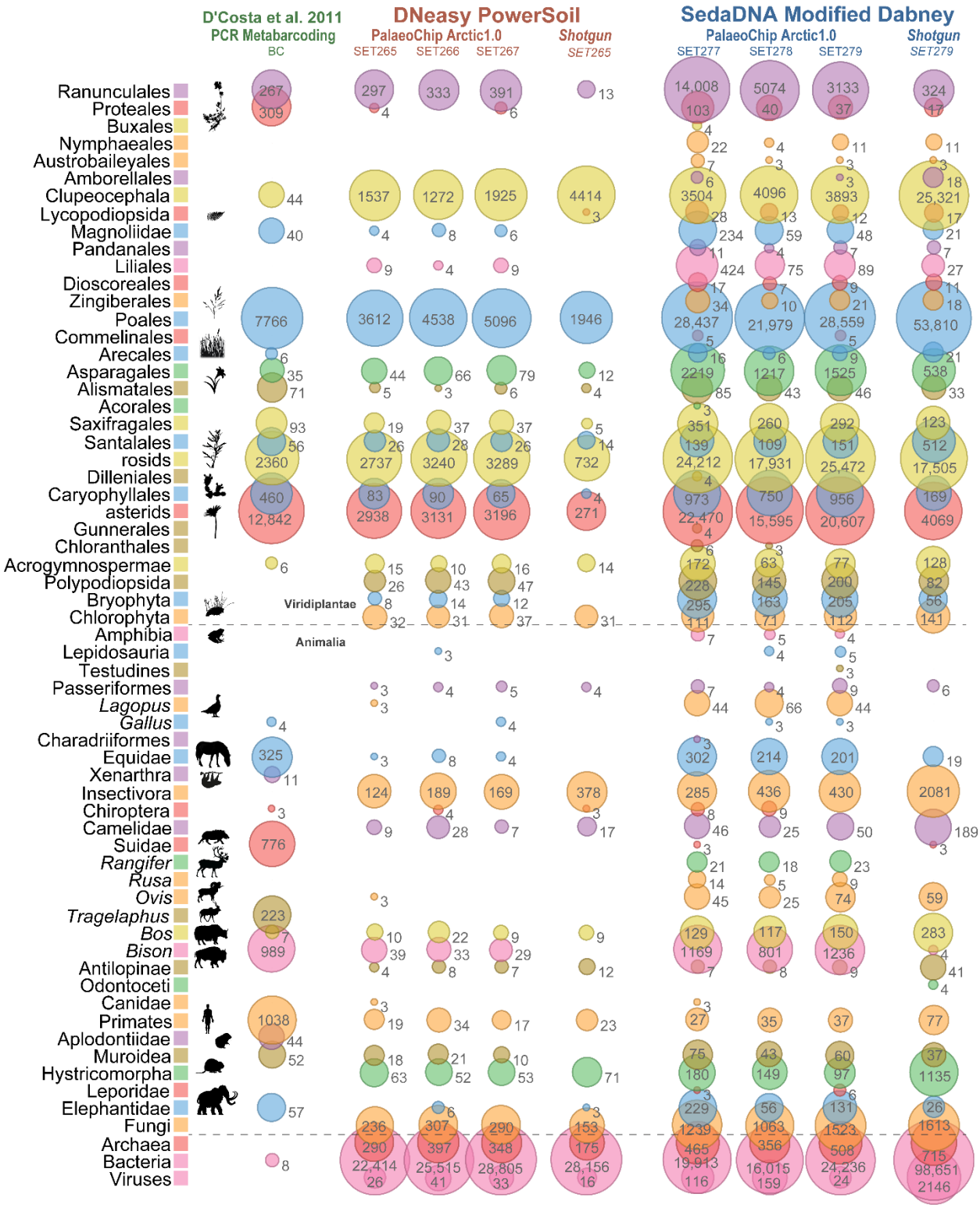

Figure S31 Metagenomic comparison of Bear Creek permafrost core BC 4-2B, all reads (not map-filtered), absolute counts, bubbles log-scaled. Core slice dated to ~30,000 cal yr BP (D'Costa et al., 2011; Sadoway, 2014; Mahony, 2015). Values indicate total reads assigned to that taxon node for Animalia, and a clade summation of reads for Viridiplantae (SET-E).

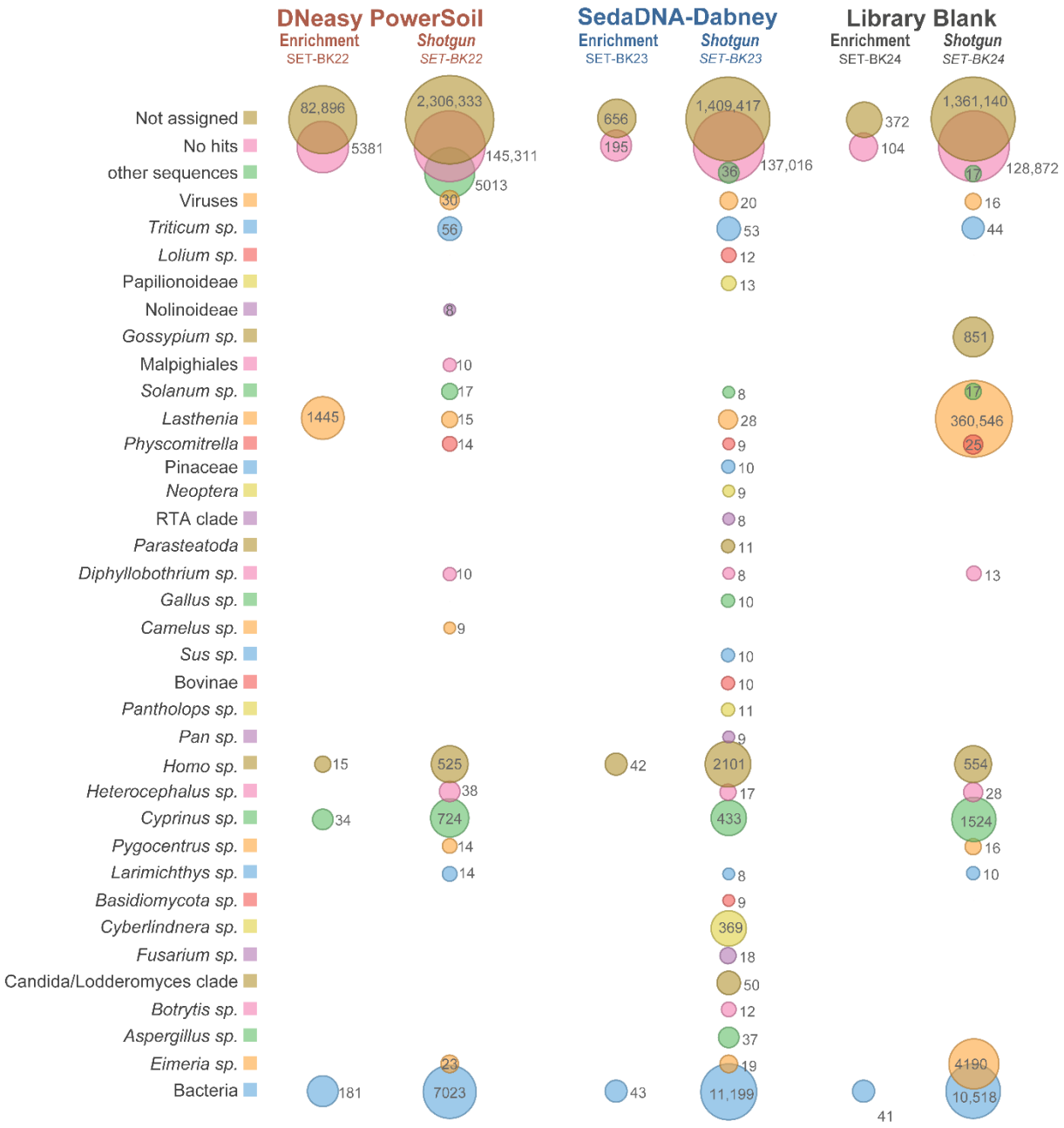

Figure S32 Metagenomic comparison of extraction and library blanks, all reads (not map-filtered), absolute counts, bubbles log-scaled. Values indicate total reads assigned to that taxon node; uncollapsed to genera (SET-E).

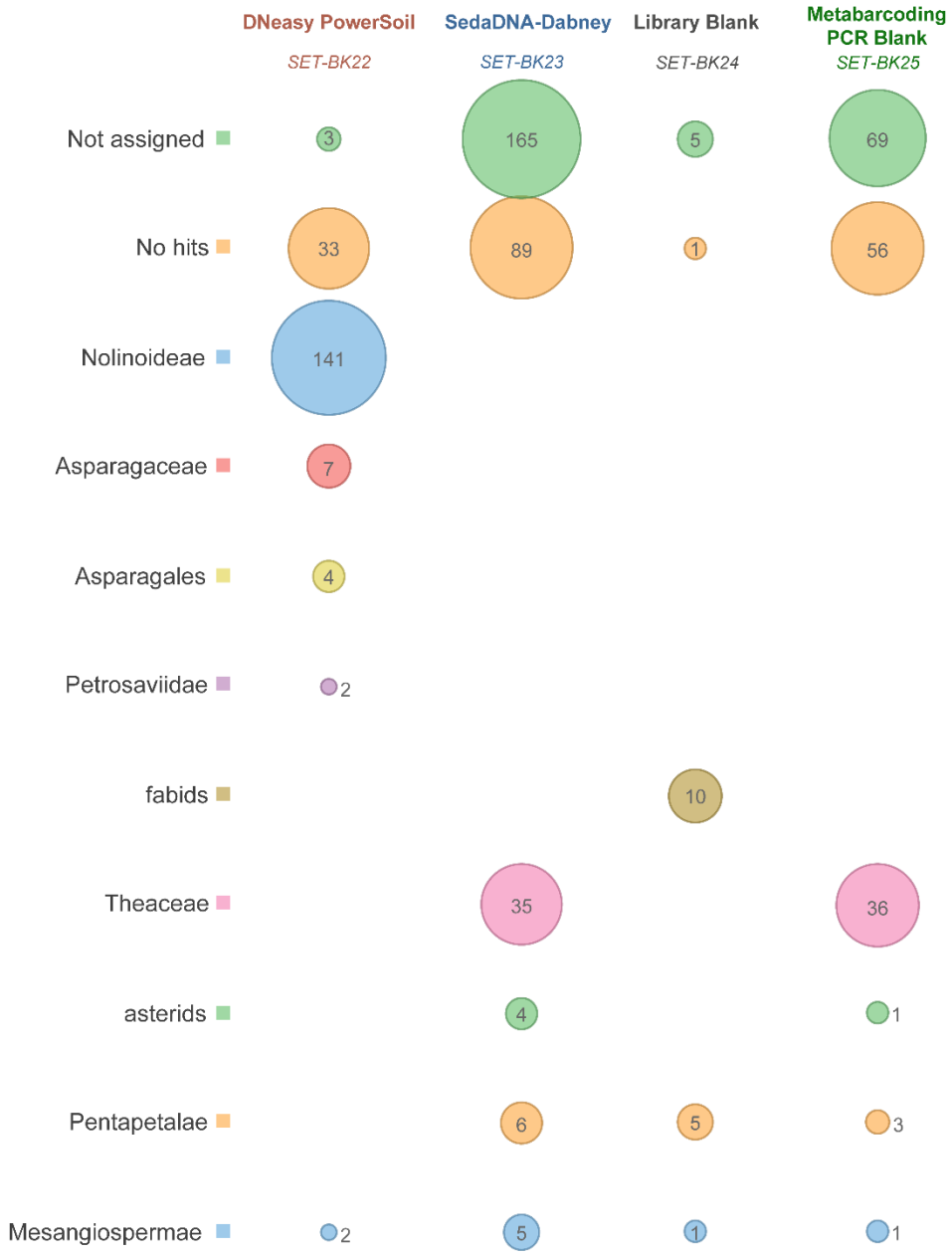

Figure S33 Metagenomic comparison of the metabarcoding blanks from extraction, library preparation, and PCR map-filtered to the plant references (*rbc*L, *mat*K, *trn*L) displaying all reads fully uncollapsed to the lowest LCA assigned nodes with log-scaled bubbles for visual normalization. Values indicate total reads assigned to that taxon node (fully uncollapsed) (SET-E). Enriched and shotgun blank controls mapped to the plant references had 0 reads that passed map-filtering (see Table S23).

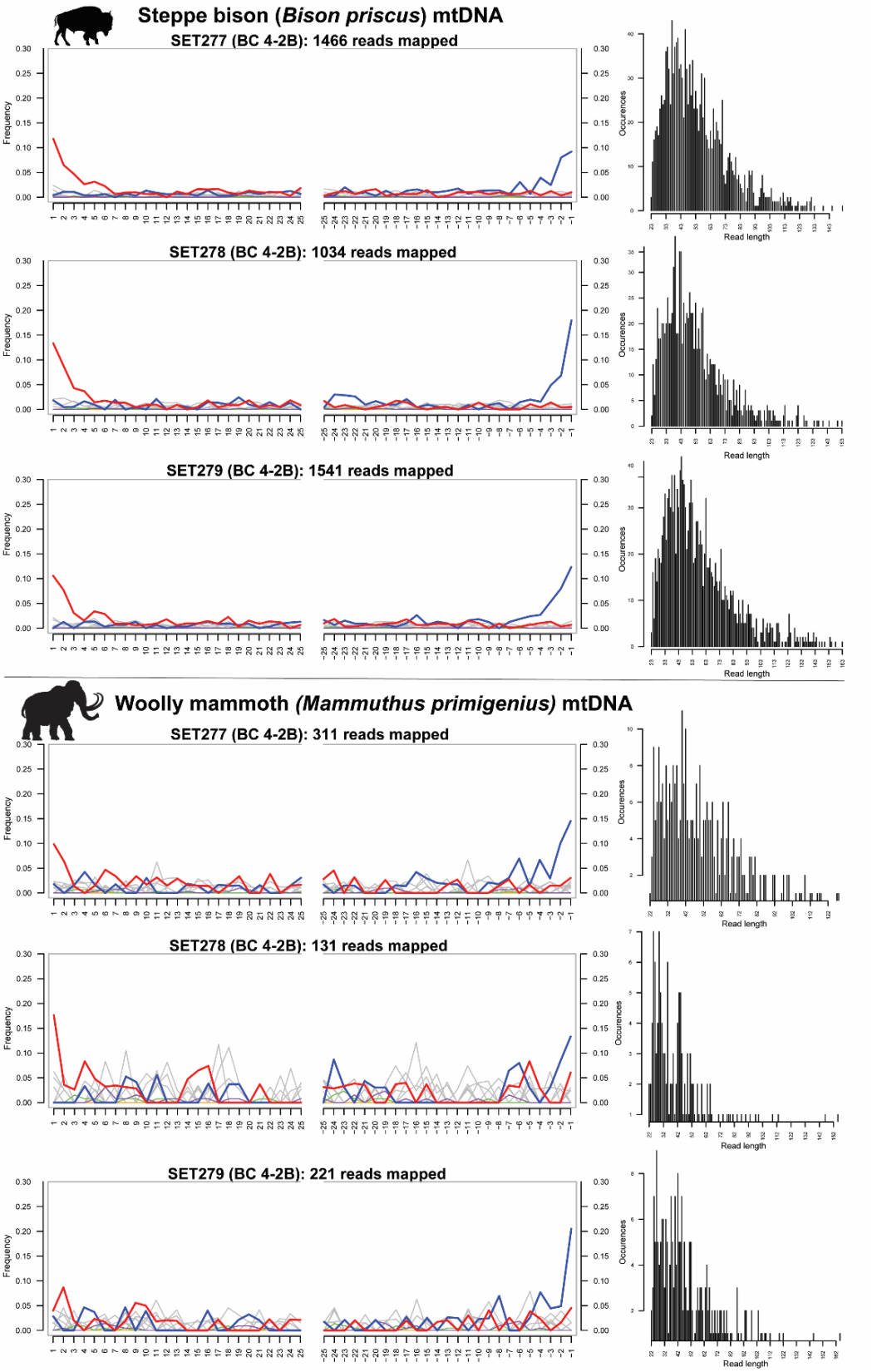

Figure S34 *MapDamage* plots for *Bison priscus* and *Mammuthus primigenius.* Minimum length = 24 bp, minimum mapping quality = 30 (SET-E).

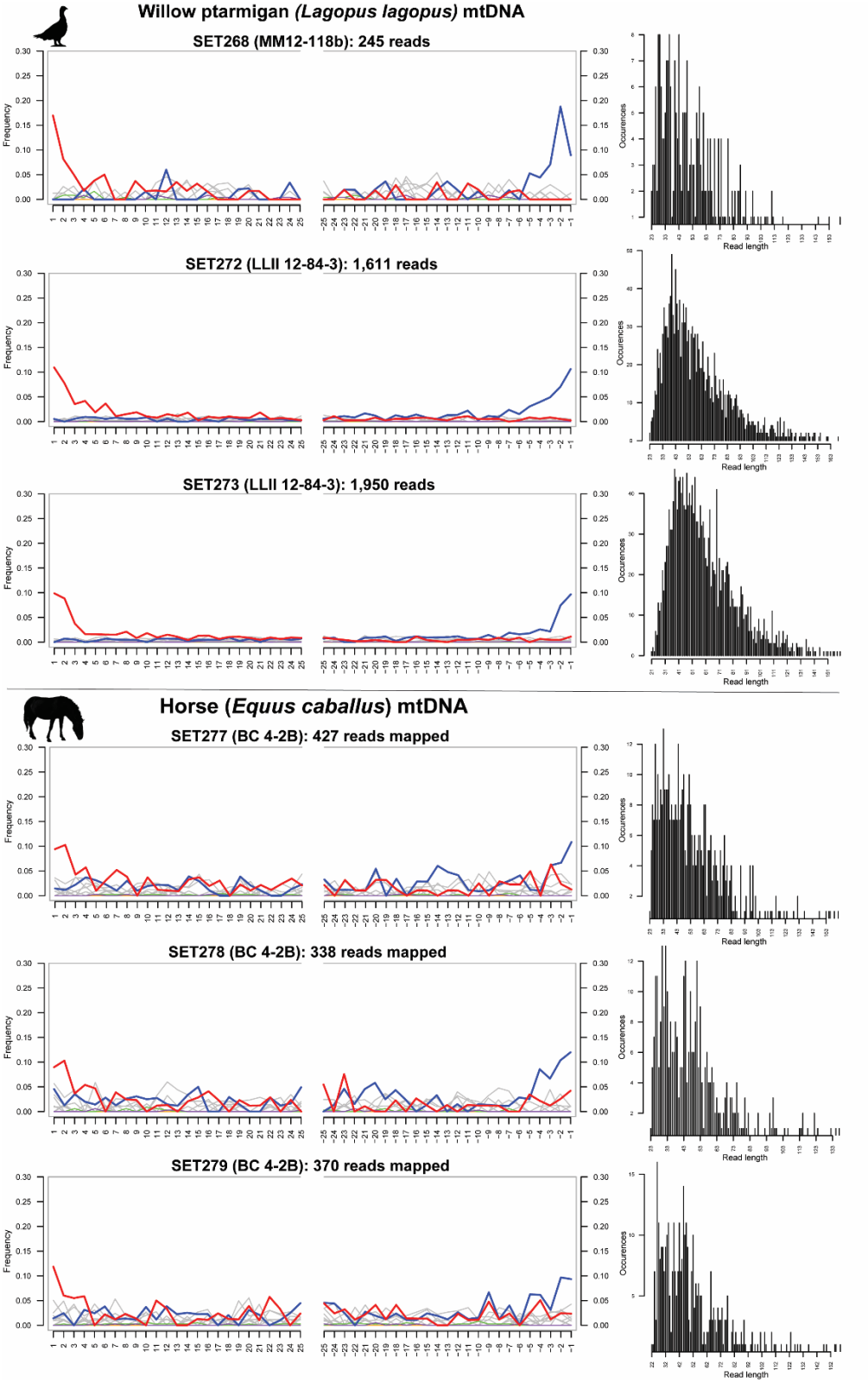

Figure S35 *MapDamage* plots for *Lagopus lagopus* and *Equus caballus.* Minimum length = 24 bp, minimum mapping quality = 30 (SET-E).

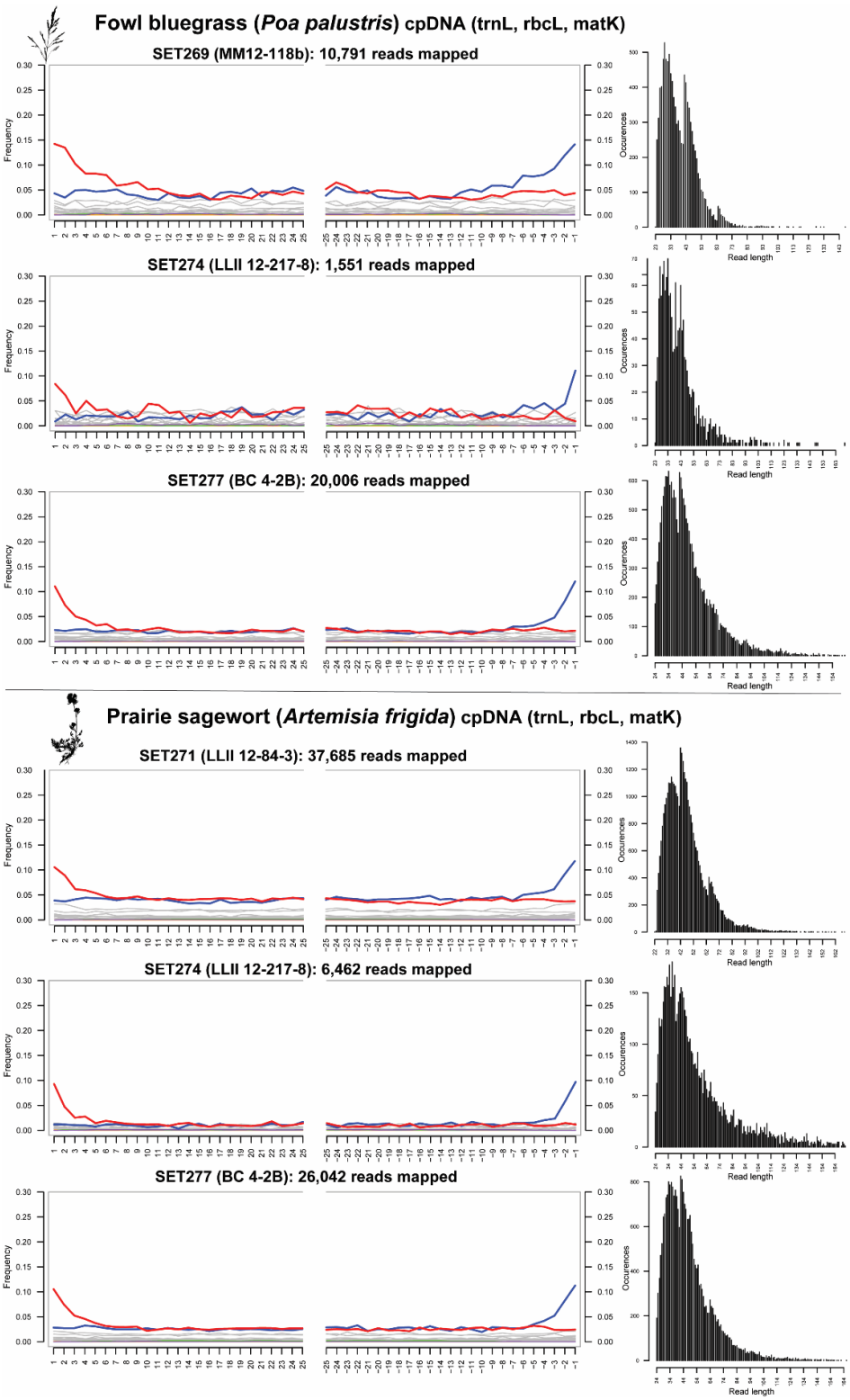

Figure S36 *MapDamage* plots for *Poa palustris and Artemisia figida*. Minimum length = 24 bp, minimum mapping quality = 30. We suspect that the biomodial distribution of the fragment length distributions is due to non-specific mapping of closely related taxa in conserved regions of these cpDNA barcoding loci (SET-E).

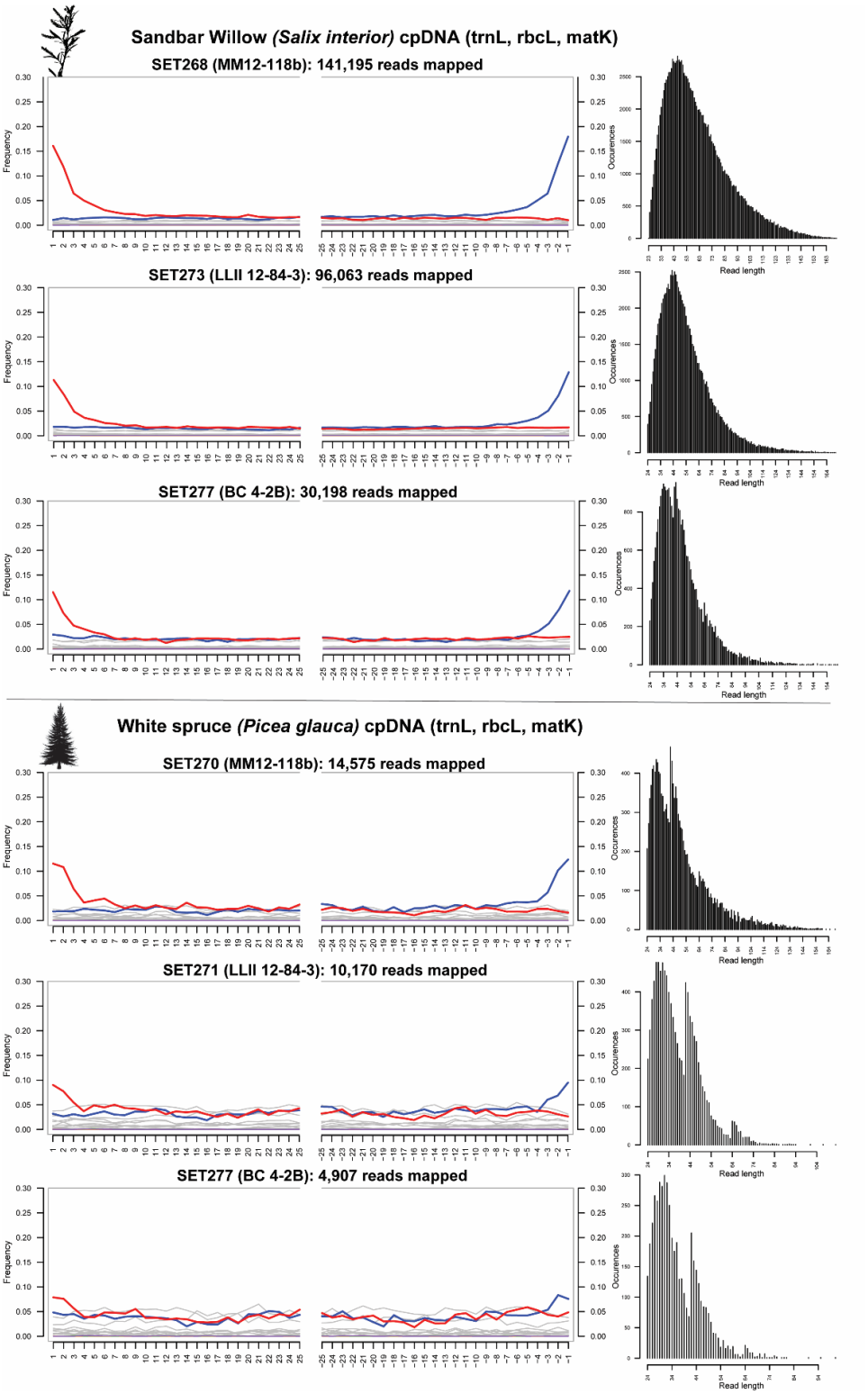

Figure S37 *MapDamage* plots for *Salix interior* and *Picea glauca.* Minimum length = 24 bp, minimum mapping quality = 30. We suspect that the biomodial distribution of the fragment length distributions is due to non-specific mapping of closely related taxa in conserved regions of these cpDNA barcoding loci (SET-E).

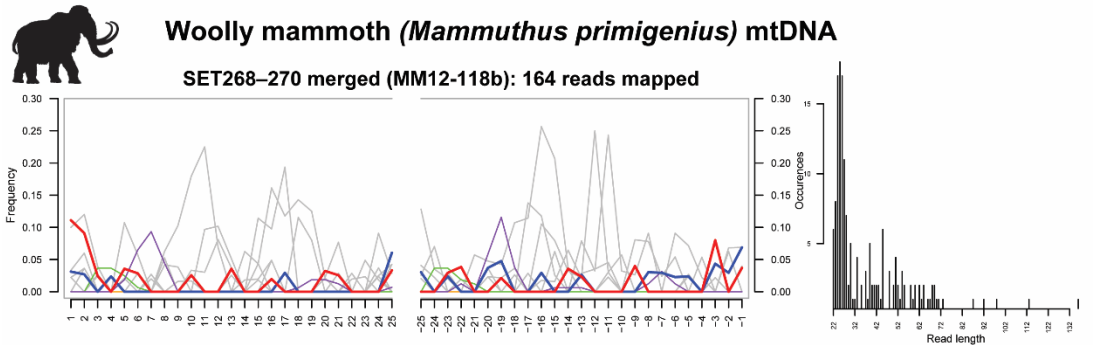

Figure S38 *MapDamage* MM12-118b merged replicates plot for *Mammuthus primigenius*. Minimum length = 24 bp, minimum mapping quality = 30. Read counts are too low (not enough overlap on the mitogenome to assess termini deamination) despite concatenating the 3 extractions to assess damage. However, fragments are characteristically short and map well to multiple loci across the mitogenome. Greater sequencing depth is needed to better assess this signal (SET-E).

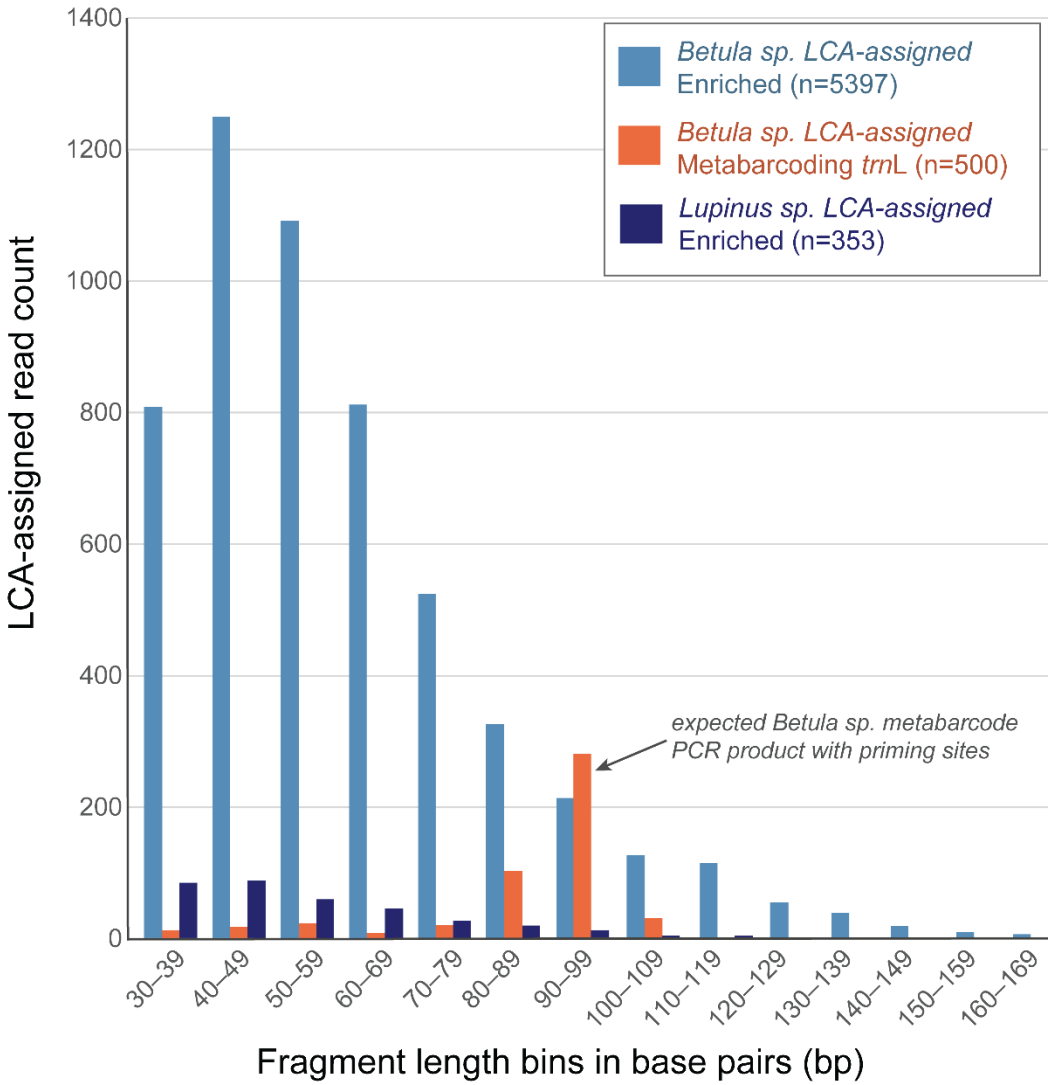

Figure S39 Histogram of fragment lengths for reads assigned to *Betula sp.* with enrichment and metabarcoding, as well those assigned to *Lupinus sp.* with enrichment for the Upper Goldbottom core (MM12-118b). The abnormally short metabarcode amplicons (30–70 bp) for *Betula sp.* might be some form of PCR artefacts or unmerged reads. Inspecting a subset of these short reads still return assignments of *Betula sp.* (100% identity) even with the top 20,000 hits on web-*BLASTn* (SET-E).

Appendix A References

Al-Soud, W.A., Radstrom, P., 1998. Capacity of nine thermostable DNA polymerases to mediate DNA amplification in the presence of PCR-inhibiting samples. Applied and Environmental Microbiology 64, 3748–3753.

Alaeddini, R., 2012. Forensic implications of PCR inhibition - A review. Forensic Science International: Genetics 6, 297–305. doi:10.1016/j.fsigen.2011.08.006

Arnold, L.J., Roberts, R.G., Macphee, R.D.E., Haile, J.S., Brock, F., Möller, P., Froese, D.G., Tikhonov, A.N., Chivas, A.R., Gilbert, M.T.P., Willerslev, E., 2011. Paper II - Dirt, dates and DNA: OSL and radiocarbon chronologies of perennially frozen sediments in Siberia, and their implications for sedimentary ancient DNA studies. Boreas 40, 417–445. doi:10.1111/j.1502-3885.2010.00181.x

Benson, D.A., Cavanaugh, M., Clark, K., Karsch-Mizrachi, I., Ostell, J., Pruitt, K.D., Sayers, E.W., 2018. GenBank. Nucleic Acids Research 46, D41–D47. doi:10.1093/nar/gkx1094

Bezanilla, M., Manne, S., Laney, D.E., Lyubchenko, Y.L., Hansma, H.G., 1995. Adsorption of DNA to Mica, Silylated Mica, and Minerals: Characterization by Atomic Force Microscopy. Langmuir 11, 655–659. doi:10.1021/la00002a050

Blum, S.A.E., Lorenz, M.G., Wackernagel, W., 1997. Mechanism of retarded DNA degradation and prokaryotic origin of DNases in nonsterile soils. Systematic and Applied Microbiology 20, 513–521. doi:10.1016/S0723-2020(97)80021-5

Camacho, C., Coulouris, G., Avagyan, V., Ma, N., Papadopoulos, J., Bealer, K., Madden, T.L., 2009. BLAST+: Architecture and applications. BMC Bioinformatics 10, 1–9. doi:10.1186/1471-2105-10-421

CBOL Plant Working Group, 2009. A DNA barcode for land plants. Proceedings of the National Academy of Sciences of the United States of America 106, 12794–7. doi:10.1073/pnas.0905845106

Cleaves, H.J., Crapster-Pregont, E., Jonsson, C.M., Jonsson, C.L., Sverjensky, D.A., Hazen, R.A., 2011. The adsorption of short single-stranded DNA oligomers to mineral surfaces. Chemosphere 83, 1560–1567. doi:10.1016/j.chemosphere.2011.01.023

Crecchio, C., Stotzky, G., 1998. Binding of DNA on humic acids: Effect of transformation of Bacillus subtilis and resistance to DNase. Soil Biology and Biochemistry 30, 1061–1067.

D'Costa, V.M., King, C.E., Kalan, L., Morar, M., Sung, W.W.L., Schwarz, C., Froese, D., Zazula, G., Calmels, F., Debruyne, R., Golding, G.B., Poinar, H.N., Wright, G.D., 2011. Antibiotic resistance is ancient. Nature 477, 457–461. doi:10.1038/nature10388

Dabney, J., Knapp, M., Glocke, I., Gansauge, M.-T., Weihmann, A., Nickel, B., Valdiosera, C., Garcia, N., Paabo, S., Arsuaga, J.-L., Meyer, M., 2013. Complete mitochondrial genome sequence of a Middle Pleistocene cave bear reconstructed from ultrashort DNA fragments. Proceedings of the National Academy of Sciences 110, 15758–15763. doi:10.1073/pnas.1314445110

Enk, J., Rouillard, J.M., Poinar, H., 2013. Quantitative PCR as a predictor of aligned ancient DNA read counts following targeted enrichment. BioTechniques 55, 300–309. doi:10.2144/000114114

Enk, J., Devault, A., Widga, C., Saunders, J., Szpak, P., Southon, J., Rouillard, J.-M., Shapiro, B., Golding, G.B., Zazula, G., Froese, D., Fisher, D.C., Macphee, R.D.E., Poinar, H., 2016. Mammuthus population dynamics in Late Pleistocene North America: Divergence, Phylogeogrpaphy and Introgression. Frontiers in Ecology and Evolution 4, 1–13. doi:10.3389/fevo.2016.00042

Greaves, M.P., Wilson, M.J., 1969. The adsorption of nucleic acids by montmorillonite. Soil Biology and Biochemistry 1, 317–323. doi:10.1016/0038-0717(69)90014-5

Greaves, M.P., Wilson, M.J., 1970. The degradation of nucleic acids and montmorillonite-nucleic-acid complexes by soil microorganisms. Soil Biology and Biochemistry 2, 257–268. doi:10.1016/0038-0717(70)90032-5

Haile, J., 2008. Ancient DNA from Sediments and Associated Remains. University of Oxford.

Hollingsworth, P.M., 2011. Refining the DNA barcode for land plants. Proceedings of the National Academy of Sciences 108, 19451–19452. doi:10.1073/pnas.1116812108

Hollingsworth, P.M., Graham, S.W., Little, D.P., 2011. Choosing and using a plant DNA barcode. PLoS ONE 6. doi:10.1371/journal.pone.0019254

Höss, M., Dilling, A., Currant, A., Pääbo, S., 1996. Molecular phylogeny of the extinct ground sloth Mylodon darwinii. Proceedings of the National Academy of Sciences 93, 181–185. doi:10.1073/pnas.93.1.181

Huson, D.H., Auch, A.F., Qi, J., Schuster, S.C., 2007. MEGAN analysis of metagenomic data. Genome Research 17, 377–386. doi:10.1101/gr.5969107

Huson, D.H., Beier, S., Flade, I., Górska, A., El-Hadidi, M., Mitra, S., Ruscheweyh, H.J., Tappu, R., 2016. MEGAN Community Edition - Interactive Exploration and Analysis of Large-Scale Microbiome Sequencing Data. PLoS Computational Biology 12. doi:10.1371/journal.pcbi.1004957

Jónsson, H., Ginolhac, A., Schubert, M., Johnson, P.L.F., Orlando, L., 2013. MapDamage2.0: Fast approximate Bayesian estimates of ancient DNA damage parameters. Bioinformatics 29, 1682–1684. doi:10.1093/bioinformatics/btt193

Kalendar, R., Lee, D., Schulman, A.H., 2011. Java web tools for PCR, in silico PCR, and oligonucleotide assembly and analysis. Genomics 98, 137–144. doi:10.1016/j.ygeno.2011.04.009

Karpinski, E., Mead, J.I., Poinar, H.N., 2016. Molecular identification of paleofeces from Bechan Cave, southeastern Utah, USA. Quaternary International 443, 140–146. doi:10.1016/j.quaint.2017.03.068

Khanna, M., Yoder, M., Calamai, L., Stotzky, G., 2005. X-ray diffractometry and electron microscopy of DNA from Bacillus subtilis bound on clay minerals. Sciences of Soils 3, 1–10. doi:10.1007/s10112-998-0001-3

King, C.E., Debruyne, R., Kuch, M., Schwarz, C., Poinar, H.N., 2009. A quantitative approach to detect and overcome PCR inhibition in ancient DNA extracts. BioTechniques 47, 941–949. doi:10.2144/000113244

Kircher, M., Sawyer, S., Meyer, M., 2012. Double indexing overcomes inaccuracies in multiplex sequencing on the Illumina platform. Nucleic Acids Research 40, 1–8. doi:10.1093/nar/gkr771

Koopal, L.K., Goloub, T.P., Davis, T.A., 2004. Binding of ionic surfactants to purified humic acid. Journal of Colloid and Interface Science 275, 360–367. doi:10.1016/j.jcis.2004.02.061

Kuch, M., Rohland, N., Betancourt, J.L., Latorre, C., Steppan, S., Poinar, H.N., 2002. Molecular analysis of a 11 700-year-old rodent midden from the Atacama Desert, Chile. Molecular Ecology 11, 913–924. doi:10.1046/j.1365-294X.2002.01492.x

Li, H., Durbin, R., 2009. Fast and accurate short read alignment with Burrows-Wheeler transform. Bioinformatics (Oxford, England) 25, 1754–60. doi:10.1093/bioinformatics/btp324

Lorenz, M.G., Wackernagel, W., 1987. Adsorption of DNA to sand and variable degradation rates of adsorbed DNA. Applied and Environmental Microbiology 53, 2948–2952.

Mahony, M.E., 2015. 50,000 years of paleoenvironmental change recorded in meteoric waters and coeval paleoecological and cryostratigraphic indicators from the Klondike goldfields, Yukon, Canada. University of Alberta. doi:10.1145/3132847.3132886

McMurdie, P.J., Holmes, S., 2014. Waste not, want not: why rarefying microbiome data is inadmissible. PLoS computational biology 10, e1003531. doi:10.1371/journal.pcbi.1003531

Meyer, M., Kircher, M., 2010. Illumina sequencing library preparation for highly multiplexed target capture and sequencing. Cold Spring Harbor Protocols 5. doi:10.1101/pdb.prot5448

NCBI Resource Coordinators, 2018. Database resources of the National Center for Biotechnology Information. Nucleic Acids Research 46, 8–13. doi:10.1093/nar/gkx985

Ogram, A., Sayler, G., Gustin, D., Lewis, R., 1988. DNA adsorption to soils and sediments. Environmental science and technology 22, 982–984.

Otto, W.H., Britten, D.J., Larive, C.K., 2003. NMR diffusion analysis of surfactant-humic substance interactions. Journal of Colloid and Interface Science 261, 508–513. doi:10.1016/S0021-9797(03)00062-6

Pina-Martins, F., Paulo, O.S., 2015. NCBI Mass Sequence Downloader–Large dataset downloading made easy. SoftwareX 5, 80–83. doi:10.1016/j.softx.2016.04.007

Poinar, H.N., Hofreiter, M., Spaulding, W.G., Martin, P.S., Stankiewicz, B.A., Bland, H., Evershed, R.P., Possnert, G., Pääbo, S., 1998. Molecular coproscopy: Dung and diet of the extinct ground sloth Nothrotheriops shastensis. Science 281, 402–406. doi:10.1126/science.281.5375.402

Renaud, G., Stenzel, U., Kelso, J., 2014. LeeHom: Adaptor trimming and merging for Illumina sequencing reads. Nucleic Acids Research 42, e141. doi:10.1093/nar/gku699

Sadoway, T.R., 2014. A Metagenomic Analysis of Ancient Sedimentary DNA Across the Pleistocene-Holocene Transition. McMaster University.

Schlager, B., Straessle, A., Hafen, E., 2012. Use of anionic denaturing detergents to purify insoluble proteins after overexpression. BMC Biotechnology 12. doi:10.1186/1472-6750-12-95

Shaban, I.S., Mikulaj, V., 1998. Impact of an Anionic Surfactant Addition on Solubility of Humic Acid in Acid-Alkaline Solutions. Chemical Papers 52, 753–755.

Sidstedt, M., Jansson, L., Nilsson, E., Noppa, L., Forsman, M., Rådström, P., Hedman, J., 2015. Humic substances cause fluorescence inhibition in real-time polymerase chain reaction. Analytical Biochemistry 487, 30–37. doi:10.1016/j.ab.2015.07.002

Soininen, E.M., Gauthier, G., Bilodeau, F., Berteaux, D., Gielly, L., Taberlet, P., Gussarova, G., Bellemain, E., Hassel, K., Stenoien, H.K., Epp, L., Schroder-Nielsen, A., Brochmann, C., Yoccoz, N.G., 2015. Highly overlapping winter diet in two sympatric lemming species revealed by DNA metabarcoding. PLoS ONE 10, 1–18. doi:10.1371/journal.pone.0115335

Sønstebø, J.H., Gielly, L., Brysting, A.K., Elven, R., Edwards, M., Haile, J., Willerslev, E., Coissac, E., Rioux, D., Sannier, J., Taberlet, P., Brochmann, C., Sonstebo, J.H., Gielly, L., Brysting, A.K., Elven, R., Edwards, M., Haile, J., Willerslev, E., Coissac, E., Rioux, D., Sannier, J., Taberlet, P., Brochmann, C., 2010. Using next-generation sequencing for molecular reconstruction of past Arctic vegetation and climate. Molecular Ecology Resources 10, 1009–1018. doi:10.1111/j.1755-0998.2010.02855.x

Sujeevan, R., Paul, D., 2007. BARCODING BOLD: The Barcode of Life Data System. Molecular Ecology Notes 7, 355–364. doi:10.1111/j.1471-8286.2006.01678.x

Taberlet, P., Coissac, E., Pompanon, F., Gielly, L., Miquel, C., Valentini, A., Vermat, T., Corthier, G., Brochmann, C., Willerslev, E., 2007. Power and limitations of the chloroplast trnL (UAA) intron for plant DNA barcoding. Nucleic acids research 35, e14. doi:10.1093/nar/gkl938

Tanford, C., 1980. The hydrophobic effect: formation of micelles and biological membranes, 2nd editio. ed. Wiley Interscience, New York.

Taylor, B.R., Parkinson, D., 1988. Patterns of water absorption and leaching in pine and aspen leaf litter. Soil Biology and Biochemistry 20, 257–258. doi:10.1016/0038-0717(88)90047-8

Willerslev, E., Hansen, A.J., Binladen, J., Brand, T.B., Gilbert, M.T.P., Shaprio, B., Bunce, M., Wiuf, C., Gilichinsky, D.A., Cooper, A., 2003. Diverse Plant and Animal Genetic Records from Holocene and Pleistocene Sediments. Science 300, 791–795. doi:10.1126/science.1084114

Willerslev, E., Davison, J., Moora, M., Zobel, M., Coissac, E., Edwards, M.E., Lorenzen, E.D., Vestergard, M., Gussarova, G., Haile, J., Craine, J., Gielly, L., Boessenkool, S., Epp, L.S., Pearman, P.B., Cheddadi, R., Murray, D., Brathen, K.A., Yoccoz, N., Binney, H., Cruaud, C., Wincker, P., Goslar, T., Alsos, I.G., Bellemain, E., Brysting, A.K., Elven, R., Sonstebo, J.H., Murton, J., Sher, A., Rasmussen, M., Ronn, R., Mourier, T., Cooper, A., Austin, J., Moller, P., Froese, D., Zazula, G., Pompanon, F., Rioux, D., Niderkorn, V., Tikhonov, A., Savvinov, G., Roberts, R.G., MacPhee, R.D.E., Gilbert, M.T.P., Kjaer, K.H., Orlando, L., Brochmann, C., Taberlet, P., 2014. Fifty thousand years of Arctic vegetation and megafaunal diet. Nature 506, 47–51. doi:10.1038/nature12921